PIGMENT DERIVED PHYTOPLANKTON COMPOSITION ALONG THE WESTERN ANTARCTIC PENINSULA

A Thesis

Presented to the

Faculty of

San Diego State University

In Partial Fulfillment

of the Requirements for the Degree

Master of Science

in

Biology

by

Wendy Anne Kozlowski

Spring 2008

SAN DIEGO STATE UNIVERSITY

The Undersigned Faculty Committee Approves the

Thesis of Wendy Anne Kozlowski:

Pigment Derived Phytoplankton Composition along the Western Antarctic Peninsula

_____

Douglas D. Deutschman, Chair
Department of Biology

_____

Charles C. Trees
Department of Biology

_____

Douglas Stow
Department of Geography

_____

Maria Vernet
Scripps Institution of Oceanography

_____

Approval Date

DEDICATION

This thesis is dedicated to three of the most influential teachers in my life: my parents, Robert and Shirley Kozlowski, and my mentor and friend, Maria Vernet. You have shared with me your grace and wisdom; may I always carry with me, and pass along to others, the things I have learned from you.

Thinking is more interesting than knowing, but less interesting than looking.

- Johann Wolfgang von Goethe

ABSTRACT OF THE THESIS

Pigment Derived Phytoplankton Composition along the Western Antarctic Peninsula

by
Wendy Anne Kozlowski
Master of Science in Biology
San Diego State University, 2008

Current bio-optical models for remote sensing of chlorophyll a (chl_a) biomass and production are sensitive to changes in specific absorption. Variability in phytoplankton composition is tied to changes in spectral absorption; our ability to follow these changes would be enhanced by a better understanding of community composition. Examined in this study was a thirteen year span (1995-2007) of high-performance liquid chromatography (HPLC) pigments collected as part of the Palmer Long Term Ecological Research (PAL LTER) project along the western Antarctic Peninsula (wAP) between roughly -64 and -68° South. Phytoplankton composition was estimated using CHEMTAX analysis software, and presented here is the temporal and spatial distribution of those assemblages in both surface (50% $E_{0,PAR}$) and deep euphotic zone (1% $E_{0,PAR}$) waters. Diatoms and cryptophytes were found to be the two dominant groups at the surface. In the deep water sample, contribution to total chl_a was more evenly distributed between groups, with only diatoms ever consisting of more than 50% of the population. Spatially, diatoms were most abundant (in terms of $\mu g\ L^{-1}$ chl_a) inshore along the entirety of the sampling grid, whereas cryptophyte and prasinophyte abundance was typically highest inshore only in the north. Mixed flagellate concentration was highest inshore in the south-eastern region but in shelf waters further north, and type 4 Haptophytes were most abundant along the length of the shelf region. Temporal distribution of groups is discussed in terms of anomalies calculated as yearly differences from the climatological means. Variability in space and time was examined using principle component analysis, and possible relationships between seasonal sea ice retreat and phytoplankton composition, as well as phytoplankton composition and primary production are discussed.

TABLE OF CONTENTS

PAGE

LIST OF TABLES

PAGE

LIST OF FIGURES

PAGE

LIST OF ABBREVIATIONS

Abbreviation	Definition	Unit
ACC	Antarctic circumpolar current	
C	carbon	
CDW	circumpolar deep water	
chl_a	chlorophyll a	$\mu g\ L^{-1}$
chl_aC	chlorophyll a attributed to cryptophytes	$\mu g\ L^{-1}$
chl_aD	chlorophyll a attributed to diatoms	$\mu g\ L^{-1}$
chl_aH	chlorophyll a attributed to haptophytes	$\mu g\ L^{-1}$
chl_aMF	chlorophyll a attributed to mixed flagellates	$\mu g\ L^{-1}$
chl_aP	chlorophyll a attributed to prasinophytes	$\mu g\ L^{-1}$
CTD	conductivity temperature depth	
DAAC	Distributed Active Archive Center	
DAD	diode array detector	
DMSP	Defense Meteorological Satellite Program	
DOM	dissolved organic material	
END15	index of sea ice retreat	d
ENSO	El Niño Southern Oscillation	
EOF	empirical orthogonal function	
GF/F	glass fiber filter	
HNLC	high nutrient low chlorophyll	
HPLC	high performance liquid chromatography	
MIZ	marginal ice zone	
MLD	mixed layer depth	m
M-UCDW	modified upper circumpolar deep water	
OA	optimal analysis	
Pal LTER	Palmer Long Term Ecological Research	
PAR	photosynthetically available radiation (400-700nm)	
PC	principle component	
PCA	principle components analysis	
pCO_2	partial pressure of CO_2	µatm
SAM	Southern Annular Mode	
SIZ	Sea Ice Zone	
SML	seasonal mixed layer	m
SSM/I	Special Sensor Microwave /Imager	
SMMR	Scanning Multichannel Microwave Radiometer	
SO	Southern Ocean	
T-S	temperature-salinity	
UCDW	upper circumpolar deep water	
VWD	variable wavelength detector	
wAP	western Antarctic Peninsula	
Z_{eu}	eupohtic zone depth	m

INTRODUCTION

Once considered merely an extension of the Atlantic, Pacific and Indian Oceans, the Southern Ocean (SO) region, now defined as waters below 60°S latitude, covers nearly 18% of the Earth's total surface area (approximately 7.85 million square miles) surrounding the continent of Antarctica. The sea floor in this region is relatively deep (4000-6000 meters) compared to other oceans (1050-4300 meters), and includes a continental shelf region which averages 400-800 meters below sea level, roughly 8 times deeper than the world average (Anderson, 1999). Despite these depths, the Southern Ocean's volume is small when compared to the sum of the world's other oceans; it nonetheless plays a crucial role in global ocean circulation. Together with the powerful Antarctic Circumpolar Current (ACC), which continuously carries water west to east (i.e., clockwise) around the continent (Orsi et al., 1995), regions of upwelling and sinking currents form circulation patterns which distribute Antarctic water masses throughout the globe (Knox, 2007). These thermohaline circulation patterns combined with biological transport (Raven and Falkowski, 1999), have been shown to play a central role in the air-sea balance of the partial pressure of CO_2 (pCO_2; Sarmiento and Toggweiler, 1984; Popova et al., 2000; Gowing et al., 2001) as well as uptake and storage of anthropogenic carbon dioxide (Caldeira and Duffy, 2000).

As phytoplankton are responsible for the entry of inorganic carbon (CO_2, HCO_3) into the food chain, this oceanic carbon sequestration is in part influenced by phytoplankton composition and the grazing that occurs on that phytoplankton (Falkowski et al., 1998). For instance, it has been shown that regions of high primary production are associated with the presence of diatoms, a relatively large, single-cell type of phytoplankton. In turn, preferential grazing by Antarctic krill (*Euphausia superba*) upon diatoms over smaller and colonial cells (Haberman et al., 2003) may impact the phytoplankton populations (top-down control) and rates of detrital formation and settlement, as well as the life-cycle of the grazers themselves. Additionally, cell size and type (e.g., flagellated vs. colonial vs. chain forming vs. single large cells) will affect the movement of phytoplankton in the water (Padisak et al., 2003) and the amount of particulate and dissolved organic matter (DOM) in the surface waters, which will in turn affect the atmospheric sink for carbon (Volk and Hoffert, 1985; Smetacek, 1999). Therefore, determination of phytoplankton composition, and understanding its patterns of variability are fundamental to our ability to follow the region's carbon pool.

Ice cover is a second key feature which impacts the Southern Ocean. Physical forcing on the continent itself has influenced the geological features of the shelf (Knox, 2007; Anderson, 1999), and the connections between both glacial and seasonal sea ice and the oceanic physical characteristics and the Antarctic ecosystem are well documented (Clarke et al., 1988; Stammerjohn, 2008; Moline and Prézelin, 1996; Buesseler et al., 2003). For instance, seasonal melting of continental glaciers influences coastal salinities (Dierssen et al., 2002), free drifting icebergs have been shown to be "hot

spots" of chemical and biological enrichment (Smith et al., 2007) and variation in extent, percent cover and duration of seasonal sea ice has been linked to changes in physical characteristics of seawater (Martinson et al., 2008; Stammerjohn et al., 2008), sedimentation rates (Ducklow et al., 2008), biomass (Smith et al., 2008), primary production (Vernet et al., 2008) and krill life histories (Quetin et al., 2003; Ross et al., 2004; Quetin et al., 2007; Ross et al., 2008).

Though considered to be high nutrient, low chlorophyll (HNLC) waters (Chisholm and Morel, 1991), there exists in the Southern Ocean regions of enhanced phytoplankton biomass, often referred to as "blooms". Such areas are typically associated with (1) stabilization of a seasonal mixed layer (Hart, 1934; Peloquin and Smith, 2007) by melting of sea ice within the marginal ice zone (MIZ; Smith and Nelson, 1986; Tréguer and Jacques, 1992; Mitchell and Holm-Hansen, 1991; Sakshaug et al., 1991; Holm-Hansen et al., 1989; Moore and Abbot, 2000), (2) major oceanic frontal systems such as the intrusion of the southern boundary of ACC water (Boyd et al., 1995; Savidge et al., 1995) or upwelling of upper-circumpolar deep water (UCDW) (Prézelin et al., 2000, 2004), (3) favorable meteorological conditions (Lancelot et al., 1993; Smith et al., 1998) or (4) ice formation (Smetacek et al., 1992). These phytoplankton blooms are thought to be controlled primarily by light (van Oijen et al., 2004; Smith et al., 2000), micronutrients such as iron (Martin et al., 1990; Coale et al., 2004; Hare et al., 2007), grazing by microzooplankton (Burkhill et al., 1995) and/or storm events (Mitchell and Holm-Hansen, 1991; Fitch and Moore, 2007). Particularly during these times of high production, phytoplankton provide a means of large scale atmospheric CO_2 uptake and through cellular excretion, lysis and grazing, can account for organic material flux of > 1-2 g C m^{-2} d^{-1} through the upper water column (Fischer et al., 2002).

Composition and distribution of phytoplankton blooms have been documented using high performance liquid chromatography (HPLC) analysis of photosynthetic pigments (Jeffrey, 1980; Geiskes and Kraay, 1986, Goericke and Repeta, 1993; Letelier et al., 1993; Peeken, 1997; Wright and van den Enden, 2000). These chemotaxonomic methods are based on the presence of characteristic pigments, mostly carotenoids, in algal phyla. One application of such methods, CHEMTAX, uses an iterative process of matrix factorization to optimize the association of pigments to compositional groups (Mackey et al., 1996). Primary concerns regarding use of chemotaxonomic methods center around (1) non-unique pigment markers (Wright and Jeffrey, 1987; Zapata et al., 2004, among others) and (2) potential fluctuations of the pigment ratios at both a species and a cellular level under various physiological stressors (Jeffrey, 1981; Demmig-Adams, 1990; Demers et al., 1991; Arsalane et al., 1994; Goericke and Montoya, 1998; DiTullio et al., 2007; Lance et al., 2007). However, with appropriate precautions and awareness of impacts and implications of physiological stressors, and some knowledge of potential populations within a sample region (Irigoien et al., 2004), CHEMTAX is a viable method for determination of phytoplankton composition (Mackey et al., 1998; Schlüter et al., 2000; Havskum, 2004; Wulff and Wängberg, 2004).

The Palmer Long Term Ecological Research (Pal LTER) project has as its focus the marine ecosystem of the western Antarctic Peninsula (wAP). The central tenet of the Pal LTER is that "the annual advance and retreat of sea ice is a major physical determinant of spatial and temporal changes in the structure and function of the Antarctic marine ecosystem" (H_1; Ross et al., 1990). One of the routes by which physical forcing modulates the wAP ecosystem is through the linkage of seasonal sea ice distribution and dynamics and primary production (Vernet et al., 2008). Variance in wAP primary production is linked to phytoplankton abundance and composition, which in turn explains 70% of the variance in growth of young krill (phytoplankton grazers) in the Pal LTER area (Ross et al., 2008). Though grazing pressure by krill and other macrozooplanktors can suppress phytoplankton accumulation, it also provides a means of nutrient regeneration (e.g., particulate organic material to NH_4), potentially facilitating the seasonal bloom cycle (Knox, 2007). The Pal LTER proposes to define ecological processes which couple the annual cycle and interannual variability of sea ice to the life histories of key species (here, phytoplankton and krill) and biogeochemical processes (primary and secondary production, CO_2 absorption and sedimentation).

In addition, the wAP has been recognized as an "example of a climate-sensitive region experiencing major changes in species abundance and composition due to changes in range and distribution (Smith et al., 1999 and 2001) that are occurring in response to regional climate change" (Ducklow, 2002). Global warming has led to an increased melting of both seasonal pack and glacial ice (Vaughan et al., 2003), and it has been hypothesized that the decreased salinity associated with such melting events may induce shifts in phytoplankton composition, and thus a secondary Pal LTER hypothesis (H_2) has been developed:

> The dominance of diatoms within the phytoplankton community is enhanced by high ice during the previous winter and spring, followed by late ice retreat and a warm summer, resulting in increased water column stability. A warming trend will decrease either average diatom distribution and/or the frequency of diatom blooms in the northern region replacing them with smaller flagellates. (Ducklow, 2002).

Though many studies have examined variability of Antarctic phytoplankton structure and dynamics, our understanding of the large-scale geographic and long-term temporal variability remains weak. Previous studies examining phytoplankton composition and distribution have primarily focused on short term, limited scale sampling. Described here are a few of the key studies regarding phytoplankton composition along the wAP. A summary of such studies in all regions of the Southern Ocean, as well as studies specifically employing CHEMTAX for taxonomic determination, their time frames, methodologies and findings relevant to this study can be found in Appendix A.

Early studies of the Bransfield and Gerlache straits include those of the Discovery expeditions, where Hart reports findings of high abundances of diatoms (1934, 1937) and *Phaeocystis* (1942). Burkholder and Sieburth (1961) document similar findings of "rich communities" of diatoms and *Phaeocystis* during the summer of 1958-1959, in the Gerlache and western Bransfield straits, adjacent to the north of the current study region. In early austral summer of 1980, Bodungen et al. (1986) again documented moderate to high biomass consisting of primarily diatoms and

haptophytes, and moderate accumulations of diatoms along the shelf break. In the mid-1980's, Holm-Hansen and Mitchell (1991) set out to explore the HNLC phenomenon in the region, and concluded protection from storm activity and proximity to fresh water was needed for blooms to form, and that large blooms (> 10 mg chl_a L^{-1}) only occurred when the upper mixed layer was less than 25 m deep. They also hypothesized that grazing by upper trophic levels, cellular sinking and advection rather than inorganic nutrient decline was the likely cause of bloom demise in the region.

Research in the wAP expanded greatly in the 1990's, and with it came advances in methodology and new insights into the dynamics of the system. Savidge et al. (1995), in the south-western Bellingshausen Sea in November and December of 1992, encountered a general dominance of diatoms and *Phaeocystis* at the ice edge, but found no "stability induced ice edge bloom". They hypothesized that development of such blooms must require a fresh water layer under the sea ice, and in that season retreat occurred too quickly for that stability to develop. Barlow et al. (1998) worked in the same region at the same time and using chemotaxonomic methods from HPLC pigments, reported very similar composition and low biomass as found by Savidge et al. (1995) who used microscopy. At Palmer Station, on the south end of Anvers Island between 1991 and 1993, Moline and Prézelin (1996) used HPLC methods to quantify presence of diatoms, cryptophytes, haptophytes and chlorophytes, and tied the variability of the groups through wind stress to water column stability. Prézelin et al. (2000, 2004) associated diatoms with topographically induced upwelling of UCDW and reported dominance of other taxa in non-UCDW shelf regions in the Pal LTER grid. Though previously documented as being a contributor to the Antarctic phytoplankton community (Villafañe et al., 1995 among others), one of the earliest reports on cryptophyte dominance (91%) in the area of the Bransfield and Gerlache straits was by Mura et al. (1995), during the austral summer of 1993. Varela (2002) divided the Bransfield and Gerlache Strait waters of summer 1995-1996 into three regions based on composition and production levels. Highest production was associated with diatoms, moderate with cryptophytes or a mixture of cryptophytes and *Phaeocystis*, and low production with microflagellates, dinoflagellates and other small diatoms. In none of the regions did they find a correlation between composition and either hydrography or nutrients. Working in the same area at the same time were Rodriguez et al. (2002), who applied CHEMTAX algorithms to HPLC data to define phytoplankton groups. Comparison of those results to microscopy based methods showed generally good agreement between methods. Rodríguez et al. (2002) also worked in that same time frame and location, and was one of the first to use flow cytometric methods for phytoplankton identification. Garibotti et al. (2003a) compared HPLC pigment regression methods to microscopic identification of phytoplankton in the Pal LTER region and also found results of the two techniques to be comparable. Finally, Garibotti et al. (2005a) analyzed Pal LTER data from 1996, 1997 and 1999 and proposed that the variability of phytoplankton community on a large scale is related to physical characteristics of the water column, but that mesoscale variability can be associated instead with seasonal succession of phytoplankton groups.

The specific goals of this study were to (1) establish and apply to the Pal LTER HPLC dataset a robust means of determining phytoplankton composition and (2) using that dataset, define and describe the temporal and spatial variability of phytoplankton composition along the Palmer LTER region of the western Antarctic Peninsula, particularly as it relates to sea ice dynamics, ecosystem dynamics and potential impacts of climate change.

METHODS

The following sections describe first the sampling region and design, sampling platforms and the temporal scope of the project; subsequent paragraphs summarize methodology for specific datasets (high performance liquid chromatography (HPLC), production, nutrients, ice, physical parameters, microscopy), including sample collection, processing and data analysis used in this thesis. Particular attention is given to HPLC sample processing and specific chemotaxonomic methods employed.

DATA COLLECTION

This data was collected as part of the Palmer Long Term Ecological Research project. The Palmer site, one of 26 within the LTER Network collaborative, was established in 1990, with the first annual austral summer cruise occurring in 1993. Palmer research is organized around six ecological components: (1) climate and sea ice, (2) physical oceanography, (3) microbial ecology and organic biogeochemistry, (4) phytoplankton ecology, (5) zooplankton and micronekton and (6) seabirds, with one of the primary goals of the project being to understand the dynamics of the marine pelagic ecosystem and how it is impacted by interannual variability in sea ice.

Study Area and Sampling Regime

The geographic area of study is along western Antarctic Peninsula (wAP), from -63.6 to -68.2°S and from -64 to -73°W. It borders the eastern boundary of the Bellingshausen Sea to the South (see map, Fig. 1, Appendix B; hereafter all figures can be found in Appendix B), and is part of the Southeastern Pacific Ocean. The region is characterized by a glacially sculpted coastline containing a series of islands, bays and passages (Anderson, 1999), and is often divided into three sub-regions based on bathymetry and associated biological and physical dynamics (Smith et al., 2008; Martinson et al., 2008; Vernet et al., 2008); these three divisions will be referred to here as coastal, shelf and slope regions (Fig. 1).

Pal LTER large-scale sampling stations are laid out on a grid system (Waters and Smith, 1992), with transects ("grid lines") 100 km apart running roughly south-east (onshore) to north-west (offshore) across the Antarctic continental shelf, approximately perpendicular to the coast. "Grid stations" are spaced 20 km apart along those lines (Fig. 1b). Stations are identified using a LLL.SSS nomenclature, where LLL is grid line position, in kilometers, relative to the southernmost position on the grid and SSS is grid station, in kilometers, relative to the average coast (e.g., station 400.120 is located 400 km north along the peninsula from the southernmost line, and 120 km offshore). Sampling used in this analysis was limited to five cardinal lines, 200 to 600, which cover the region from Southern end of Anvers Island to Marguerite Bay, and included all cardinal grid stations as well

as other off-grid stations (e.g., near Palmer Station on Anvers Island, stations north and inland of Renaud Island and stations in the vicinity of southern Adelaide Island in the mouth of Marguerite Bay) occupied during yearly sampling efforts.

Water sampling included in this study was done as part of the Pal LTER annual Austral summer cruise series from 1995 to 2007. Cruise timing coincided with the critical Adélie penguin growth period (Smith et al., 1995), and stations were occupied in most years between the first week in January and the first week of February. Sampling was carried out from the R/V Polar Duke in 1995, 1996 and 1997 and from the ASRV Laurence M. Gould from 1998 to 2007. Not all stations were sampled on all cruises due to ice, weather or scheduling issues; Table 1 in Appendix C contains a summary of timing and stations visited during cruises included in this study (hereafter all tables can be found in Appendix C). HPLC data from January 2002 is not included in this study.

Sampling and Processing Methods

At all stations sampled, water was collected in 10 L Go-Flo (1995-1997) or 12 L Niskin (1998-2007) bottles, at the surface and at depths corresponding to 50, 25, 10, 5 and 1% (± 4%) of surface photosynthetically available radiation (PAR, 400-700 nm). Light depths were determined using a Biospherical Instruments QSP 200L4S sensor from 1995-2000 and 2003 and the PAR channel from a Biospherical Instruments Profiling Reflectance Radiometer (600 Series 2001-2002, 800 Series 2004-2007) cast immediately prior to the water collection cast. To ensure adequate light availability for instrumentation, water sampling was limited to daytime hours when the ambient PAR irradiance (4π) was greater than 100 $\mu E\ m^{-2}*s^{-1}$. This typically bound water sampling hours to between 0430 and 2200 hours local. For purposes of this study, the euphotic zone depth (Z_{eu}) is defined as the 1% irradiance depth.

Attached to the sampling rosette was conductivity, temperature and depth (CTD; Sea Bird Electronics (SBE) 19 from 1995 to 1997, SBE 911 from 1998-2007) instrumentation, as well as a fluorometer (SeaTech from 1995 to 1997, Chelsea Aquatracka MkIII from 1998-2004, WetLabs ECO-FL from 2005-2007), transmissometer (except 2004, WetLabs C-Star) and PAR sensors, which continuously collected data for the duration of the cast.

Specifics for the major variables used in this study are discussed below.

HPLC

From each depth sampled, 0.5-2 L of seawater was filtered, at < 12 psi vacuum, under dim light conditions (no direct overhead or outside light), onto 25 mm Whatman glass fiber filter (pore size nominally 0.7 µ; hereafter referred to as “GF/F”), and stored in liquid nitrogen until analysis. Samples were extracted and injected as soon as possible after collection (minimum of 24 hours in liquid nitrogen); for years other than 2000, time between filtration and analysis was typically less than one month and no more than three months. Due to instrumentation problems, samples from January

2000 were transported (in liquid nitrogen) to Scripps Institution of Oceanography and analyzed within thirteen months of collection.

Filters were extracted in 90% HPLC grade acetone and either (a) manually crushed with a clean Teflon pestle, stored at -80°C for 24 hours, and pre-filtered through another GF/F before injection (1995-2001) or (b) ultrasonicated while held in a -20°C bench-top cooler for 10 seconds, stored at -80°C for 24 hours and pre-filtered through a 1 µ syringe tip glass fiber filter (2003-2005) or 0.45 µ Whatman nylon Puradisk filter (2006-2007) before injection. Testing confirmed that the changes in pre-injection filter type affected only pre-column and column longevity, not separation or retention times.

For cruises between 1995 and 1999, pigments were separated using a Hitachi system (D-6500 in 1995; D-7000 from 1996 to 1999) with L-4250 fixed wavelength (440 nm) and L-4500 diode array (DAD, scanning 350-650 nm) detectors. HPLC grade mobile phase eluents followed the method of Wright et al. (1991):

Solvent A: 80:20 methanol : 0.5 M aqueous ammonium acetate (pH 7.2)
Solvent B: 90:10 acetonitrile : water
Solvent C: 100% ethyl acetate

The analytical gradient was modified from Wright et al. (1991) to reduce spreading of the early eluting, highly polar chlorophyll c3, and is listed in Table 2. Ultimately, the chlorophyll c3 data was not used in the analysis due to this peak spreading and the associated difficulties of calibration. Solvents were degassed by sparging with 99% pure Helium gas, and separations were performed on a Waters Resolve C18, 300 mmx3.9 µ, 5 µ column. Hitachi's ConcertChrome software package was used for system control and data collection, and peaks were quantified at 440 nm on the DAD.

January 2000 cruise data was analyzed on a Waters 600 controlled system with a Thermo Separation Products (TSP) AS3000 sampler, a TSP Spectra 1000 variable wavelength detector (VWD) for peak quantification and a Waters 470 Scanning fluorescence detector for peak identification when applicable (excitation at 440 nm, emission at 665 nm). Data was collected using the Waters Millennium 32 software package, and peaks were quantified at 440 nm on the VWD.

For cruises between 2001 and 2007, samples were separated using an Agilent Technologies (Hewlett-Packard) 1100 Series HPLC system, equipped with G1314A variable wavelength (fixed at 440 nm), G1315A diode array (scanning 330-800 nm) and G1321A fluorescence (440 nm excitation, 650 nm emission) detectors. Solvents were degassed using a vacuum degasser and column temperature was maintained at 25°C with a G1316A column thermostat. Agilent Technologies ChemStation for LC 3D software was used for system control and data collection and peaks were quantified at 440 nm on the VWD.

From 2000 to 2007 (both Waters and Agilent Technologies systems), HPLC grade mobile phase eluents followed the method of Zapata et al. (2000):

Solvent A: 50:25:25 methanol : acetonitrile : 0.25 M aqueous pyridine
Solvent B: 20:60:20 methanol: acetonitrile : acetone

The analytical gradient was modified slightly from Zapata et al. (2000) to allow adequate separation of the mid-chromatogram range xanthophylls, and is listed in Table 2. Separations with this method were performed on Waters Symmetry C8, 150 mm x 4.6 µ, 3.5 µ columns, and samples were injected as either (a) a 2:1 sample:water mixture in 2000 or (b) a 5:4 sample:water mixture from 2001-2007.

In 1995 and 1996, chlorophylls a and b and alpha and beta carotene were quantified using measured spectral absorbance and published extinction coefficients; all other standards were isolated and quantified by Moss Landing Marine Laboratory and all were injected as external standards to determine signal response and retention times. From 1997-2007 commercially produced plant pigment standards (Sigma Chemical for chlorophylls a and b and alpha and beta carotene until 2000; DHI (formerly VKI), Denmark (http://www.c14.dhi.dk/PhytoplanktonPigmentStandards.htm) for all others) were used for system calibration. Four to six point response curves were built using standard peak areas measured at 440 nm, and daily injections of chlorophyll a (chl_a), as well as random single-point injections of all other pigments, were made to confirm system stability and monitor column degradation throughout the duration of sample processing. Sample peaks were identified based on retention times and confirmed spectrally using the diode array and fluorescence detectors, and pigment concentration was calculated by regression in Excel. Pigments quantified and used in this study, average retention times, and extinction coefficients used for determining standard concentrations are listed in Table 3.

PRIMARY PRODUCTION

Net primary production was estimated at each station using standard radiocarbon (^{14}C) incorporation methods (Steeman-Nielsen, 1952). Briefly, water was collected at light depths as described in section 2.1.1, spiked with 5 µCi $NaH^{14}CO_3$ per 100 ml sample bottle. Incubations were carried out in a shade free area of the ship's deck, in UV blocking acrylic tubes with running seawater for maintenance of ambient temperature. Parallel duplicate light and dark incubations were carried out, and specific activities were calculated based on a 0.1 ml sample taken from a time zero bottle. After 24 hours, particulate material was collected on GF/F filters, acidified with 20% hydrochloric acid to off-gas remaining inorganic radiocarbon, and activities read on a scintillation counter after the addition of 5 ml UniverSol ES scintillation cocktail. Daily (24 hour) production was calculated as the difference of the average light and the dark readings, assuming 24,000 mg HCO_3 kg^{-1} concentration in seawater (Carrillo and Karl, 1999). Data was adjusted for the 1.05 preferential uptake rate of ^{12}C to ^{14}C and monitoring of time zero and dark values (always <5% sample values) assured no interference from bacterial incorporation. Detailed methodology can be found in Vernet et al. (2008) and Vernet and Smith (2007).

DISSOLVED INORGANIC NUTRIENTS

Water was collected into acid washed polypropylene containers for nutrient analysis at all light depths, and analyzed immediately after collection whenever possible. When necessary,

samples were refrigerated at 4°C for up to 4 hours or frozen at -20 to -80°C until processing, thawed in a warm water bath (40°C) and mixed thoroughly before analysis. Samples from 1995 to 1998, 2000 and 2002 to 2005 were processed using segmented flow analysis on an Alpkem Flow Solution IV system with Winflow/Softpac data collection software. Samples from 1999 and 2001 were analyzed at the University of California Santa Barbara Marine Science Institute's Analytical Facility, and from 2006-2007 on board using continuous flow analysis on Lachat QuickChem 8000 Flow Injection Nutrient Analyzers with Omnion data collection software. Nitrate plus nitrite and silicic acid were analyzed following the methods of Armstrong et al. (1967), and the phosphate analysis was a modification of the Bernhardt and Wilhelms (1967) methods.

MIXED LAYER DEPTH

From 1995 to 2006, the summer mixed layer depth (MLD) was calculated from the sigmaT measurements from the CTD, and calculated as the local maxima in the second derivative of the downcast density profile. For more information see Martinson and Iannuzzi (1998).

SEA ICE INDICES

Using satellite measurements of sea ice concentration from NASA's Scanning Multichannel Microware Radiometer (SMMR) and the Defense Meteorological Satellite Program's (DMSP) Special Sensor Microwave/Imager (SSM/I) and provided by the EOS Distributed Active Archive Center (DAAC) at the National Snow and Ice Data Center (Boulder, Colorado, http://nsidc.org), Stammerjohn et al. (2008) developed seasonal sea ice variability metrics. Used in this analysis is the index representing day of retreat (END15), which is defined as the year day (measured from March 15 to March 14 of the following year) within each grid point when the sea ice concentration decreased past 15% and "remained below that threshold for at least five consecutive days until the end of the sea ice year" (Stammerjohn et al., 2008). For example, a sea ice retreat year day of 280 (as typically seen in the northern slope region of the grid) indicates that the sea ice concentration stayed below 15% of solid for five consecutive days starting October 7; a year day of 370 translates to a sea ice retreat on January 5. Note that it is possible to have sea ice year days greater than 365 because March 15 translates to sea ice year day 75, and the ice year ends on 365 days later, on March 14 of the following calendar year, sea ice day 439. Sea ice indices were derived from the SMMR-SSM/I satellite polar stereographic 25 km by 25 km grid and remapped onto the Pal LTER grid to facilitate comparisons with biological data. Due to differences in timing of water column sampling and ice characteristic indexing, all sea ice / composition comparisons were done with phytoplankton variables lagged by one year (i.e., ice from 1997 impacts phytoplankton from January 1998).

PHYTOPLANKTON COMPOSITION

The following sections first describe methodologies that can be used for determination of phytoplankton composition, then continue in detail about the specific method employed in this study.

General Methodologies

Common methods for estimation of phytoplankton abundance and composition include microscopy (Garibotti et al., 2003b and 2005a; Gomi et al., 2007; Kang et al., 2001; Savidge et al., 1995; Varela et al., 2002, among others), flow cytometry (Smith et al., 2007; Dubreuil et al., 2003; DiTullio et al., 2003; Sosik and Olson, 2002, among others), genetic analysis (Wilmotte et al., 2002; Medlin et al., 2000 and 2006; Andersen et al., 1993; Countway and Caron, 2006; Suzuki et al., 2005, Massana et al., 2004) and several versions of methods that can be categorized as chemotaxonomic, e.g., groupings based on presence of chemical (pigment) markers. The later category includes the use of single or multiple pigment markers and multiple linear regression analysis to determine contribution by various groups to the total chl_a pool (Gieskes et al., 1988; Buma et al., 1990; Barlow et al., 1998 and 2002; van Leeuwe et al., 1998; Garibotti et al., 2003a; Prézelin et al., 2000 and 2004; Moline and Prézelin, 1996; Peekin, 1997, among others), the application of inverse methods to develop a least-squares solution to a matrix algorithm (Tarantola et al., 1987; Letelier et al., 1993, Andersen et al., 1996), as well as an iterative method of matrix factorization for determination of algal class abundance (Mackey et al., 1996; DiTullio et al., 2003; Jeffrey et al., 1999; Rodriguez et al., 2002; Wright and van den Enden, 2000; Wulff and Wängberg, 2004, among others).

Each method has both advantages and limitations. Used since the 1930's (Utermöhl, 1931), microscopy might be considered to be the most authoritative assessment of phytoplankton composition. However, its accuracy is dependent on preservation methods (Montagnes et al., 1994, Breteler, 1985), and on the skill and consistency of those doing the identification (Duarte et al., 1990), and although relatively inexpensive, sample processing is highly labor and time intensive. Additionally, uncertainty in calculation of cell volumes and subsequent conversion to biomass (C) can lead to inconsistent results (Mullen et al., 1966; Montagnes et al., 1994). Despite current advances in methodolgy (Olson and Sosik, 2007; Sosik and Olson, 2007; Eller et al., 2007) and the advantage of real-time enumeration and visualization, flow cytometry can also be cost prohibitive and identification is dependent primarily on cell size differentiation. Similarly, once a genome is mapped, polymerase chain reaction is a reliable and accurate means of identification to phylogenetic level (Iglesias-Rodríguez et al., 2006), but the use of these methods is time consuming, presently limited in scope and can be expensive.

There are also several weaknesses in the use of HPLC pigments for estimation of phytoplankton composition. Like microscopy, proper pigment preservation is critical; both heat and light cause rapid isomerization and decay. Additionally, pigment analysis does not reveal any information about cell size structure of a population. Of primary concern in any chemotaxonomic method is the complex distribution of pigments throughout varying taxa (Latasa et al., 2004; Stolte et al., 2000) and thus the ambiguity related to assigning pigments as group markers (Schlüter and Møhlenberg, 2003). Despite these challenges, pigment analysis provides high consistency between users and laboratories and low variability/high reproducibility (Hooker et al., 2005), requires less time

and labor than microscopy, and is a lower cost alternative to genetics analysis. With proper consideration given to expected distribution and assignment of markers, HPLC pigments and chemotaxonomy offer a viable, robust method for determination of phytoplankton composition and abundance.

Microscopy

In 1996, 1997 and 1999, water was sampled for quantitative microscopic analysis from the 50% light depth and preserved with 2% Lugol's iodine solution (Parsons et al., 1984). Following the Utermöhl (1958) method, phytoplankton was identified and counted using an Iroscope IS-PH inverted microscope. Cells were identified to the lowest possible taxonomic level, and reported as follows: diatoms, cryptophytes, *Phaeocystis antarctica*. (type 4 haptophyte), dinoflagellates and a group referred to as phytoflagellates which included all unidentified small spherical flagellated specimens (Garibotti et al., 2005a). Cell biovolumes were measured according to Hillebrand et al. (1999) and corrected for cell shrinkage due to sample fixation (Montagnes et al., 1994). Cell carbon (C) content was calculated using carbon-to-volume ratios from Montagnes and Franklin (2001) for diatoms and from Montagnes et al. (1994) for all other groups. See also Garibotti et al. (2003a)) for additional details and discussion regarding microscopic analysis.

CHEMTAX

Phytoplankton composition was determined using CHEMTAX (Mackey et al., 1996), a program that uses factor analysis and a steepest descent algorithm to determine the best fit to the data with a given input matrix of pigment ratios. Using an iterative process for a given input matrix, the software optimizes the pigment ratios for each group and applies the final ratio to the total chl_a in each sample to determine composition. For this work, the Microsoft Excel based CHEMTAX version 1.95, a beta version received directly from the CHEMTAX authors, was used. The data is output in terms of absolute amounts (μg L^{-1}) of chl_a attributed to each group, or as a relative amount (percentage) of the total chl_a in a sample; group distribution will be discussed using both output methods.

There are several factors that influence the accuracy of class estimation when using CHEMTAX. These issues, specifics of the software input parameters used in this study and a summary of the quality testing carried out are detailed in the following sections.

Initial Pigment Ratio Matrix

To accurately allocate chl_a to phytoplankton groups, CHEMTAX requires an input matrix containing the expected classes and initial ratios of pigments contained in those classes. The same start ratio was used in all years of this analysis. Specific issues addressed in the determination of this start matrix are discussed in the following sections.

Phytoplankton Groups

For this study, the 1996, 1997 and 1999 microscopy data sets (Garibotti et al., 2005a) provided the anticipated groupings, and were allocated as described in the microscopy section, with the "dinoflagellate" and "phytoflagellate" groups combined to form the derived "mixed flagellates" group. The chosen groups likely do not include all taxa present in the ecosystem of this area, but other studies completed in region confirm the consistent dominance of diatoms, cryptophytes, haptophytes, flagellates and prasinophytes (Prézelin et al., 2000, Savidge et al., 1995; Varela et al., 2002).

Pigment Ratios

The CHEMTAX method for determination of phytoplankton composition has been extensively used in the Southern Ocean, including East Antarctica (South West of Australia; Wright and van den Enden, 2000; Wright et al., 1996), the eastern Atlantic region (South of South Africa; Wulff and Wänberg, 2004), the Southern Pacific sector (South East of New Zealand; DiTullio et al., 2003) and in the Gerlache and Bransfield Straits along the Antarctic Peninsula (Rodriguez et al., 2002; hereafter referred to as RVZ02). Given the geographic proximity of their data set to the current study, and the similarity in included groups to those found in the Palmer LTER microscopy data sets, the start matrix from the RVZ02 work was used as the working base matrix for this study (Table 4a).

Of the listed matrices, RVZ02 also proved most tolerant to the modifications made to accommodate the reduced pigment suite available in this study (data not shown). For those pigments in the initial RVZ02 matrix but which were not routinely collected in this project, two options were considered: (1) associated chl_a from the non-measured pigment eliminated from the matrix, and (2) associated chl_a from the non-measured pigment attributed instead to the highest chl_a-contributing pigment that was measured. A comparison of the two methods showed reassignment of the missing pigment concentration gave results closer to results achieved by the original matrix. The initial pigment ratio matrix used in this study is listed in Table 4b; note that in this study region, type 4 haptophytes (hereafter "haptophytes") consist primarily of *Phaeocystis antarctica,* in both its single cell and colonial phases (Bidigare et al., 1996).

To address the concern that variation in irradiance can lead to changes in ratios even within the same region and within species (Mackey et al., 1998), the relationship between MLD and Z_{eu} (allowing for a 5 m total error in the estimation of either parameter) was examined and only 5.5% of the samples were found to have a MLD deeper than the Z_{eu} (Fig. 2). The existence of so few 1% samples being mixed up into higher, variable irradiance suggests there was minimal impact on the average pigment ratios within the cells. As a second check of potential irradiance impacts on cellular pigment content, the data for each year was analyzed as a whole, as well as broken into 1-10% and 25-100% light depth bins. There were no significant differences between the light bins in any output

matrix values (Fig. 3), confirming the appropriate use of the same initial ratio matrix for all depths analyzed.

Previous studies using multiple regression methods have improved chl_a association estimate with a binning of data based on chl_a biomass (Garibotti et al., 2003a). To see if similar division would improve this CHEMTAX analysis, data was processed for each year with chl_a <1 μg L^{-1}, 1-4 μg L^{-1} and >4 μg L^{-1} bins. Again, no significant differences in any of the output matrix values were found (Fig. 4), and data from all depths were analyzed together in this study.

CONFIGURATION PARAMETERS

CHEMTAX was run using the start matrix as described in the pigment ratios section, and data was binned by year to optimize the final matrix ratios applied to the data. Configuration parameters required by CHEMTAX were set as follows (see Mackey et al., 1997 for a complete explanation of each setting): ratio limits = 500 (allowed ratio (r) to vary from r/6 to 6r), weighting = bounded relative, weighting = 3 and weight bound = 30 (used to specify error distribution in the ratio matrix), iteration limit = 500 (maximum number of iterations), epsilon limit = 0.0001, initial step size = 10, step ratio = 1.3 (used to set size and amount by which it can change with each iteration), cutoff step = 1000 (limits size of iteration step), and elements varied = 7 (all pigments). All settings were individually modified by one order of magnitude in either direction but no significant change (data not shown) was seen in the output, and all final settings were left as set as described.

DATA PROCESSING AND ANALYSIS

Data handling was primarily done in Microsoft Excel 2003; additional plotting and statistics were carried out using Ocean Data View (Alfred-Wegner-Institute for Polar and Marine Research, http://odv.awe.de), Systat Version 12 (Systat Software, Inc., www.systat.com) and Matlab 2007b (Mathworks, Inc., www.mathworks.com). Specific data handling procedures are described in the following sections.

Climatologies and Anomalies

Spatial and temporal variability of all variables was calculated on a grid centered between grid lines at 100 km intervals and between grid stations at 40 km intervals (e.g., south-easternmost grid cell contains stations between the 150 line and the 250 lines, and stations between the -010 and 030 grid stations). Since the -010 to 030 station region of the 300 line falls in the area of Adelaide Island (Fig. 1b), the resulting grid contained 29 individual cells. Climatologies were produced by first calculating the arithmetic mean of all the values within a grid cell for a given year (in most grid cells n = 2), then calculating an 8-14% trimmed mean (minimum and maximum for each cell removed) of all the yearly averages within that cell. The trimmed mean was chosen as the most robust representation of the typical value in a cell given that the right skew of the super data was frequently due to a single high value. Median improvement of the G1 skewness coefficient of the raw data

before and after trimming was 40.1% (Zar, 1999). Comparison with climatologies calculated using the arithmetic mean, the median, and with a delta distribution correction (Aitchison, 1955; Pennington, 1983; Gilbert, 1987) showed the trimmed mean method to be the least sensitive to extreme outliers while being robust enough to capture true central tendency of the data.

Yearly anomalies were calculated as the difference between the climatology and the yearly averages. Anomalies were used instead of raw data as they allow small deviations from the mean to be more clearly articulated. Presented here are spatial maps of both climatologies and yearly anomalies, showing for each grid cell the mean and departure from that value for each year. In these maps, data was interpolated onto the grid in locations equidistant between nominal stations using a Gaussian weighting term. The interpolated data was then contoured onto the maps, which provides a clear presentation of the data without losing significant features.

Principle Components and Empirical Orthogonal Function Analysis

Further quantification and insight into the interannual variability and its spatial structure is obtained via principle components analysis (PCA, Martinson et al., 2008). The PCA approach is most effective when there are no gaps in the data, so a sample covariance matrix was estimated from the anomaly time series. This matrix quantifies how the data covary in space and time across the grid. From this matrix, the eigen, or empirical orthogonal function (EOF) structure was calculated, where lower order EOFs represent spatially coherent structures with temporally consistent shapes (Martinson and Iannuzzi, 2003). The variance in amplitude of the EOF shape over time is captured in the modes of the principle components (PCs), where the first (gravest) few modes of the PCs describe the largest amounts of variance in the data.

PC/EOF analysis is mathematical means of defining patterns that exist in often noisy, higher-dimensional space. Total anomaly in one location is described by the sum of all modes, but not all modes necessarily have physical meaning. If the modes do capture meaningful variance, they will behave according to the mechanisms responsible for that particular mode. Thus, individual modes can be higher than the value of an anomaly as other modes may be removing variance in that same location.

When needed, spatial data gaps within sampling years (due to either missed sampling due to weather, sample processing error etc.) were filled using a reduced-space optimal analysis (OA, Kaplan et al., 1997). Briefly, OA uses the dominant EOF's from the covariance matrix to provide an interpolant for the data across both space and time (see also Martinson and Iannuzzi, 2003; Martinson et al., 2008). In this way, missing data was interpolated (smoothed) using a data-adaptive method rather than a fixed mathematical function, which took into account how a particular grid cell had most consistently varied in time relative to other locations in the domain. To test the sensitivity of the interpolation, 10% of the observed data was removed and the OA repeated with this reduced data set for the absolute ($\mu g\ L^{-1}$ chl_a) 50% light depth. The Pearson product moment correlation

coefficient was calculated, and found to be a robust 0.92 ± 0.03. Note that these interpolated anomalies were used only in the PC portion of the two-variable comparisons; in all other work actual (non-interpolated) anomaly values were used.

Trend Analysis

Temporal trends within each grid cell were calculated using raw data anomalies. To minimize the influence of large values at the chronological ends of the data sets, data was fit with a robust linear regression, using an iteratively weighted least squares process with a Huber weighting (Ψ) function (tuning constant of 1.7) on the residuals. This method allows minimization of the coefficient estimates without shifting the curve toward outlying points, and has no impact on the curve fit when no outliers exist. Trend values are presented as the robust regression coefficient, R, (i.e., slope) within each data cell. Significance was defined as $Z > 1.96$ (at α 0.05), where $Z \approx R$ / standard error. Because it is unlikely to detect periodicity in a time series spanning only 13 years, the possibility of non-linear trends was not addressed.

Assemblages

To determine if consistent assemblages (ie. recurring patterns of one or more compositional groups or clusters) exist in either pigments or phytoplankton groups, three tests were performed. First, for each data set examined, principle components factor analysis was used, and loadings were examined to determine amount of variance explained. Second, cluster analyses using both K-means (3 groups) and hierarchical algorithms with Euclidean distance metrics and centroid linkages were performed. For these analyses the pigments input data set was the chl_a-normalized raw data (see Table 3 for pigments included) at the 50% light depth and for phytoplankton groups was the 50% light depth in both relative and absolute contribution terms. Finally, the hierarchical cluster analysis (Euclidean distance metrics with average linkages) was performed again on each year of relative (ie., chl_a-normalized) composition data.

Timing between presence of an assemblage and the time since ice retreat in that location was calculated as follows:

1. Average ice retreat for the coastal, shelf and slope regions was calculated from the climatologies (e.g., average retreat along the slope was on ice day 311).
2. Average anomalies for “very early” (> 2 standard deviations earlier than the mean), “early” (> 1 but < 2 standard deviations earlier than the mean), “average” (within one standard deviation of the mean), “late” (> 1 but < 2 standard deviations later than the mean), and “very late” (> 2 standard deviations later than the mean) were calculated (e.g., during a “late” year, sea ice retreated 19 days after the mean). Average retreat in each region for each year was categorized using the same nomenclature.
3. Average time (in ice days) of each of the time frames for each of the regions was calculated (e.g., late retreat in the slope region resulted in an average retreat sea ice day of 311 + 19 = 330)
4. Days between time of last ice presence and observation at each location under each time frame was calculated using the average mid-cruise date (in ice days) of 387, as the time of

observation (e.g., late retreat in the slope region translated to 387 – 330 = 57 days between presence of ice and observation of the assemblage).

5. Using assemblage maps (Figs. 48 and 49) to identify presence, time between observation of an assemblage in a region and last ice was tabulated and averaged (exponential transformation applied in cases of left skew).

Two Variable Comparisons

Evaluation of correlations between more than one variable, or between depths within one variable, included the following protocols. With the exception noted below, spatial correlations between climatologies of the two variables were calculated using Spearman rank correlation (R_S) to minimize the importance of the extreme outliers. Significance was determined at the $\alpha(2)_{0.05,29}$ critical value of 0.368 (Zar, 1999). For correlations between diatoms and primary production and between diatoms and sea ice retreat, non-linear models were fit with a robust estimator with a Huber weighting (Ψ) function (tuning constant of 1.7) on the residuals. Where applicable, correlations of yearly anomalies between variables were also calculated using Spearman rank correlation, and was done on non-interpolated data that was standardized by dividing the value of the anomaly by the standard deviation of that value (Z score or Wald statistic). Significance was evaluated using $\alpha(2)_{0.05}$ at the critical value appropriate for the number of years in the anomaly pair being examined (between 6 and 12 depending on grid cell). These are visualized by (1) a heterogeneous correlation map of the entire grid (one value per grid cell per variable) showing the Spearman correlation coefficient, and/or (2) on a grid-cell by grid-cell basis, showing the relationship between the anomalies over time within a single cell. Average spatial correlation can differ from grid cell correlation; the former shows what can be expected in general across the study region and the later reveals more localized patterns or processes that whose mechanism may be different than those driving the average. Finally, to evaluate processes that might be impacting the anomalies in paired variables, Spearman rank correlation between the gravest PC's was calculated. In all cases negative correlation coefficients indicate patterns in the variables (or PCs) that move in opposite directions; positive coefficients reflect patterns moving in phase with one another.

RESULTS

Presented first is a summary of the comparison of phytoplankton composition between microscopy and CHEMTAX for 1996, 1997 and 1999. Following that, results for each of the main phytoplankton groups are presented in both absolute and relative amounts of chl_a attributed to a group and at both the 50% and 1% light depths. Relative contributions are viewed in terms relative to themselves spatially in the grid, as well as relative to other groups in both space and time. A descriptive summary highlighting important features of each group and year can be found in Tables 5 and 6. Finally, year to year assemblages are described and factors used to the relationships between groups and assemblages and their surrounding ecosystem are reviewed.

Results and discussion of the study follow the general convention of "northern" as the 600 and 500 lines, "central" or "mid" as the 400 and 300 lines, and "southern" as the 200 lines of the Pal LTER grid. It is recognized that theses designations do not adhere to strict magnetic directionality; the sampling grid is set up not along a true north-south axis but rather parallel to the peninsula and so is oriented on a northeast to southwest axis.

MICROSCOPY VS CHEMTAX

Direct comparison of biomass data between phytoplankton groups using microscopy and the CHEMTAX methods showed consistently significant correlation between methods for diatoms and cryptophytes. The strongest correlation was seen in the 1999 data for the cryptophytes (R^2 = 0.90, m = 0.77). Correlation between methods was lower and less consistent between years for prasinophytes and mixed flagellates. Haptophytes were recorded much less often using microscopy than was found by CHEMTAX; in 1999 haptophytes were documented at only one station using microscopic methods, where CHEMTAX indicated haptophytes relative concentrations of 10% or higher at 37 of 61 stations. Data is summarized in Table 7; plots of raw data vs CHEMTAX results are contained in Appendix D.

SPATIAL DISTRIBUTIONS (CLIMATOLOGIES)

Typical spatial variance of phytoplankton composition and variables representing the possible physical parameters acting as mechanisms and those that might be influenced by the composition can be assessed by examining the climatological maps. Results for composition are organized by light depths, in order of decreasing contribution to biomass.

Physical and Biological Parameters

Climatologies of sea ice retreat, primary production, mixed layer depth, dissolved inorganic nitrate+nitrite, silicate and phosphate are shown in Figure 5. All the variables showed general

onshore to offshore gradients, easily described using the slope, shelf and coastal province designations. Year day of sea ice retreat generally increased offshore to onshore, with earliest retreat typically seen in late October (year day 297) in the northern, offshore stations and latest retreat along the northern coastal area around early February (year day 402). Rates of primary production showed a similar pattern, with average slope production nearly an order of magnitude lower than seen on average along the coast. The average depth of the summer mixed layer varied from as shallow as 7 m in the northern coastal regions to as deep as 45 m along the slope. It too followed a general onshore-offshore gradient where slope regions had deeper mixed layers, with the exception of Marguerite Bay whose average summer MLD resembled more the shelf and slope regions than the northern coastal ones. The three primary macronutrients measured in this study on average remained above what is considered to be limiting to phytoplankton growth (>10μM L^{-1} Nitrate (Holm-Hansen and Mitchell, 1991), >30 μM L^{-1} Silicate (Knox, 2007) and > 1.0 μM L^{-1} Phosphate (Hartmann, 1997).

Composition, 50% $E_{(0,PAR)}$

On average between January 1995 and January 2007, up to 0.96 μg $_{[chl\_aD]}$ L^{-1} could be attributed to diatoms in coastal surface waters of the grid (Fig. 6). A distinct decrease in diatom biomass occured in both shelf and slope regions, where amounts of diatoms were typically between 0.05 and 0.39 μg $_{[chl\_aD]}$ L^{-1} (shelf and slope, respectively). The high inshore abundance was consistent along the North-South gradient with the exception of the inside of the 500 line where diatom biomass typically remained 0.24 μg $_{[chl\_aD]}$ L^{-1}. Relative to other phytoplankton groups, diatoms were most abundant in both coastal and slope regions of the grid, and less so in the shelf region (Fig. 7). Coastal and shelf populations on average were between 37 and 55%; diatoms on the shelf typically were between only 22 and 41% of the total (pigmented) population biomass. This general distribution was maintained along the north-south gradient, with the highest shelf relative abundances occurring along the 300 line.

Cryptophytes showed a different spatial pattern of distribution, with average absolute biomass greater than 0.27 μg $_{[chl\_aC]}$ L^{-1} occurring consistently only in the northern, inshore portion of the grid (Fig. 6). The rest of the Palmer LTER area typically had only between 0.01 and 0.26 μg $_{[chl\_aC]}$ L^{-1}. In relative terms though, cryptophytes consistently contributed only 3 to 12% in the slope regions, 34% in the Southern, shelf area but typically 34-62% in the northern, inshore region (Fig. 7).

Though contributing less to total surface biomass than either the diatoms or cyryptophytes, the mixed flagellates group was most abundant along the length of the shelf and in the southern coastal region, typically contributing between 0.12 and 0.18 μg $_{[chl\_aH]}$ L^{-1} in those areas (Fig. 6). Those concentrations equate to between 12 and 28% of the total population on the shelf, slope and southern coastal areas (Fig. 7). Mixed flagellates averaged only 4 to 7% of the total population in the central and northern coastal regions.

Nearly an order of magnitude lower in concentration than the most abundant groups, the haptophytes made their highest contribution to total biomass at between 0.05 and 0.07 μg $_{[chl\_aH]}$ L^{-1} along the length of the shelf region (Fig. 6). Slope concentrations were lower than shelf and coast areas but still typically contributed 0.03 μg $_{[chl\_aH]}$ L^{-1}. The relative spatial distribution of the haptophytes revealed a different pattern however, with typical average contribution to the total population highest in slope waters and a consistent decreasing gradient heading toward coastal waters (Fig. 7). Haptophytes typically constituted 18 to 23% of the population of the slope waters, 10 to 16% along the length of the shelf and only 4 to 10% along the coast.

Of the groups predicted to exist in PAL wAP waters, prasinophytes contributed the least to both total and relative biomass. In absolute terms, they are highest in northern coastal waters, where the average concentration is just under 0.04 μg $_{[chl\_aP]}$ L^{-1}. Elsewhere on the grid, levels were typically less than 0.01 μg $_{[chl\_aP]}$ L^{-1} (Fig. 6). These low concentrations equate to an average population contribution of no more than 3.7%, seen across all of the northern part of the grid, and in one area on the inside of the 500 line (Fig. 7).

Composition, 1% $E_{(0,PAR)}$

Similar to surface waters, highest contribution to total biomass at the bottom of the Z_{eu} was by the diatoms. Highest overall levels were regularly seen on the inside of the 400 and 200 lines, at 0.53 and 0.37 μg $_{[chl\_aD]}$ L^{-1}, with the remainder of the grid on average at 0.13 μg $_{[chl\_aD]}$ L^{-1} (Fig. 8). These concentrations equate to a high relative presence throughout the entire grid, with average contributions of 31 to 60% of the total biomass (Fig. 9).

Differing slightly from the pattern in the surface waters, the next most abundant group at depth was the mixed flagellates. In absolute concentrations they were typically found at highest levels at the break between the coastal region and the shelf, along the 400 and 500 lines (Fig. 8). Here, their concentrations were between 0.10 and 0.18 μg $_{[chl\_aMF]}$ L^{-1}; elsewhere in the grid they averaged only slightly lower at 0.06 μg $_{[chl\_aMF]}$ L^{-1}. These values represent on average 25% of the population across the entire grid (Fig. 9).

The next most abundant group in the deep Z_{eu} was the cryptophytes. Their abundance was highest in the northern coastal and shelf area, averaging there 0.06 to 0.13 μg $_{[chl\_aC]}$ L^{-1} (Fig. 8c). Throughout the rest of the grid their concentrations were lower, averaging only 0.01 μg $_{[chl\_aC]}$ L^{-1} (Fig. 8). Where cryptophyte biomass was high, their contribution to the total population was on average 12 to 17%, but elsewhere concentrations equated to an average of only 1 to 8% (Fig. 9).

Haptophyte dominance in absolute terms showed a slightly different spatial pattern than the rest of the phytoplankton groups in the deep waters. Their biomass was usually highest in the southern, offshore (far shelf and slope) region; levels there on average were between 0.04 and 0.05 μg $_{[chl\_aH]}$ L^{-1}. Elsewhere on the grid haptophyte biomass was typically slightly lower, between 0.01 and 0.03 μg $_{[chl\_aH]}$ L^{-1} (Fig. 8). These concentrations equate to a consistent relative population

distribution of 11 to 19% on the slope, 8 to 12% on the shelf and 7 to 10% in coastal areas through the length of the grid (Fig. 9).

Again the lowest total contributor to chl_a biomass, prasinophytes were most abundant in the northern, coastal waters of the PAL grid. Concentrations there averaged under 0.03 $\mu g_{[chl\_aP]} L^{-1}$ and dropped to between 0.01 and 0.02 $\mu g_{[chl\_aP]} L^{-1}$ (Fig. 8). Prasinophytes on average thus contributed between only 3 and 11% of the total phytoplankton population throughout the grid (Fig. 9).

TEMPORAL VARIABILITY (ANOMALIES)

How each group differed from the average (climatological) pattern is displayed in the anomaly plots. For each year, the climatology for a grid cell was subtracted from the measured mean for that cell, and these uninterpolated results are presented. For the primary phytoplankton groups, results are described in both absolute and relative terms at both depths sampled.

Physical and Biological Parameters

Timing of sea ice retreat along the Pal LTER grid varied by as much as 59 days from the mean in either direction. Impacting nearly the whole grid, large early anomalies occurred in the 1998-1999 (affecting the phytoplankton in January of 1999) and 2006-2007 (affecting January 2007) sea ice seasons, when the overall grid averages were 29 and 21 (respectively) days earlier than average. Late retreats occurred in the 2004-2005 (impacting January 2005) and 2005-2006 (impacting January 2006) sea ice seasons, with grid averages 31 and 15 (respectively) days later than average. Localized anomalies were also seen; retreat was earlier than usual in the northern coastal regions which impacted 2001. Retreat was later than usual along the northern coast affecting January of 1996, and later than average in the southern slope region influencing January of 2004.

The range of primary production in any given year and location varied by as much as two times below the value of the climatology, and as much as five times above. Such notable deviations from the mean occurred in 1999 along the central coast (low production), in 2002 in the southern coast region (Marguerite Bay, high production) and across nearly the entire grid in 2006 (very high production).

The depth of the summer mixed layer varied greatly year to year as well as location to location along the grid. Years where the anomalies were seen across nearly the entire grid were 1995 (as much as 44 m deeper than the mean with a grid average 13 m deeper), 2005 and 2006 (as much as 29 m and 23 m shallower than the mean with grid averages 8 m and 10 m shallower, respectively). Localized high anomalies were seen off of Renaud Island in 1999 and off of Adelaide Island in 2002 and 2003. Negative MLD anomalies were seen in the southern coastal region in 1997 and 2000, and in the central and north shelf areas in 1996 and 2003.

Relative to the mean values, nutrient anomalies generally did not vary as greatly year to year, with regional variations being more common than across-grid highs or lows. Low nitrogen anomalies were seen off of Anvers Island in 1996 and 2002, in the southern coastal region (Marguerite Bay) in

2002, off of Renaud and Adelaide Islands and along the southern shelf in 2006 and across nearly all the grid in 2007. Low silicate anomalies were seen along the shelf in 1998 and 1999, along the coast in 1999, across the northern portion of the grid in 2001 and 2002, and offshore in 2007. Phosphate had no major deviations from the mean. It is important to note that in only very few cases in any of the years were limiting levels of either Nitrogen or Silicate seen.

Composition, 50% $E_{(0,PAR)}$

As absolute concentration, diatoms occurred at anomalously high levels in two years of the study; regions of particularly high concentration occurred in the northern, inshore region in 1996 and shelf and inshore areas of the central and southern region of the grid in 2006 (Fig. 10). 1995, 2000 and 2007 also had positive average anomaly values (0.21, 0.26 and 0.07 $\mu g_{[chl\_aD]} L^{-1}$), with highest positive anomaly values generally located along coastal and shelf regions. Although the grid average was just slightly lower than average, diatoms in 2005 were also higher than normal in central and southern coastal regions (anomaly values >0 average: 0.36 $\mu g_{[chl\_aD]} L^{-1}$). The remaining years of the study were as a whole lower than average, but concentrations across the grid on those years were only 0.01 to 0.23 $\mu g_{[chl\_aD]} L^{-1}$ lower than typical. These values equate to considerable variance year to year in relative diatom contribution to the population, with high years being up to 80% higher than typical and low years up to 50% lower (Fig. 11).

Surface cryptophytes showed anomalously high levels in five years of the study: 1995, 1996, 1999, 2000 and 2005 (Fig. 12). In those years, highest concentrations of cryptophytes occurred on either the shelf area (1995, 1996, 2005), or along the coast (1999, 2000). Average grid cryptophyte concentrations ranged from 0.18 to 0.46 $\mu g_{[chl\_aC]} L^{-1}$ higher than usual, with high values ranging from 1.8 to 4.7 $\mu g_{[chl\_aC]} L^{-1}$ above average. Years 1997, 2003 and 2007 can be considered “average” cryptophyte years at the surface, where anomalies were near zero throughout the grid. Low cryptophyte concentrations were seen in 1998, 2001, 2004 and 2006; average grid concentrations in those years were between 0.11 and 0.14 $\mu g_{[chl\_aC]} L^{-1}$ lower than typical, and minimum observed concentrations were as low as 0.74 $\mu g_{[chl\_aC]} L^{-1}$ below average. These cryptophyte concentrations translate to only a slightly smaller relative range of variance than those of the surface diatoms. Yearly anomaly values ranged from extremes of 62% below (2006 inshore north) to 77% higher (1995 northern shelf) than average (Fig. 13). Average yearly grid values ranged between 20% below and 33% above the climatological concentrations of cryptophytes.

The next most populous phytoplankton group on average was the mixed flagellates. During most years (1998, 1999, 2000, 2003, 2005), when averaged across the entire grid, the surface mixed flagellate population remained very close to its average value (Fig. 14). In 1995, 1996 and 2006 slightly higher than average concentrations occurred in selected gridcells along the coastal and shelf areas (maximum concentrations 0.55, 0.56 and 0.63 $\mu g_{[chl\_aMF]} L^{-1}$ higher than normal, respectively). Note that in 1995 however, other than those selected high grid cells, the remainder of the grid experienced average to lower than normal concentrations of mixed flagellates. On the other hand,

2001 was an extremely high year for mixed flagellates throughout nearly the entire grid; concentrations as high as 2.29 μg $_{[chl\_aMF]}$ L^{-1} above average were measured in the northern coastal area and the overall grid average was 0.50 μg $_{[chl\_aMF]}$ L^{-1} higher than usually seen. These concentrations translate to extreme relative values of 85% higher than average in 2001, 23 to 67% higher than normal in 1995, 1996, 2003 and 2005, 35 to 62% lower than average in 1997, 1998, 1999, 2000, 2004 and 2007 (Fig. 15). On average across the entire grid however, other than 2001 which was 52% higher than normal, annual anomalies varied no more than 12% in either direction.

Absolute values of haptophyte concentrations varied the least of the four major phytoplankton groups. Four years had both specifically high locations on the grid and overall averages greater than one standard deviation larger than the average: 1999, 2003, 2006 and 2007 (Fig. 16). Spatially, high concentrations were seen throughout the grid; some years the high haptophyte biomass was in coastal and slope regions (2007) and in others, highest concentrations were seen on the shelf (2003, 2006). In the two highest years of haptophytes, concentrations were estimated to be over 0.40 μg $_{[chl\_aH]}$ L^{-1} higher than the mean. Remaining years of the study can be considered average (typical) years, where the variance was never exceeded 0.13 μg $_{[chl\_aH]}$ L^{-1} in either direction and was on average across the entire grid no greater than 0.02 μg $_{[chl\_aH]}$ L^{-1} larger or smaller than usual. For years described as having high concentrations of haptophytes, local maxima were seen as high as 37% greater than normal in 1999 (slope), 41% in 2003 (shelf), 29% (shelf) in 2004 and 49% (slope) in 2007 (Fig. 17). Typical and low haptophyte years ranged from extremes of 22% higher than average in 1998 (5% higher than average across the entire grid), to 21% lower than average in 2000 (8% lower than usual when averaged across the grid).

Finally, although they had the lowest absolute climatological concentrations, yearly variance of prasinophytes was higher than that of haptophytes (Fig. 18). Absolute biomass measurements indicate that 1996 was a higher than average year for prasinophytes in the mid and northern coastal and northern shelf regions, with concentrations as high as 0.69 μg $_{[chl\_aP]}$ L^{-1} above average. Elsewhere in the grid in 1996, prasinophyte concentrations remained at usual levels. Two years, 2006 and 2007, also had small portions of the grid that were extremely high; blooms both years were in the mid and South-coastal area of the grid, with concentrations reaching 3.38 μg $_{[chl\_aP]}$ L^{-1} and 1.86 μg $_{[chl\_aP]}$ L^{-1} above average, respectively. Unlike 1996 however, both 2006 and 2007 had slightly lower than typical concentrations in non-bloom locations on the grid. Also slightly higher than average, 2001 did not have the extreme concentrations seen in 1996, 2006 and 2007. On the other end of the range, 1997, 1998 and 2004 showed slightly lower than average concentrations in locations on the grid, with overall grid averages falling in all three years 0.01 μg $_{[chl\_aP]}$ L^{-1} lower than average. The remaining years can be considered “typical”, with a mix of average, slightly high and slightly lower than average concentrations throughout the study area and overall grid averages never varying more than 0.004 μg $_{[chl\_aP]}$ L^{-1} from the mean. The relative concentrations of prasinophytes in the population followed a slightly different yearly pattern than the absolute values (Fig. 19). As

expected, regions of high absolute concentration in 2006 and 2007 equate to higher than average relative concentrations (up to 43% higher than typical), but not only did 1996 have relatively high concentration, so too did 2001, 2003 and 2004. Those years had regions as high as 18% (1996, 2001), 24% (2003) and 13% (2004) above normal, and those high regions were located primarily on the shelf and along the coast in 1996, on the shelf in 2001, throughout the grid in 2003 and along the shelf and slope in 2004. The only year that was consistently below average throughout the grid was 1998, with an overall grid average 2% and a maximum of 3% lower than usual. Although typical in concentration of prasinophytes, 1995, 2000 and 2005 had both slightly lower and slightly higher than normal regions of prasinophyte contribution, and overall grid averages in those years remained 1% lower than average. Both 1997 and 1999 also had regions of high and low contribution, but in those years, overall grid averages remained less than 1% different than normal.

Composition, 1% $E_{(0,PAR)}$

At the bottom of the Z_{eu}, yearly variability in diatom concentration generally followed the pattern of the surface concentrations (Fig. 20). High years include 1995, 1996 and 2006, with the latter two having extreme high anomalies at as much as 6.75 and 10.67 μg $_{[chl\_aD]}$ L^{-1} higher than average. Years with the most extreme lows were 1997, 2001, 2003 and 2004, where overall grid averages were between 0.08 and 0.13 μg $_{[chl\_aD]}$ L^{-1} lower than average, and coastal regions reached minimums of between 0.38 and 0.51 μg $_{[chl\_aD]}$ L^{-1} lower than average. Localities of both highs and lows across the entire grid were seen in 1999, 2000 and 2007; these years' average grid values were no more than 0.10 μg $_{[chl\_aD]}$ L^{-1} higher than normal and were very close to "typical" levels at this depth. Relative contribution of diatoms to the population revealed a slightly different variability than seen by the absolute concentrations (Fig. 21). Here, 1995, 1996, 1998, 1999, 2000, 2006 and 2007 all had regions between 41% and 61% higher than average, and although patchy, those high anomalies were spread spatially throughout the grid. Years where the grid was dominated by lower than average diatom contribution are 2001 and 2003, with overall grid averages varying by as much as 23% below typical and extremes as low as 60% below average. The remaining study years, 1997, 2004 and 2005 showed the least variability and diatom contribution can be considered to be very close to typical years.

Variation in cryptophyte concentration at 1% light depth also generally followed that of the surface values (Fig. 22). Years of high anomalies were 1995 (maximum of 2.11 μg $_{[chl\_aC]}$ L^{-1} above average along the 500 line shelf), 2003 and 2005 (maxima of 0.75 and 0.95 μg $_{[chl\_aC]}$ L^{-1} respectively, in coastal areas). Slightly higher than average concentrations of diatoms occurred in 1996, but the overall grid average was still only 0.02 μg $_{[chl\_aC]}$ L^{-1} higher than the mean. Two years had lower than expected from the climatology; in 1998 and 2004, only a single grid cell in each year had values slightly higher than the average. The remaining years of the study, 1997, 1999, 2000, 2001, 2006 and 2007 had no cryptophyte anomalies greater than 0.11 μg $_{[chl\_aC]}$ L^{-1}. In terms of relative contribution to the phytoplankton population at the bottom of the Z_{eu}, the absolute values translate to

similar patterns of variability (Fig. 23). High years were 1995, 2003 and 2005, where extremes reached 88%, 89% and 47% higher than average, respectively. Spatially, the extreme highs occurred along the northern shelf, and along the mid-shelf and southern coastal regions. Low cryptophyte contribution anomalies of as much as 10 to 17% below average were seen throughout nearly the entire sample region in 1998, 2001, 2004, 2006 and 2007. Years that were close to average were 1996, 1997, 1999 and 2000, where grid averages varied by no more than 1% from average.

Like at the 50% light depth, mixed flagellate concentration at 1% light depth was anomalously high in 2001 (Fig. 24). Spatial extent of this variance was smaller, expressed in deep water only in the inshore area of the 600 line, but was actually greater in terms of concentration – levels as high as 3.74 $\mu g_{[chl\_aMF]} L^{-1}$ above average were measured there. 1995, 1996 and 2006 also had higher than typical amounts of mixed flagellates, but in those years overall grid means were no more than 0.09 $\mu g_{[chl\_aMF]} L^{-1}$ above average and maxima were not measured any higher than 0.33 $\mu g_{[chl\_aMF]} L^{-1}$ higher than average. Lower than normal concentrations were seen 1998, 2000, 2003, 2004 and 2007, but even the most extreme lows were only 0.17 $\mu g_{[chl\_aMF]} L^{-1}$ below normal. Very close to average concentrations of mixed flagellates were seen in these low light depths 1997, 1999 and 2005. These absolute values translate to relative population contribution showing slightly different patterns (Fig. 25). As expected, 2001 mixed flagellates contributed much more than average across nearly the whole grid. Levels were as high as 80% above normal, and the overall grid average was 46% higher than the mean. Higher than normal contribution by the mixed flagellates was also seen in the northern coastal region in 1998 (54% above average) and in the southern slope region in 2003 (56% above average). In 2003 however, the reminder of the grid was nearly 16% below average. Not quite as extreme and much less localized highs were observed in 1996, 1997, 1999 and 2005. In these years, overall grid averages ranged from 5 to 18% above average, with localized highs spread throughout the grid. Despite having some areas higher than average, 1995, 2000, 2006 and 2007 had overall averages between 4 and 13% below the mean. Finally, mixed flagellate levels were lower than normal in all but one grid cell in 2004, with a local minimum of 24% below normal and an overall grid average of 11% below average.

Like their surface counterparts, the highest concentrations of deep Z_{eu} haptophytes occurred in 2006 and 2007 (Fig. 26). In those years, localized highs primarily along the mid and southern shelf and slope reached 1.02 and 0.62 $\mu g_{[chl\_aH]} L^{-1}$ above the mean, and grid averages were 0.6 and 0.8 $\mu g_{[chl\_aH]} L^{-1}$ (respectively) higher than normal. At these depths 1995 and 1996 were also slightly higher than average; localized extremes reached 0.09 and 0.10 $\mu g_{[chl\_aH]} L^{-1}$ those years and grid averages were also above normal by as much as 0.03 $\mu g_{[chl\_aH]} L^{-1}$. Lowest absolute concentrations occurred in 2001 and 2004, where nearly every cell across the grid was lower than average in both years, and grid averages were between 0.02 and 0.03 $\mu g_{[chl\_aH]} L^{-1}$ below the mean. The remaining years, 1997, 1998, 1999, 2000, 2003 and 2005 all had regions of highs and lows, but overall grid averages remained close to average, varying no more than 0.01 $\mu g_{[chl\_aH]} L^{-1}$ from the mean. The

contribution of haptophytes to the total population exhibits yet another spatial pattern (Fig. 27). The high concentrations in 2006 and 2007 translate to localized high (42 to 70% above average) contribution to phytoplankton population, particularly in the slope regions. Despite low biomass, haptophytes contributed to the overall phytoplankton community by as much as 37% over normal and on average 12% above normal in 2004, with those high values spread across nearly all grid cells. Localized high anomalies (as much as 36% and 19% respectively) occurred in 1998 and 2003, yet enough of the grid had average to low anomalies which lead to overall grid averages of less than 1 and just 3% above normal. Conversely, low values in 2001 translated to low relative contributions of haptophytes in 2001 (as much as 18% below normal and a grid average of 11% lower than usual), but the nearly-average biomass observed in 2000 also translates to lower than average contribution to the population (as much as 11% lower in the southern region and 4% lower on average). Again the remaining years (1996, 1997, 1999 and 2005) had both high and low anomalies but none varied more than 16% in either direction from the mean.

At the 1% light depth, prasinophytes both contributed the least in terms of biomass and also had the smallest absolute range of variance (Fig. 28). Highest localized anomalies were seen in 1996, where concentration reached 0.37 $\mu g_{[chl\_aP]} L^{-1}$ above average in the northern coastal area. Despite that extreme, the overall grid average that year remained at only 0.3 $\mu g_{[chl\_aP]} L^{-1}$ above normal, with other higher than average grid cells located along the slope and shelf regions. Other localized highs were observed in 2000, 2001 and 2006 (maximum anomalies 0.14, 0.15 and 0.10 $\mu g_{[chl\_aP]} L^{-1}$, respectively), and similar to 1996, overall grid averages remained between only 0.01 and 0.02 $\mu g_{[chl\_aP]} L^{-1}$ higher than normal. The remaining years all had various slightly low, average and slightly positive anomalies in various locations and strengths. Low extremes were no greater than 0.03 $\mu g_{[chl\_aP]} L^{-1}$ below average, high extremes of these “intermediate” years were no greater than 0.05 $\mu g_{[chl\_aP]} L^{-1}$, and overall grid averages ranged only from -0.01 to 0.01 $\mu g_{[chl\_aP]} L^{-1}$ from the mean. Anomalies of the relative prasinophyte contribution at the 1% light depth showed a different temporal pattern than did the absolute concentration anomalies (Fig. 29). High anomalies were observed across nearly the entire sampling grid in 1997, 2004, and 2005, with local extremes ranging from 13% higher than normal in 1997 and 2005 to 27% above normal in 2004. Absolute concentrations translated to high localized extremes again in 2000, 2001 and 2006 (maximum anomaly values 0.22, 0.19 and 0.29 respectively), but in those years the majority of the grid was below average, leading to overall grid average anomalies of not more than 1%. The most extreme low anomalies were seen in 1995 (-7%), 1999 (-11%) , 2003 (-7%) and 2007 (-9%), and were mixed with small areas of close to or just above average prasinophyte contribution leading overall grid contributions to vary no more than 3% below average.

LIGHT DEPTH STRATIFICATION

Using Spearman rank correlation, the relationship between composition at the 50% and 1% light depths was evaluated. Comparisons of climatologies for the phytoplankton groups in terms of absolute concentration to biomass show a significant positive correlation between the two depths in all groups except the haptophytes. Relative abundance in the surface waters and deep Z_{eu} waters was positively related in only the cryptophytes, diatoms and haptophytes. Details of the correlations are shown in Figure 30 (top panels).

These significant relationships weakened somewhat when the yearly anomaly values were compared, but despite lack of statistical significance, consistent patterns did develop across the grid for most phytoplankton groups. In terms of absolute concentration of chl_a associated with the group, diatoms, mixed flagellates and haptophytes had strong positive correlation between the two depths across much of the grid (details of the correlations and significance for all groups are shown in Fig. 31, top panels). Although only 4 of 29 grid cells were significantly correlated, the absolute concentrations of prasinophytes also showed a generally positive correlation in the northern coastal region of the grid. Despite strong climatological correlation, the group with the weakest correlation between anomaly concentration at the surface and at the bottom of the Z_{eu} was the cryptophytes. Significant positive correlation occurs in the northernmost coastal grid cell only with the remainder of the grid showing close to no correlation throughout.

The climatological correlations of the relative contributions differed slightly from those of the absolute concentrations. Significant positive correlations existed between the surface and the deep Z_{eu} in the diatoms, cryptophytes and haptophytes. The relationship remained positive but was not statistically significant for the mixed flagellate group and the prasinophytes. Specifics of the correlations are shown in Figure 30 (bottom panels).

Correlations between the anomalies of the two depths for relative contribution followed similar patterns to those seen for the anomalies of the absolute concentrations in all groups except the mixed flagellates (details of the correlations and significance for all groups are shown in Fig. 31, bottom panels). Strong positive correlations were again seen throughout nearly all the grid in the diatoms and haptophytes; visualization of the temporal correlations of both relative and absolute haptophyte correlations are shown in Figure 32. Significance was lost in the northern coastal region for the prasinophytes, but the pattern of increased correlation in the central coastal, mid slope and southern shelf regions were maintained. Similar to the anomalies for the absolute concentrations, the relative contributions of cryptophytes between the two depths sampled were correlated only in localized grid cells in the northern portion of the grid. Finally, the mixed flagellate relative contribution anomalies were nearly opposite to those of the absolute concentrations. No correlation between depths was seen through most of the grid, and the only significant relationships were negative in sign and located in the northern outer shelf and slope region.

TRENDS

No consistent, significant trends across time were detected across the grid in any major phytoplankton group at either depth during the course of this study. However, though not always statistically significant given the relatively high error associated with the anomaly measurement, certain patterns do appear to repeat themselves and are worth consideration

At both light depths, and in both absolute concentration and relative contribution, diatoms showed no consistent statistical trend in any region of the grid, but there is some indication of a decreasing trend in the inner 600 line (Fig. 33). Cryptophytes however did not appear to be "replacing" the diatoms, as no increasing trends are measurable in that location. To the contrary, a general neutral (ie. m = 0) to negative trend (non-significant) can be seen for the cryptophytes at all depths in both absolute and relative terms (Fig. 34).

Similarly, a general, non-significant neutral to decreasing trend pattern was observed for the mixed flagellates (Fig. 35). Haptophytes may be moving in the opposite direction however, with some consistent (still non-significant) positive trends seen throughout the mid and southern portions of the grid, particularly in the shelf and slope regions (Fig. 36). Finally, the prasinophytes showed no consistent, discernable trend during the study period, with only inconsistent changes in slope in individual grid cells at each depth and output type (Fig. 37).

To evaluate if any of the observed patterns in an individual group were merely reflective of changes in total biomass in the water, trends of chl_a were also examined (Fig. 38). No significant consistent spatial or temporal patterns were observed at either the 50% or 1% light depths.

PRINCIPLE COMPONENTS ANALYSIS

Principle components analysis results are presented for the absolute concentration of the 50% light depth. For diatoms, 88.4% of the variance was explained in the first two modes, with the largest variance observed 1996, 2000 and 2006 in PC1 and again in 1996 and 2006 in PC2 (Fig. 39). Although the first two PC's both expressed themselves in 1996 and 2006, PC2 acted in the same direction as PC1 in the North coastal region in 1996 and in the central coastal region in 2006, but removed some variance from the central coastal area in 1996 and from the North coastal area in 2006. Despite this seeming contradiction, the additive sign for the covariance in these regions remained positive. Also picked up in PC2 was some of the positive anomaly in the Southern coastal region in 2006.

For the cryptophytes, 84.9% of the total variance was explained in the first three modes of the PCs, with the EOF's (spatial expression) of these modes primarily occurring in the shelf region of the 500 line (Fig. 40). Primary years where these modes were expressed were 1995, 1999 and 2005.

90.5% of the variance in the absolute concentration of the mixed flagellate group was explained in the first two modes of the PCs (Fig. 41). Expression of PC1 was seen to a major extent in 2000, and less so in 1996, 1999 and 2006, all in the same direction and in a region in the northern

region along the break between the coastal and shelf region. Unlike mode one, mode two of the mixed flagellates was expressed in different directions in different years. Regions impacted were the southern coastal and shelf, and northern coastal/nearshore shelf areas.

For the haptophytes, the first two modes combined explained 70.9% of the total variance (Fig. 42). Mode one was primarily expressed positively in 2006 along the shelf region of the 200 and 300 lines. Mode 2 was also expressed in high haptophytes concentration in 1999, 2003 and 2007 primarily in the inside of the 300 line.

The first two modes of the prasinophytes accounted for 95.4% of their variance, with clear, positive concentrations in 2006 in the inside of the 400 line, 1996 and 2006 in the inside of the 300 line and again in 1996 in the inside of the 600 line (Fig. 43).

TWO-VARIABLE COMPARISONS

Significant correlations between primary production and abundance of diatoms at the 50% light depth were seen along the Pal LTER region of the wAP. On average, as diatom abundance increased, so too did the rate of primary production (Fig. 44a); the relationship is best fit not by a linear regression however. As diatom biomass increased beyond 0.6 $\mu g_{[chl\_a]}\ L^{-1}$, production rates hit a climatological maximum of just over 1200 mgC $m^{-2}\ d^{-1}$. The relationship was fit with a robust lognormal model, and the resulting correlation coefficient is significant at the $\alpha(2)_{0.05}$ critical value. The relationship of the anomalies across the grid is shown in Figure 44b, and also showed a pattern of significant positive correlation across nearly the entire grid. Following a similar pattern, the first modes of the PCA also correlated highly ($R^2 = 0.65$), with the high Z-scores of 1996 and 2006 mirroring each other in both variables (Fig. 44c).

Significant correlations between abundance of diatoms at the 50% light depth and the timing were also seen along the Pal LTER region of the wAP. The correlations of the climatologies of sea ice retreat showed an increase in diatom abundance as sea ice retreated later (Fig. 45a). The relationship was fit with a robust exponential model, and the resulting correlation coefficient is significant at the $\alpha(2)_{0.05}$ critical value, but there exists clear outliers where diatom abundance is higher than can be explained by timing of the sea ice retreat. Correlation of the anomalies also showed patterns of significant relationships (Fig. 45b). Along the length of the coastal region the two parameters were positively correlated, but this relationship weakened and eventually changed sign entirely so that in the central and north slope region high diatom abundance was actually correlated with early ice retreat. The first modes of the PCs of diatom abundance and sea ice retreat followed similar patterns, with high Z-Scores in 1996 and 2006, but the late ice of 2005 was picked up in this mode for the ice with no corresponding signal in mode one of the diatoms (Fig. 45c).

Correlations between presence of diatom and cryptophyte anomalies at the 50% light depth are illustrated in Figure 46. Across nearly all the grid, there was a strong, significant negative relationship between the two groups (Fig. 46a). Temporal correlation of specific grid cells are shown in Fig. 46b - d.

Finally the relationship between the ratio of diatoms to cryptophytes and mixed flagellates is shown in Figure 47. Note no significant correlations were found, though there is some indication of a negative relationship in the southern portion of the grid.

ASSEMBLAGES

Factor analysis of the pigment data at 50% revealed no unambiguous groupings. Factor analysis of the relative contribution to total chl_a biomass by the five main phytoplankton groups analyzed with the full twelve years of data as a whole, showed significant loading of diatoms and cryptophytes on factor one and mixed flagellates on factor two. Those two factors however account for 60.2% of the total variance. Comparing the climatologies of the diatoms to those of the cryptophytes (biomass at 50% for each), no significant correlation (Spearman rank) was found. To further illustrate the relationship between these two groups, anomalies across time for three grid cells were examined. Figure 46 shows the spatial anomaly correlation (a), with the majority of the grid cells exhibiting a negative correlation. Also shown are time series anomaly plots for four representative grid cells. Strong correlation typically exhibit either large anomalies of opposing signs (1995, 1996, 1999, 2004, 2006) or anomalies where both groups are very close to average (1997, 2003, 2005, 2007), as shown in grid cell 200.010 (Fig. 46e). The correlation weakened in locations where anomalies were observed in only one of the two groups (1995, 1999, 2003) as seen in grid cells 600.090 and 500.050 (Fig. 46b and c). No significant correlation was seen in locations where the anomalies actually tracked each other, particularly in grid cell 200.210 between 1995 and 2001 (Fig. 46d). A similar comparison was then done on the ratio of diatoms to cryptophytes and the mixed flagellates (factor two above) and though again the climatologies revealed no significant correlation ($R = -0.33$), the anomalies showed a general, qualitiative pattern of an inverse correlation in the south and no or slightly positive correlation in the north (Fig. 47).

Factor analysis was done using the absolute concentrations of each phytoplankton group to total chl_a, and results showed 68% of the variance explained in the first three factors, with prasinophytes loading on vector one, cryptophytes on vector two and the diatoms and mixed flagellates on vector three.

Cluster analysis of the same data sets showed no consistent spatial clusters occurring within the sampling grid over the course of time of the study. Cluster analysis of the data on a year-by-year basis however did reveal some temporally recurring assemblages whose geographic locations and patterns varied across the years of the study. A description of the most common assemblages, which years and in what region of the grid they were seen can be found in Table 8, and distribution plots of these assemblages in Figures 48 and 49.

Results from the analysis of the timing of the presence of an assemblage in a region and the time since ice was present in that area are shown in Figure 50. Average time between observation and sea ice presence for the diatoms > 90% assemblage was 9 days, and was statistically different than the timing for all other groups except cryptophytes > 50% and prasinophytes > 50%.

DISCUSSION

A brief consideration of findings and insights relating to the methods of determining phytoplankton composition is followed by a more detailed discussion of composition and its variability along the wAP. Possible forcing mechanisms, phytoplankton's role in the dynamics of the Antarctic ecosystem, and potential impacts of climate change on the system are then considered.

METHODOLOGICAL CONSIDERATIONS

The first goal of this study was to develop and apply a means of determining phytoplankton composition to the class level along the wAP. The samples analyzed included those from 12 cruises encompassing a span of 13 years, with an average of 366 samples collected per year at six different depths, across an 80,000 km^2 grid. The scope of the project required that the method used be efficient enough to process the large volume of samples, be flexible in order to accommodate potential physiological differences between sampling locations, yet be robust enough to tolerate some uncertainty in input parameters and provide realistic results with a low computational margin of error.

Several factors go into the decision of which method to employ when needing to determine compositional makeup of a water sample. As described in the methods section, two of the most commonly used techniques include microscopy and chemotaxonomic methods such as CHEMTAX. Though microscopic techniques can provide a detailed species-level inventory, the process is extremely time consuming and is particularly susceptible to errors introduced by preservation methodology (Menden-Deuer et al., 2001) and variability introduced by the skills and consistency of the analysts. CHEMTAX analysis of HPLC pigments data can provide only group-level resolution and requires an a priori knowledge of both anticipated phytoplankton groups and their pigment content.

This study benefited from the microscopy data analysis already completed for the surface waters of the 1996, 1997 and 1999 data sets (Garibotti et al., 2005a), which provided confirmation of phytoplankton groupings to include in the CHEMTAX initial input ratios. This information was specific to the samples used in the study, but also coincided well with previously published literature for main species found in the vicinity of the study region (Prézelin et al., 2000; Rodriguez et al., 2002). One exception was the near lack of haptophytes and the assignment of more biomass to the mixed flagellates in the Pal LTER microscopy samples compared to the CHEMTAX analysis. Qualitative observation during sample collection (Kozlowski, unpublished; see also Appendix D) and other work done in the region provided the impetus to include the haptophyte group in the study, and the presence of the marker-pigment 19'-hexanoyloxyfucoxanthin confirmed that this group frequently existed in wAP waters during the time frame of this work. Additionally, the main haptophyte in the region is *P. antarctica* and underestimation by microscopy, particularly when in its gelatinous colonial stage, has been documented (Perrin et al., 1987). It is possible that haptophytes cells were

misidentified and assigned to the mixed flagellate group. Although microscopy was invaluable to confirm the range of taxa to include in the CHEMTAX algorithms, it alone would not have provided a complete picture of the phytoplankton composition.

A fundamental assumption of the CHEMTAX methodology is to supply appropriate initial ratios, both as groups expected to be found in the samples (as discussed above), and initial pigment ratios which are realistic and representative of the physiological state of the organisms (Mackey et al., 1996, Mackey et al., 1998). It has been recommended even to build initial ratios from data from cultures or to collect data from local populations (Mackey et al., 1996), but others have concluded that literature-derived pigment ratios are a more reliable estimate of pigment data (Goericke and Montoya, 1998). Previous studies have employed initial start ratios from literature based solely on the region under study (Wulff and Wänberg, 2004; Delizo et al., 2007). In this study, CHEMTAX proved to be particularly robust in its tolerance to both reduced pigment sets (chl_c3 and violaxanthin data were missing as compared to RVZ02), and to introduced error (up to 25%) in the initial pigment ratios, supporting the idea that precise a priori knowledge is not mandatory for the analysis to provide accurate estimations of phytoplankton composition. Further considerations regarding light adaptation are discussed with relationship to depth stratification in the composition section.

Different questions require resolution on a range of scales and have differing tolerances for error, and it is critical that the above issues are not ignored when selecting a method and protocol for determining phytoplankton composition. However, if additional information is learned about the system or pigments involved, one final advantage of the use of CHEMTAX over microscopy is the ability to re-analyze the data at any point to improve composition estimates.

Specifically given the large number of cruises and samples included in this data set and the group-level resolution of questions being asked, CHEMTAX proved to be the most robust and powerful means to estimate phytoplankton composition along the wAP.

GROUP COMPOSITION AND DISTRIBUTION

The second goal of this study was to define and describe the temporal and spatial variability of phytoplankton along the wAP. Across the twelve year time frame of this study, diatoms were most frequently found to be the dominant group, with as much as 55%, on average, of the total biomass associated with this group. Cryptophytes, mixed flagellates and haptophytes were also common at times, but high abundances tended to be either localized (regional blooms, such as with cryptophytes), or associated with smaller biomasses (29% and 23% of the total, on average, for mixed flagellates and haptophytes, respectively). Prasinophyte blooms were uncommon but did occur in very high abundance on occasion within the study region. Generally, when one group was not dominant (> 50% abundance), the four main groups were mixed fairly evenly, with lower levels of prasinophytes also present. These findings agree well with other published studies in the region, where contribution by various groups dominate at different times in the seasonal cycle and at different locations.

Similar to other Southern Ocean regions, the variability in abundance is extremely large along the wAP, in space and time, as well as in overall phytoplankton biomass and composition. Average values within the grid varied by an order of magnitude (mixed flagellates, haptophytes and cryptophytes in both surface and deep Z_{eu} water) and at times up to two orders of magnitude (surface diatoms). Phytoplankton blooms increased this variability even more; with respect to the climatology, diatom biomass increased by three orders of magnitude along the coast in 2006.

Factors influencing the distribution are commonly cited to be (1) water masses, with their associated impacts on water column stability and nutrient availability due to upwelling, (2) sea ice, whose melting contributes fresh water which stabilizes the water column and whose recession exposes the water column to increased irradiance and potentially "seeds" the water column with bloom forming phytoplankton, (3) depth of the mixed layer, which is impacted as described by sea ice and glacial melt water as well as by mixing due to major weather events and in turn can impact phytoplankton physiology, (4) micro- and macro-nutrients and (5) grazing by zooplanktors. The first four are addressed directly in this study; the fifth remains to be examined.

In turn, phytoplankton have an affect on their surrounding ecosystem, impacting food availability to upper trophic levels, and rates of primary production. The relationship between diatoms and primary production, and possible impacts in changes in community composition are discussed in the sections below.

Importance of Diatoms

Each of the four main phytoplankton groups can, at times, occupy 50% or more of the total biomass in a given location. There are only a few times and locations where populations of prasinophytes, the fifth group included in the study, were greater than 0.4 $\mu g_{[chl\_aP]}$ L-1 or 20% of the population. Diatoms on the other hand were somewhat ubiquitous, compromising 50% or greater of the total population at 37% of the stations sampled and 70% or greater at 21.5% of the stations sampled.

Such predominance of diatoms in the SO is not a new phenomenon. During Antarctic expeditions under James Clark Ross in from as early as 1839 JD Hooker reported the "countless myriads" of summer diatoms (Hooker, 1844). More recently Fryxell and Kendrick (1988) in the Weddell Sea, Kopczyńska et al. (1995) in Prydz Bay (South East of South Africa), Barlow et al. (1998) in the Bellingshausen Sea, van Leeuwe et al. (1998) in the western Bellingshausen Sea, and Arrigo et al. (1999) in the Ross Sea, among others, have all documented diatoms as a dominant taxon of phytoplankton.

Diatom contribution to overall primary production in the SO has also been reported. Kopczyńska et al. (2007) correlate diatom presence to primary production levels along a transect into the Seasonal Ice Zone (SIZ) south of New Zealand, and Prézelin et al. (2004) documente that diatoms were responsible for nearly all of the primary production along the wAP shelf in the austral fall of 1993 and attribute this to presence of UCDW intrusions along the shelf. Vernet et al., (2008)

correlate high production anomalies with presence of diatoms within the Pal LTER grid, particularly in cases of deeper SML, which is theorized to expose the cells to higher irradiance.

Analysis of the correlations between the presence of diatoms ($\mu g_{[chl\_aD]}\ L^{-1}$) and primary production reveals further insights into the relationship described in Vernet et al. (2008). The non-linear relationship found when comparing the average response of each factor (climatology vs climatology) across the grid (Fig. 44a) suggests a physiological limitation to growth of diatoms. One possibility is nutrient limitation, but in those locations silicate (common diatom-limiting macronutrient) never fell below 46 $\mu M\ L^{-1}$, well above the 25 $\mu M\ L^{-1}$ considered to be limiting. The three stations with high diatom biomass are located along the coast (inside-most grid cells of the 200, 400 and 600 lines), and Garibotti et al. (2005b) describe a spatial variability in carbon to chl_a ratios with coastal values only half as high as those in open waters. Less pigment per unit carbon (therefore per cell) could have a negative impact on growth efficiency in the coastal regions, yet a comparison of primary production to chl_a of the three high diatom grid cells to the rest of the grid reveals no significant differences (20.76 ± 1.51 vs 19.56 ± 1.67 mgC m^{-3} chl_a^{-1} d^{-1}). It is also unlikely that micronutrients such as iron are limiting at inshore stations (Garibotti et al., 2005b).

Diatom and production anomalies show that the variations from the mean of the two groups are also tightly correlated across nearly the entire grid (Fig. 44b). A scatter plot of the anomalies (not shown) reveals the relationship is linear, though it weakens somewhat as diatom biomass increases; the highest production anomalies (> approx 3000 mgC m^{-2} d^{-1}) do correlate with high diatom anomalies.

Finally the correlation between the first modes of diatom abundance and primary production further support the idea that diatoms are the primary drivers of production in the region (Fig. 44c). The mechanism behind the temporal and spatial patterns of the two variables is yet to be evaluated, but this study shows that diatoms correlate with average primary production as well as to its spatial and temporal variability.

Studies in the SO have frequently linked the high primary production to sea ice dynamics (Buesseler et al., 2003; Arrigo and Thomas, 2004), particularly to the timing of spring retreat along the wAP (Vernet et al., 2008). There is a spatial dependence though, where late retreat is correlated with increased production on the shelf and in coastal regions, but no or low influence was detected in slope waters (Garibotti et al., 2005a; Vernet et al., 2008). It is theorized that the increased stabilization caused by ice melting (Mura et al., 1995), the increase in irradiance both by physical removal of ice cover from the water as well as by the decrease in MLD due to the freshwater and the possible seeding of the water column with ice algae (Mangoni et al., 2004) are possible mechanisms behind this relationship. Given that as much as 80% of the variability of primary production can be explained by the variability of diatom abundance (Fig. 44b), it is reasonable to expect a relationship between sea ice retreat and diatoms.

On average, as sea ice retreat occurred later, diatom abundance also increased (Fig. 45a). Variability between the two parameters was also correlated, with late sea ice retreat correlating with higher diatoms (Fig. 45b). This was clearly exhibited in the coastal regions of the grid, and though not statistically significant likely due to the high variability in abundance of diatoms, that pattern held for nearly the entire shelf region as well. The opposite relationship holds for the offshore stations, where the two parameters were negatively correlated. There are two scenarios that could create this negative correlation: above average diatom abundance when ice retreat was early or lower than average diatom abundance even when sea ice retreat was late. A look at the individual grid cells along the slope region reveals that both scenarios exist. For instance, in 1998, 2000, 2001 and 2003, sea ice retreat was later than average at the offshore stations yet diatom biomass was slightly below average in those same locations. In 2006 the opposite occurred, and there was higher than average diatoms in the area, despite early sea ice retreat. It is interesting to note high diatom / early retreat scenario was only one year, yet its magnitude was much greater than any of the late ice retreat / low diatom abundance years. The offshore correlations are weaker than those for the shelf and coast ($R \approx 0.3$ vs $0.4 – 0.7$), yet still statistically significant from zero, implying that the variability is less in these offshore regions. It is likely that the positive correlation is the primary one, and the presence of diatoms offshore is not necessarily negatively correlated with sea ice retreat but instead is driven by other factors such as the presence of UCDW (Prézelin et al., 2004; Vernet et al., 2008).

Correlation of the first PC modes of variability shed additional insight into this relationship (Fig. 45c). The timing of the two modes follow similar patterns, with two notable exceptions. First, the negative sign in PC1 of sea ice in 1999 relates to early retreat throughout the entire grid (EOF not shown), yet no corresponding decrease in diatom abundance occurs in locations of the first or second EOF of the diatoms (see also Fig. 37). Both of the first two modes of the diatoms influence the inshore regions of the grid only, yet mode one of the sea ice retreat affects the entire grid. Thus, sea ice is not the component that explains much of the variance in that year. Second, the positive sign of the sea ice PC in 2005 is not reflected with a positive signal in the first PC mode of the diatoms. Here, it is possible that the lack of impact has to do with the extreme lateness of the signal. Sampling for this study was always done in the January; 2005 sea ice retreat was, on average across the grid, 31 days later than normal. It is possible that though diatom abundance is correlated with the timing of the retreat, there is a delay between the actual retreat and the development of the diatom bloom, and the timing of sampling in that year was too early to measure the resultant bloom.

No consistent correlations were found between diatoms and MLD or nutrients, nor between abundance of the remainder of the principal phytoplankton groups and any of the main physical and biological parameters evaluated so far. Further analysis of drivers of these groups and how the might impact the ecosystem will be addressed in a separate study.

Depth Effects

Turbulent mixing, by either wind driven waves and currents, or density dependent convection, leads to the formation of a layer of uniform salinity and temperature at the ocean's surface. Common methods for evaluating water column stratification include examination of density (which is dependent on both temperature and salinity), in order to find the depth where a certain change (frequently 0.2 or 0.5 kg m^{-3}) occurs relative to a reference depth (frequently the surface or 10 m). Put simply, the bottom of the mixed layer is the top of the pycnocline, or the point at which some abrupt change in density occurs; this steep gradient serves as a barrier to mixing, allowing phytoplankton within this top layer to be exposed to essentially uniform water properties.

These layers have two primary components: depth and strength. The extent to which this more stable layer extends is considered the depth of the mixed layer. The strength, or intensity of stratification, refers to the rate of change of the density within the mixed layer. A "well mixed" water column may be of any depth, but it implies that the density gradient occurs quickly, creating a "strong" barrier to mixing below that depth. The schematics in Figure 51 show examples of common mixed layer regimes which demonstrate: (a) a deep MLD with a strong density gradient, (b) a deep MLD with a weak density gradient, (c) a shallow MLD with a strong density gradient, and (d) a shallow MLD with a weak density gradient, all of which are at times seen along the grid.

The extent of vertical mixing within the MLD itself is related to the stability of the water column, or the extent of the density gradient within that layer. It is heavily influenced by duration and intensity of wind events and storms (Holm-Hansen et al., 1989; Prézelin et al., 1991). In this region it is typical that the more stable (larger gradient, strongly stratified) waters are associated with shallower MLDs, and these in turn have been shown to be commonly found in coastal regions (due in part to glacial meltwater) (Moline, 1997; Dierssen et al., 2002; Garibotti et al., 2005a), and along the MIZ (due in part to sea ice meltwater). These shallow, stable MLD waters have long been associated with bloom formation (Smith and Nelson, 1985; Perissinotto et al., 1990). In the Ross Sea, shallow MLDs have been shown to be associated with the presence of diatoms, and deep with *P. antarctica* (Arrigo et al., 1999; Smith and Asper, 2001). Conversely, Moline and Prézelin (1996) associate increased water stability in the Anvers Island region with the presence of cryptomonads. Contrary to all these studies, no consistent, significant correlation with MLD alone was found in any of the main phytoplankton groups (data not show).

A second stratification that occurs in oceanic surface waters has to do with the depth to which sufficient light for photosynthesis penetrates (Z_{eu}). Within the Z_{eu} itself, it is possible to be in high light (surface), low light (bottom) or variable light (when mixing conditions permit). Phytoplankton have the ability to adapt to changes in light to protect themselves against high irradiance (photoinhibition) as well as to optimize photosynthesis at low light levels. Therefore, the interaction of the MLD and the Z_{eu} can be critical for phytoplankton. When the MLD is below the Z_{eu}, phytoplankton are exposed to irradiance levels which can lead to low light stress (Fig. 52a). A MLD which is shallower than the Z_{eu}

prevents mixing of the phytoplankton populations to a light depth which could induce such photoadaptation (Fig. 52b).

In turn, photoadaptation can manifest itself in several ways. Such light regimes may impact pigment ratios; a particular concern involves low light stress (Hammer et al., 2002). However, as discussed in the methods section, no such changes in pigment ratios were detected when different light depth bins were analyzed separately with CHEMTAX (Fig. 4). There are several reasons such changes might not have been detected.

First, given that not all of the 10% light depth samples were below the MLD (average 10% depth, 23.0 m; average MLD, 24.9 m), it is possible that subtle changes in pigment ratios were not detected. Additional resolution might be achieved with a more detailed sub-sampling of the input data (i.e., run 1% samples separate from all others). However, considering the extreme similarity of the output results as tested (100-25% vs 10-1%), strikingly different ratios are not likely to be found.

Second, the selection of the pigments included in the initial ratios may not reflect changes associated with light adaptation. The RVZ02 initial ratios do not depend on photoprotective pigments such as diadinoxanthin, diatoxanthin or violaxanthin, antherazanthin and zeaxanthin, which are known to undergo rapid but short-term shifts under high-light stress (Lohr and Wilhelm, 1999; Moisan et al., 2002). The region does exhibit some variations in Carbon per unit chl_a (Garibotti et al., 2005b) but these adaptations appear to be a short term response to changing light regimes, likely reflected in changes in pigments not used for composition determination.

Third, it is possible that the range of light intensity in this region of the SO is not sufficient to produce low light adaptation (“too light” scenario), or conversely, all the cells regardless of light depth are already low light adapted (“too dark” scenario). However, average cruise irradiance during January of 2006 was 633 μE m^{-2}*s. With an average day length of 18.5 hours, this equates to 17.1 and 0.34 μE m^{-2}*s d^{-1} for the 50% and 1% samples, respectively. A review of recent lab and field studies evaluating the impact of light stress on phytoplankton showed “low” irradiance to vary from 0.83 to 3.33 μE m^{-2}*s and “high” irradiance to range from 6.9 to 34.6 μE m^{-2}*s. In all of the examined studies, various pigment changes between light regimes were observed (although results varied). Given that the typical low light irradiance in this study was below, and the high irradiance was within the range that which has been previously documented to impact pigments, it is unlikely that either the “too light” or “too dark” scenario is occurring.

Photoadaptation may also impact growth rates (Geider, 1987), where higher light conditions allow for higher growth rates. It is important to note that though low light adapted growth is slower, if light was the only variable (laboratory culture conditions, for example), low light cells would eventually reach the same total accumulation as those under high light. Oceanic conditions are much more complex, and through processes such as grazing and advection, low growth rates may be manifested as lower accumulation.

Though no changes in pigment ratios were detected with changes in depth, it is possible that through the combined impacts of different light regimes (and associated changes in growth rates) and the differences in physical and biological characteristics dictated by a MLD barrier, there could be changes in phytoplankton composition with depth. DiTullio et al. (2003) documented high haptophytes abundance (both relative composition and as absolute chl_a biomass) at or below the 1% light depth levels in waters south of 45° S latitude. Moline et al. (1996) and Garibotti et al. (2003b) report correlation of changes in density (MLD) with changes in phytoplankton composition. Given that nearly all the samples included in this study were divided as 50% (high light-adapted) within the MLD and 1% (low light adapted) below the MLD, it provided natural experimental conditions to test the hypothesis that phytoplankton composition is affected by extremes in light and density gradients.

To evaluate this, the 50% vs 1% light depth climatology and anomaly plots can be examined. The question focuses around the impacts of light on the individual phytoplankton groups, not how they react as a system, so discussion here is limited to the absolute abundance of each of the groups.

The correlations of the climatologies show that on average, concentration at one depth can predict concentration at the other for all groups except for the haptophytes (Fig. 29, top panel). It is interesting to note though that there is always a difference in concentration above and below the MLD (relationship is not one to one). This result can be expected given the differences in light, with the low light samples having lower rates of accumulation. This result implies that whatever favors growth of a certain group at a certain location is not impacted in the depth dimension (i.e., in general, the MLD does not act as a barrier).

The year to year variability also tracks well across depth for the diatoms and the mixed flagellates, across nearly the entire grid (Fig. 30, top panel). This implies that not only what drives these two groups on average, but also what drives their variability in time acts across the MLD. A notable exception to this relationship is seen in the slope waters for the mixed flagellates, where the correlation between the depths weakens substantially. It is possible that the conditions which cause large variation in growth of the mixed flagellates occur only on the shelf and in coastal areas. For instance, optimal mixed flagellate growth could correlate with presence of M-UCDW, which only forms as UCDW moves across the shelf. Further analysis will be required before this hypothesis can be tested.

Although the climatologies of the haptophytes at 50% and 1% light depths were not significantly correlated, the anomalies show a significant positive correlation also across nearly the entire grid (with the exception of the central and southern coastal regions, where there is no correlation). Figure 46 exemplifies the temporal correlation of the anomalies between the two depths, with strongest negative correlation being driven by extreme opposites in sign of the anomaly values. This result suggests that the average haptophytes abundance is not impacted by the same forces

that drive the extremes of its variability, and when the conditions do occur to cause haptophytes blooms, they are stronger than those driving the average, overcoming any barrier depth (or light) might otherwise present.

Two other factors should be considered when evaluating these results. First, light history has been shown to have as strong an impact as absolute irradiance (Cullen and Lewis, 1988; van Leeuwe et al., 2005; Dimier et al., 2007); since the MLD used in this study in merely a "snapshot" of the water column at the time of sampling, effects of recent changes (or lack of changes) in irradiance are not accounted for. Also, it is important to recognize the limitation of the CHEMTAX method to resolve taxa at a species-level. It is possible that despite correlation between the 50% and 1% samples, the actual populations might consist of different types (e.g., large chain forming diatoms might be at the surface while small, pennate diatoms might dominate deep Z_{eu} waters) and the method used in this study is not able to differentiate between those.

Assemblages

Cluster analysis of all twelve years of chl_a normalized composition at 50% did not reveal any consistently recurring assemblages. Principle component analysis resulted in diatoms and cryptophytes occupying factor one and two, explaining a little over half of the variance in the system. On average the two groups do move opposite each other (correlation of the climatologies explain less than 50% of the variance), but under bloom conditions this negative correlation appears. The negative correlation between the diatoms and the cryptophytes is evident throughout the entire grid, as seen by the correlation map of the anomalies (Fig. 46). Looking more closely at individual grid cells reveals obvious exceptions. In locations that were highly correlated, there were frequently large anomalies with opposing signs (Fig. 46e). Locations where the relationship was not as strong displayed some discord (Fig. 46c; 1999, 2004-2006), but also had multiple years where both groups were close to average (Fig. 46b; 1996-1999) or even years where one group's anomaly was high and the other differed little from the mean (Fig. 46b, 1995 and Fig. 46c, 2007). Finally, no correlation was seen in the slope region of the 200 line, where frequently neither anomaly was large, or the deviations moved in the same direction (Fig. 46d). The southern slope region is thought to be strongly influenced by UCDW, possibly over-riding the usual diatom-cryptophyte dynamic. The interaction between diatoms and cryptophytes can explain some of the variance in the overall population but the "noise" in the timing and magnitude of the blooms prevents these groupings from being significant when analyzed across the entire time series.

Year-by-year cluster analysis removed enough variability to reveal some recurring assemblages, based primarily on the dominance of one group, with one assemblage representing a mixture of all groups (Table 8). Thus, phytoplankton in the wAP tends toward single-taxon dominant groups.

In addition, this result supports previous studies which have proposed scenarios describing a seasonal succession of phytoplankton groups. Working at Palmer Station during summers of 1991 to

1994, Moline and Prézelin (1996) describe a dominant community of ice-edge associated diatoms appearing in the spring as sea ice melted and daily irradiance increased. The diatoms were replaced by cryptophytes, which dominated the population until they were in turn replaced by a community of diatoms and *Phaeocystis*. The timing of the appearance and demise of the cryptophyte bloom was correlated with changes in density in the water column; increased fresh water in the surface layers (likely from increased glacial melt-water during austral summer) correlated strongly with cryptophyte biomass. Garibotti et al. (2005a) proposed a similar scenario along the wAP, with diatom blooms being associated with the retreat of the winter sea ice, progression to a population consisting of a mixture of cyrptophytes and other phytoflagellates, and return of the population to a diatom dominated assemblage later in the season. After work in the southern Bransfield and northern Bellingshausen Sea in spring and summer of 1990, Bidigare et al. (1996) proposed that it was not diatoms that are associated with the sea ice edge, but rather haptophytes, with the population shifting to diatoms as the ice recedes.

To evaluate if any of these progressions are regularly seen along the Pal LTER grid, the assemblages described above were evaluated for their presence in locations along the grid (coast, shelf, slope) with relationship to timing of the sea ice retreat. Specifically, the average time between when ice was last in an area of a particular assemblage and the time that the assemblage was seen (ie., the time of sampling during the January LTER cruise) was calculated to determine if seasonal succession could be detected given the fixed time frame of the sampling regime.

Analysis of the time between when certain assemblages were seen and the time since ice was in that location indicated that diatoms at high concentration (> 90%) have on average the shortest time between observation and time since ice retreat (Fig. 50). Statistically, there is no difference between the timing of the high concentration diatoms, the cryptophytes > 50% and the prasinophytes and, and the later two groups and the haptophytes > 50%, mixed flagellates > 50%, the diatoms > 50% and the mixed community (ie., no group > 50%). The high concentration diatoms are different than the later four groups. These results support the succession ideas presented by Garibotti et al., (2005a) where diatoms are associated with ice-edge stabilized water columns, and those of Moline and Prézelin (1996), where diatoms are the first to appear after ice melt. Though not statistically significant, these results do not preclude the possibility that cryptophytes follow the ice-edge diatoms. The longer time between observation of the mixed population and the diatoms > 50% assemblage also supports the possibility that these groups occur later in the succession. Examples of years where a progression from high concentration diatoms to a crytophyte and/or flagellate dominated community returning to a diatom dominate community are 1995, 1996, 1997, 1999, 2000 (Fig. 48), 2004, 2005 and 2007 (Fig. 49). However, no evidence for this succession is seen in 2001, where mixed flagellates dominated nearly the entire grid, with only a single station showing diatom dominance even with more than three months since ice retreat in the slope regions (Fig. 49a). Assemblage patterns in 1998 also do not support the “diatoms first” hypothesis; there, no high

concentration diatoms were observed at all, despite late/very late ice retreat along the shelf and slope (Fig. 48c).

There is no statistical evidence in this study to support the hypothesis that haptophytes are the first to appear after ice retreat (Bidigare et al., 1996). One possible exception is 2003, when haptophytes were observed to be dominant along the shelf, in a region where sea ice retreat was recent. The signal there is very localized however, and the data show no evidence of diatom dominance following the haptophyte blooms (Fig. 49b).

The analysis conducted in this study does not in any way evaluate the mechanism that might be driving the assemblage succession. The retreat of the sea ice is theorized to create conditions in the water column conducive to growth of a certain group or combination of groups. A full evaluation of the theory would need to entail several factors not addressed here, including physical characteristics of the water column such as density and/or stability, zooplankton, micro-nutrient levels (ie., iron), in-ice seed populations, the relationship of timing of ice retreat to levels of incident irradiance (PAR), and impacts of recent mixing events. Each of these variables contains their own intrinsic questions, and development of measurements to that best represents each parameter will be required. The results seen thus far suggest that additional analysis, particularly if accompanied by these ancillary data, might provide a better understanding of the link between sea ice and phytoplankton composition, but it is beyond the present scope of this project.

Water Masses in the Pal LTER Region

Phytoplankton composition is frequently associated with large-scale water masses or frontal systems (Longhurst, 1998). The southern edge the Antarctic Circumpolar Current (ACC) regularly flows over the slope and shelf break regions of the Pal LTER sampling grid (Orsi et al., 1995). The ACC brings with it the warm Circumpolar Deep Water (CDW) which is seen along the entire region, and so can be further resolved into a layer containing temperatures between 1.70 and 2.13° C and a salinity of between 34.58 and 34.75 ‰ known as upper CDW (UCDW). This UCDW is then cooled as it moves coastward across the shelf, becoming modified UCDW (M-UCDW; Martinson et al., 2008).

Analysis of temperature-salinity (T-S) diagrams from CTD profiles of the waters in the study region reveals two fundamental shapes which relate to the above water masses: a sharp “V” and a more rounded “U” (Fig. 53). The narrow range of the V-shape is water which is renewed frequently by fresh winter water from the ACC. These waters are always apparent over the slope region (Fig. 53a). The U-shaped curves are waters which are more isolated from the ACC, renewed less frequently, and are more subject to vertical mixing. They are most predominant in the coastal region of the study area (Fig. 53b). Waters along the shelf display curves that appear to be transitional between the two, indicating variable amounts of freshening in both time and space (Fig. 53c). Distribution of these T-S shapes across the grid is consistent with bathymetric features ranging from deep slope waters to the coastal region of shallow bays and islands which may serve to protect against UCDW renewal (Martinson et al., 2008).

One possible proxy for presence of UCDW might be temperature; with deep warmer temperatures representing influence of the ACC, but the formation of the M-UCDW along the shelf confounds this relationship (Martinson et al., 2008). A linear relationship has been defined between the degradation of the V shape of the T-S curve and the time since last being refreshed, with the shape of the curve itself another potential proxy. By defining this "canonical structure" (using waters less than 0.5° C, or the region of the V that shows the most variation) and using it as a "tracer" of recent UCDW renewal, it may possible to define the annual distribution of ACC along the grid (Martinson, personal communication). Finally, use of optimal multi-parameter analysis may allow determination of the fraction of pure UCDW flowing across the grid (Martinson et al., 2008), but all of these avenues will require additional refinement and testing before exploring the relationship between UCDW masses and phytoplankton composition along the wAP.

Because there is no direct measure of presence of M-UCDW on the shelf, the best descriptor of water masses in the system is the regional delineation between shelf, slope and coast. Descriptively, several features appear to be related to the regional divisions associated with these water masses. The most distinct of these are seen in the diatoms and the haptophytes. First, looking at abundance, diatoms are most abundant along the coast, and surface haptophytes are more abundant on average in shelf waters than along the coast or in slope waters (Figs. 6 and 8). In terms of proportion of the total community, contribution of surface diatoms is greater along the coast and in slope waters than along the shelf (Fig. 7), and on average, haptophytes throughout the water column contribute more to the community in slope waters than elsewhere along the grid (Figs. 7 and 9). Finally, deep water diatoms are more abundant along the coast and in slope waters than in shelf waters (Fig. 9). It is possible that with the ACC along the slope and the movement of the UCDW across the shelf brings upwelled sources of micronutrients such as iron, or perhaps the turbulence caused by the currents create conditions conductive to abundance of diatoms and haptophytes.

Sea Ice and Climate Change

According to the Intergovernmental Panel on Climate Change, mean global temperature has increased 0.6±0.2 °C in the last century (Houghton et al., 2001). The Antarctic peninsula has been identified as one of three high latitude areas that in the last 50 years has undergone recent rapid regional (RRR) warming, with increases more rapid than the global average (Vaughan et al., 2003). In particular, the Antarctic Peninsula has undergone a 2-3 °C increase in the last 50 years, with strongest warming seen in the autumn and winter (3-6 °C warming vs 1.3-1.5 °C in the spring and summer) (Vaughan et al., 2003). Such warming has already been associated with physical parameter changes such as increases ocean heat content (Martinson et al., 2008) and biological changes such as increases in salp abundances (Ross et al., 2008) and local declines in Adélie penguin populations (Fraser et al., 1992; Ducklow et al., 2007). Similarly, Stammerjohn et al., (2008) present evidence of ocean-atmosphere-ice interactions that are consistent with this warming trend,

with the average date of sea ice formation occurring 20-30 days later and the date of sea ice retreat 15-25 days earlier in 1992-2004 compared to 1979-1991.

A central hypothesis of the Pal LTER is that the seasonal and interannual variability of sea ice affects all levels of the Antarctic marine ecosystem. Tréguer and Jacques (1992) defined four main hydrographical and biogeochemical regions in the Southern Ocean; two are applicable to this study area. The Pal LTER region is annually covered by sea ice and so is considered part of the SIZ; the MIZ is delimited by those waters influenced by the meltwater of the receding sea ice, and can extend from 50-100 km from the edge of the seasonal pack ice. The location of the MIZ during the January cruise time frame is dependent on the ice during the previous spring.

Variability in the seasonality of sea ice has in turn been shown to be influenced by El Niño Southern Oscillation (ENSO) and the Southern Annular Mode (SAM) climate variability (Stammerjohn et al., 2008). Unfavorable sea ice conditions have been associated with La Niña and/or positive SAM years, when cyclonic (clockwise) winds bring warm, northerly air over the region. Having already established the relationship between sea ice and diatom abundance, it follows that long term changes in diatoms, and other key phytoplankton groups may be discernable.

To determine if this is the case, robust trends, as slopes of the grid cell anomalies for each of the groups, across the Pal LTER grid were examined. Overall, no statistically significant, grid-wide trends were observed, in either overall biomass (as chl_a), or in abundance (contribution to chl_a) or community contribution (%) of the major phytoplankton groups. A few changes and general patterns of change are discussed below, but due to the high variability of the signal of phytoplankton contribution, it appears a longer time series will be necessary before conclusive evidence for trends in phytoplankton contribution can be detected.

First, total chl_a (μg L^{-1}) did not show any significant trend across the whole grid, implying that overall biomass along the wAP is not responding to the warming trends (Fig. 38). Upon closer examination, the slight decreasing slope seen in the northern coastal region of the grid was due primarily to high chl_a in the region in 1996. Due to its high variability in those grid cells, the decrease is not statistically significant.

Second, a generally decreasing trend in absolute abundance of cryptophytes can be seen in the northern portion of the Pal LTER grid (Fig. 33, left panels), though it was not statistically significant in most locations. This is in opposition to the suggestion by Moline et al. (2004) who report a shift in phytoplankton population from diatoms to cryptophytes in the coastal waters near Anvers Island between 1991 and 1996. Moline and Prézelin (1996) associate the presence of cryptophytes with changes in salinity, and hypothesize that the increased in temperatures in the region will lead to increased freshwater from glacial runoff, thus creating conditions supporting cryptophyte growth over diatom growth. It is known that diatoms are preferentially grazed over cryptophytes (Jacques and Panouse, 1991), and Moline et al. (2004) suggest that the decrease in diatom abundance would lead to a decrease in the krill population. This would lead to an increase in the salp population, which

would in turn impact higher trophic levels whose diets depend on the more energy-rich krill. Although no significant population shift was detected in this study, it is possible that the sampling scale is impacting the ability to detect such a change. As glacial melt was the primary source of freshwater in the Palmer inshore study region it is possible that the phenomenon is only a local, inshore shift in cryptophyte presence and the signal is not detectable at the stations annually sampled as part of the Pal LTER cruises. These results suggest that no large scale changes in the wAP are being observed to date; trends that are detected are either those of very short time scales, or are confined to a localized region of the grid. Note also that no increase occurred in diatoms in the Anvers Island region (Fig. 32); slight increases were detected, but were spatially inconsistent and offshore of the region discussed by Moline et al. (2004).

Other analyses of the impacts of climate change and warming scenarios predict that a 25% loss in sea ice cover would increase primary production in the SO by between 0.7-8.1% (Sarmiento et al., 2004; large range due to temperature dependence variability estimates of primary production) and 10% (Arrigo and Thomas, 2004). This could in turn have a slight negative feedback on climate warming. Again given the tie already established between diatoms and primary production, it will be of key interest and importance to track phytoplankton, particularly diatom, abundance in the region over the next few decades.

Additional Considerations and Future Analysis

Perhaps the most conclusive statement that can be made after evaluation of the composition of the Pal LTER region of the wAP is that it is an exceedingly complex system. As such, it encourages further questioning about a various possible mechanisms as well as impacts that would require careful evaluation in both space and time before gaining additional insight into additional factors both influencing the system and being influenced by the phytoplankton composition. A few of the main avenues I hope to follow to both improve and augment this study are briefly described below.

First, analysis of the 2002 composition samples and their inclusion into the data set is of utmost importance. From the full time series of sea ice retreat anomalies (Stammerjohn et al., 2008), sea ice retreat of 2001 is one of few years of early anomaly impacting nearly the entire LTER grid region. Addition of the 2002 composition that would potentially been impacted by this early retreat could shed additional insight in factors driving the variability of phytoplankton composition.

Second, several parameters mentioned in this study are deserving of further analysis. As methods improve for the tracking of UCDW onto the shelf, improved resolution of its relationship to composition may be revealed. Additionally, the range of methods for both defining and determining “stability” found while researching this work was large. Further analysis of the impacts of this vertical structure and the best way to define it in the wAP region may also help elucidate the linkage between water column stability and composition.

Further insights into mixed layer depth might be gained by examination of major weather (mixing) events. There exists a data set similar to the grid data used in this work from seasonal sampling at Palmer Station, on Anvers Island. Because the Palmer data would allow introduction of an annual cycle to the interannual variability already seen on the grid, and because the fixed sampling locations would allow easier quantification of weather and "life history" information, a similar analysis of the composition in that region may also provide useful insight into understanding the ecosystem

The addition of the physical parameters to the assemblage / sea ice timing analysis is also of great interest. The Pal LTER data set includes the variable that could be used to answer questions about the mechanisms brought about by sea ice dynamics.

Two other variables are frequently discussed as possible mechanisms of change for Antarctic phytoplankton: micronutrients such as iron (Martin, 1990), and the impacts of grazers, such as krill (Jacques and Panouse, 1991) and salps (Walsh et al., 2001). Examination of photosynthetic efficiency from fast repetition rate fluorometry may shed insight into possible effects of low-iron stress in this region, and collaboration with Palmer principle investigators Ross and Quetin is planned to test of impacts of macrozooplankton grazing on composition.

Last, but certainly not least is to return to the original impetus for the project: evaluation of the impacts of composition on water column optics. Tied tightly into the understanding of all the above topics, development of a simple, direct way to relate composition to in-water and ultimately remotely sensed optics in this region will help in our understanding of the potential impacts of climate change.

SUMMARY

A robust means of determining phytoplankton composition was tested and applied to data collected between 1995 and 2007 along the wAP region. Using these results, the spatial and temporal variability was defined and described. Results were examined in relationship to primary production and sea ice dynamics in the region, and impacts of light and mixing regimes and climate changes on the ecosystem were also discussed. The following is a summary of key findings:

Results from the CHEMTAX analysis of HPLC data show four groups which commonly contribute to the phytoplankton population in this area: (1) diatoms, (2) cryptophytes, (3) mixed flagellates and (4) haptophytes. A fifth group (prasinophytes) is frequently present, but rarely contributes more than 10% to the total biomass signal. Diatoms were found to be both the most common, and on average the most abundant of all the phytoplankton groups.

The region can be best characterized by its extremes of variability, in both space and time, with large phytoplankton blooms contributing up to three times the average biomass. Between 67 and 90% of the variability within each group is explained in the first two principle component modes, the timing and location of which is correlated to large blooms.

For all groups except the haptophytes, surface (50% light depth) biomass is linearly related to biomass at the bottom of the Z_{eu} (1% light depth). Extreme anomalies (bloom occurrences) in cryptophytes and across much of the grid for prasinophytes do exhibit some vertical differentiation; whether this is due to a barrier brought about by water column differences at the MLD, or by differences in light intensity remains to be tested.

The abundance of diatoms was shown to be positively correlated with the timing of sea ice retreat and to rates of primary production. In contrast, no significant relationships were found between these parameters and any other major phytoplankton group.

No consistent significant trends were observed in either absolute or relative biomass of any group, in spite of observed changes in upper trophic levels. A longer time series will likely improve the ability to detect such long term changes in the system.

The most common assemblages found in the region are those dominated (> 50% relative abundance) by one single phytoplankton group, or one which is dominated by no single group. High concentrations of diatoms (> 90%) were observed soonest after sea ice retreat, frequently in the region of Marguerite Bay.

The wAP ecosystem is extremely complex, as exemplified by the non-linear response of primary production to presence of diatoms, and the spatial gradient in the response of diatoms to sea ice. The phytoplankton in the area are influenced by both biological and physical factors, which are in turn impacted by the interannual signal of the sea ice. Additionally, the region is also undergoing a major warming shift and so potential impacts of climate change must also be included in the attempt to extract the signal from the information in hand. Of key importance will be continued collection of long term data, in order to continue to add to our knowledge of this critical and sensitive region of the world's oceans.

ACKNOWLEDGEMENTS

Funding for this work was provided to Maria Vernet through NSF / OPP grants # OPP-90-11927 OPP-96-32763 and OPP-02-17272. I am grateful for the generous financial support of a NASA Graduate Student Research Program fellowship from 2005-2007. Thank you to my committee for guiding me through this process and sharing with me your expertise; it was a pleasure to learn from each of you.

I would like to thank the Palmer LTER principal investigators for the opportunity to participate in this long term project. Maria Vernet, Langdon Quetin and Robin Ross, you shared with me not just your extensive knowledge of the area and its ecology, but opened my eyes to the many advantages and joys of working within a scientific family. Ray Smith, thank you for your help in the development of the ideas which became this thesis. Doug Martinson and Rich Iannuzzi, you contributed greatly to my understanding of the interplay between physical oceanography and biology. Thank you Rich, for your great patience and thoughtful explanations, and for teaching me so much about Matlab. Thank you Sharon Stammerjohn, for sharing your data and knowledge of sea ice. Namaste.

Thank you to the LTER technicians and the MSI lab at UCSB for nutrient data analysis. The beta version of CHEMTAX was provided upon request from Simon Wright; thank you for your interest in my work. Microscopy data was provided by Irene Garibotti – gracias. Antarctic and Chilean logistical support was provided by Antarctic Support Associates, Raytheon Polar Services Company, AGUNSA and the Captains and crews of the R/V Polar Duke and ARSV Laurence M. Gould.

Data collection for this study could not have been done without the many, many hours of hard work by and companionship of too many volunteers to name here; thank you all for your enthusiasm, energy and joy. Karie Sines, Heidi Geisz, Karen Pelletreau, Janice Jones, Peter Horne, Jeffrey Bechtel, Joe Grzymski, Jordan Watson and so many others – it wouldn't have been the same without you.

Lynn Yarmey, thank you teaching me that Illustrator and Matlab can be fun, and for reminding me to breathe. Tom Anderson and Laurie Harvey, you were my sanity-savers in this now-triumphant return to graduate school; I'm so glad you were there with me. My gratitude goes out to my parents and sister who show me every day the benefits, joys, and true meaning of the word "knowledge". Thank you.

Finally, to my best friend and husband, Doug Fink: I simply could not have done this without you. Thank you sharing my love of Antarctica, and for staying by my side, there and always.

REFERENCES

Aitchison, J., 1955. On the distribution of a positive random variable having a discrete probability mass at the origin. Journal of the American Statistical Association 50: 901-908.

Andersen, R.A., Bidigare, R.R., Keller, M.D., Latasa, M., 1996. A comparison of HPLC pigment signatures and electron microscopic observations for oligotrophic waters of the North Atlantic and Pacific Oceans. Deep-Sea Research II 43: 517-537.

Andersen, R.A., Saunders, G.W., Paskind, M.P., Sexton, J.P., 1993. Ultrastructure and 18s Ribosomal-RNA gene sequence for Pelagomonas-Calceolata Gen Et Sp-Nov and the description of a new algal class, the Pelagophyceae. Journal of Phycology 29: 701-715.

Anderson, J.B., 1999. Antarctic marine geology. Cambridge University Press, Cambridge

Armstrong, F.A., Stearns, C.R., Strickland, J.D.H., 1967. Measurement of upwelling and subsequent biological processes by means of Technicon Autoanalyzer and associated equipment. Deep-Sea Research 14: 381-389.

Arrigo, K.R., Robinson, D.H., Worthen, D.L., Dunbar, R.B., DiTullio, G.R., VanWoert, M., Lizotte, M.P., 1999. Phytoplankton community structure and the drawdown of nutrients and CO2 in the Southern Ocean. Science 283: 365-367.

Arrigo, K.R., Thomas, D.N., 2004. Large scale importance of sea ice biology in the Southern Ocean. Antarctic Science 16: 471-486.

Arsalane, W., Rousseau, B., Duval, J.C., 1994. Influence of the pool size of the xanthophyll cycle on the effects of light stress in a diatom - competition between photoprotection and photoinhibition. Photochemistry and Photobiology 60: 237-243.

Barlow, R.G., Aiken, J., Holligan, P.M., Cummings, D.G., Maritorena, S., Hooker, S., 2002. Phytoplankton pigment and absorption characteristics along meridional transects in the Atlantic Ocean. Deep-Sea Research I 49: 637-660.

Barlow, R.G., Mantoura, R.F.C., Cummings, D.G., 1998. Phytoplankton pigment distributions and associated fluxes in the Bellingshausen Sea during the austral spring 1992. Journal of Marine Systems 17: 97-113.

Bernhardt, H., Williams, A., 1967. The continuous determination of low level iron, soluble phosphate and total phosphate with the AutoAnalyzer, Technicon Symposium: Automation in Analytical Chemistry, New York, pp. 385-389.

Bidigare, R.R., Iriarte, J.L., Kang, S., Karentz, D., Ondrusek, M.E., Fryxell, G.A., 1996. Phytoplankton: quantitative and qualitative assessments. In: R.M. Ross, E.E. Hofmann and L.B. Quetin (Editors), Foundations for Ecological Research West of the Antarctic Peninsula. AGU Antarctic Research Series. American Geophysical Union, Washington, DC, pp. 173-198.

Bjørnland, T., Guillard, R.R.L., Liaaen-Jensen, S., 1988. *Phaeocystis sp.* Clone 677-3 - a Tropical Marine Planktonic Prymnesiophyte with Fucoxanthin and 19'-Acyloxyfucoxanthins as Chemosystematic Carotenoid Markers. Biochemical Systematics and Ecology 16: 445-452.

Bodungen, B.V., Smetacek, V.S., Tilzer, M.M., Zeitzschel, B., 1986. Primary production and sedimentation during spring in the Antarctic Peninsula region. Deep-Sea Research A 33: 177-194.

Boyd, P.W., Robinson, C., Savidge, G., leB Williams, P.J., 1995. Water column and sea-ice primary production during Austral spring in the Bellingshausen Sea. Deep-Sea Research II 42: 1177-1200.

Breteler, W.C.M.K., 1985. Fixation artifacts of phytoplankton in zooplankton grazing experiments. Hydrobiological Bulletin 19: 13-19.

Buck, K.R., Garrison, D.L., 1983. Protists from the ice-edge region of the Weddell Sea. Deep Sea Research A 30: 1261-1277.

Buesseler, K.O., Barber, R.T., Dickson, M.L., Hiscock, M.R., Moore, J.K., Sambrotto, R., 2003. The effect of marginal ice-edge dynamics on production and export in the Southern Ocean along 170 degrees W. Deep-Sea Research Part Ii-Topical Studies in Oceanography 50: 579-603.

Buma, A.G.J., Treuger, P., Kraay, G.W., Morvan, J., 1990. Algal pigment patterns in different watermasses of the Atlantic sector of the Southern Ocean during fall 1987. Polar Biology 11: 55-62.

Burkholder, P.R., Sieburth, J.M., 1961. Phytoplankton and chlorophyll in the Gerlache and Bransfield Straits of Antarctica. Limnology and Oceanography 6: 45-52.

Burkill, P.H., Edwards, E.S., Sleigh, M.A., 1995. Microzooplankton and their role in controlling phytoplankton growth in the marginal ice zone of the Bellingshausen Sea. Deep-Sea Research II 42: 1277-1290.

Caldeira, K., Duffy, P.B., 2000. The role of the Southern Ocean in uptake and storage of anthropogenic carbon dioxide. Science 287: 620-622.

Carreto, J.I., Montoya, N.G., Benavides, H.R., Guerrero, R., Carignan, M.O., 2003. Characterization of spring phytoplankton communities in the Rio de La Plata maritime front using pigment signatures and cell microscopy. Marine Biology 143: 1013-1027.

Carrillo, C.J., Karl, D.M., 1999. Dissolved inorganic carbon pool dynamics in northern Gerlache Strait, Antarctica. Journal of Geophysical Research 104: 15873-15884.

Chisholm, S.W., Morel, F.M.M., 1991. Preface: What controls phytoplankton production in nutrient-rich areas of the open sea? Limnology and Oceanography 36.

Clarke, A., 1988. The annual cycle of temperature, chlorophyll and major nutrients at Signey Island, South Orkney Islands, 1969-82. British Antarctic Survey Bulletin 80: 65-86.

Coale, K.H., Johnson, K.S., Chavez, F.P., Buesseler, K.O., Barber, R.T., Brzezinski, M.A., Cochlan, W.P., Millero, F.J., Falkowski, P.G., Bauer, J.E., Wanninkhof, R.H., Kudela, R.M. et al., 2004. Southern ocean iron enrichment experiment: carbon cycling in high- and low-Si waters. Science 304: 408-414.

Countway, P.D., Caron, D.A., 2006. Abundance and distribution of Ostreococcus sp in the San Pedro Channel, California, as revealed by quantitative PCR. Applied and Environmental Microbiology 72: 2496-2506.

Cullen, J.J., Lewis, M.R., 1988. The kinetics of algal photoadaptation in the context of vertical mixing. Journal of Plankton Research 10: 1039-1063.

Delizo, L., Smith, W.O., Hall, J., 2007. Taxonomic composition and growth rates of phytoplankton assemblages at the Subtropical Convergence east of New Zealand. Journal of Plankton Research 29: 655-670.

Demers, S., Roy, S., Gagnon, R., Vignault, C., 1991. Rapid light-induced-changes in cell fluorescence and in xanthophyll-cycle pigments of *Alexandrium-Excavatum* (Dinophyceae) and *Thalassiosira-Pseudonana* (Bacillariophyceae) - a photo-protection mechanism. Marine Ecology-Progress Series 76: 185-193.

Demmig-Adams, B., 1990. Carotenoids and photoprotection in plants - a role for the xanthophyll zeaxanthin. Biochimica Et Biophysica Acta 1020: 1-24.

Dierssen, H.M., Smith, R.C., Vernet, M., 2002. Glacial meltwater dynamics in coastal waters west of the Antarctic peninsula. Proceedings Of The National Academy Of Sciences Of The United States Of America 99: 1790-1795.

Dimier, C., Corato, F., Tramontano, F., Brunet, C., 2007. Photoprotection and xanthophyll-cycle activity in three marine diatoms. Journal of Phycology 43: 937-947.

DiTullio, G.R., Garcia, N., Riseman, S.F., Sedwick, P.N., 2007. Effects of iron concentration on pigment composition in *Phaeocystis antarctica* grown at low irradiance. Biogeochemistry 83: 71-81.

DiTullio, G.R., Geesey, M.E., Jones, D.R., Daly, K.L., Campbell, L., Smith, W.O., 2003. Phytoplankton assemblage structure and primary productivity along 170 degrees W in the South Pacific Ocean. Marine Ecology Progress Series 255: 55-80.

Duarte, C.M., Marrase, C., Vaque, D., Estrada, M., 1990. Counting error and the quantitative-analysis of phytoplankton communities. Journal Of Plankton Research 12: 295-304.

Dubreuil, C., Denis, M., Conan, P., Roy, S., 2003. Spatial-temporal variability of ultraplankton vertical distribution in the Antarctic frontal zones within 60-66 degrees E, 43-46 degrees S. Polar Biology 26: 734-745.

Ducklow, H., 2002. Palmer, Antarctica LTER: Climate change, ecosystem migration and teleconnections in an ice-dominated environment. Palmer Station Antarctica Long Term Ecological Research, Retrieved 21 April 2008, from http://pal.lternet.edu/docs/publications/proposals/0208proposal/ (Path: text.pdf).

Ducklow, H., Erickson, M., Kelly, J., Montes-Hugo, M., Ribic, C.A., Smith, R., Stammerjohn, S.E., Karl, D.M., 2008 (accepted). Particle export from the upper ocean over the continental shelf of the west Antarctic Peninsula: A long-term record, 1992-2007. Deep-Sea Research II.

Ducklow, H.W., Baker, K., Martinson, D.G., Quetin, L.B., Ross, R.M., Smith, R.C., Stammerjohn, S.E., Vernet, M., Fraser, W., 2007. Marine pelagic ecosystems: The West Antarctic Peninsula. Philosophical Transactions of the Royal Society B-Biological Sciences 362: 67-94.

Egeland, E.S., Eikrem, W., Throndsen, J., Wilhelm, C., Zapata, M., Liaaenjensen, S., 1995. Carotenoids from further prasinophytes. Biochemical Systematics & Ecology 23: 747-755.

Eller, G., Toebe, K., Medlin, L.K., 2007. Hierarchical probes at various taxonomic levels in the Haptophyta and a new division level probe for the Heterokonta. Journal of Plankton Research 29: 629-640.

Falkowski, P.G., Barber, R.T., Smetacek, V., 1998. Biogeochemical controls and feedbacks on ocean primary production. Science 281: 200-206.

Ferrario, M.E., Sar, E.A., Vernet, M., 1998. Chaetoceros resting spores in the Gerlache Strait, Antarctic Peninsula. Polar Biology 19: 286-288.

Fischer, G., Gersonde, R., Wefer, G., 2002. Organic carbon, biogenic silica and diatom fluxes in the marginal winter sea-ice zone and in the polar front region: interannual variations and differences in composition. Deep-Sea Research II 49: 1721-1745.

Fitch, D.T., Moore, J.K., 2007. Wind speed influence on phytoplankton bloom dynamics in the southern ocean marginal ice zone. Journal of Geophysical Research-Oceans 112.

Fraser, W.R., Trivelpiece, W.Z., Ainley, D.G., Trivelpiece, S.G., 1992. Increases in Antarctic penguin populations - reduced competition with whales or a loss of sea ice due to environmental warming. Polar Biology 11: 525-531.

Fryxell, G.A., Kendrick, G.A., 1988. Austral spring microalgae across the Weddell Sea ice edge - spatial relationships found along a northward transect during Ameriez-83. Deep-Sea Research Part A 35: 1-20.

Furuya, K., Hayashi, M., Yabushita, Y., Ishikawa, A., 2003. Phytoplankton dynamics in the East China Sea in spring and summer as revealed by HPLC-derived pigment signatures. Deep-Sea Research II 50: 367-387.

Garibotti, I., Vernet, M., Kozlowski, W., Ferrario, M., 2003a. Composition and biomass of phytoplankton assemblages in coastal Antarctic waters: a comparison of chemotaxonomic and microscopic analyses. Marine Ecology Progress Series 247: 27-42.

Garibotti, I.A., Vernet, M., Ferrario, M.E., 2005a. Annually recurrent phytoplanktonic assemblages during summer in the seasonal ice zone west of the Antarctic Peninsula (Southern Ocean). Deep-Sea Research I 52: 1823-1841.

Garibotti, I.A., Vernet, M., Ferrario, M.E., Smith, R.C., Ross, R.M., Quetin, L.B., 2003b. Phytoplankton spatial distribution in the Western Antarctic Peninsula (Southern Ocean). Marine Ecology Progress Series 261: 21-39.

Garibotti, I.A., Vernet, M., Smith, R.C., Ferrario, M.E., 2005b. Interannual variability in the distribution of the phytoplankton standing stock across the seasonal sea-ice zone west of the Antarctic Peninsula. Journal of Plankton Research 27: 825-843.

Geider, R.J., 1987. Light and temperature dependence of the carbon to chlorophyll *a* ratio in microalgae and cyanobacteria: implications for physiology and growth of phytoplankton. New Phytology 106: 1-34.

Gieskes, W.W., Kraay, G.W., 1986. Floristic and physiological differences between the shallow and the deep nanophytoplankton community in the euphotic zone of the open tropical Atlantic revealed by HPLC analysis of pigments. Marine Biology 91: 567-576.

Gieskes, W.W.C., Kraay, G.W., Nontji, A., Setiapermana, D., Sutomo, 1988. Monsoonal alternation of a mixed and a layered structure in the phytoplankton of the euphotic zone of the Banda Sea (Indonesia) - a mathematical-analysis of algal pigment fingerprints. Netherlands Journal of Sea Research 22: 123-137.

Gilbert, R.O., 1987. Statistical methods for environmental pollution monitoring. Van Nostrand Reinhold Co., New York, 320 pp.

Goericke, R., Montoya, J.P., 1998. Estimating the contribution of microalgal taxa to chlorophyll a in the field - variations of pigment ratios under nutrient- and light-limited growth. Marine Ecology Progress Series 169: 97-112.

Goericke, R., Repeta, D.J., 1993. Chlorophyll-a and chlorophyll-b and divinyl chlorophyll-a and chlorophyll-b in the open subtropical North-Atlantic Ocean. Marine Ecology-Progress Series 101: 307-313.

Gomi, Y., Taniguchi, A., Fukuchi, M., 2007. Temporal and spatial variation of the phytoplankton assemblage in the eastern Indian sector of the Southern Ocean in summer 2001/2002. Polar Biology 30: 817-827.

Gowing, M.M., Garrison, D.L., Kunze, H.B., Winchell, C.J., 2001. Biological components of Ross Sea short-term particle fluxes in the austral summer of 1995-1996. Deep-Sea Research I 48: 2645-2671.

Haberman, K.L., Ross, R.M., Quetin, L.B., 2003. Diet of the Antarctic krill (Euphausia superba Dana) II. Selective grazing on mixed phytoplankton assemblages. Journal of Experimental Marine Biology and Ecology 283: 97-113.

Hammer, A., Schumann, R., Schubert, H., 2002. Light and temperature acclimation of *Rhodomonas salina* (Cryptophyceae): photosynthetic performance. Aquatic Microbial Ecology 29: 287-296.

Hare, C.E., DiTullio, G.R., Riseman, S.F., Crossley, A.C., Popels, L.C., Sedwick, P.N., Hutchins, D.A., 2007. Effects of changing continuous iron input rates on a Southern Ocean algal assemblage. Deep-Sea Research I 54: 732-746.

Hart, T.J., 1934. On the phytoplankton of the South-west Atlantic and the Bellingshausen Sea, 1929-31. Discovery Reports, 8. University Press, Cambridge.

Hart, T.J., 1937. *Rhizosolenia Curvata Zacharias*, an indicator species in the Southern Ocean. Discovery Reports, 16. University Press, Cambridge.

Hart, T.J., 1942. Phytoplankton periodicity in Antarctic surface waters. Discovery Reports, 21. University Press, Cambridge.

Hartmann, C., Kattner, B.H.G., Richter, K.U., Terbrueggen, A., 1997. Nutrients, dissolved and particulate matter. Berichte zur Polarforschung 0: 44-52.

Havskum, H., Schluter, L., Scharek, R., Berdalet, E., Jacquet, S., 2004. Routine quantification of phytoplankton groups - microscopy or pigment analyses? Marine Ecology Progress Series 273: 31-42.

Henriksen, P., Riemann, B., Kaas, H., Sorensen, H., Sorensen, H., 2002. Effects of nutrient-limitation and irradiance on marine phytoplankton pigments. Journal of Plankton Research 24: 835-858.

Hillebrand, H., Durselen, C., Kirschtel, D., Pollingeher, U., Zohary, T., 1999. Biovolume calculation for pelagic and benthic microalgae. Journal of Phycology 35: 403-424.

Holm-Hansen, O., Mitchell, B.G., 1991. Spatial and temporal distribution of phytoplankton and primary production in the Western Bransfield Strait region. Deep-Sea Research A 38: 961-980.

Holm-Hansen, O., Mitchell, B.G., Hewes, C.D., Karl, D.M., 1989. Phytoplankton blooms in the vicinity of Palmer Station, Antarctica. Polar Biology 10: 49-57.

Hooker, J.D.S., 1844. The botany of the Antarctic voyage of H. M. discovery ships Erebus and Terror in the Years 1839-1843, under the command of Captain Sir James Clark Ross, LVI. Reeve Brothers, London.

Hooker, S.B., Van Heukelem, L., Thomas, C.S., Claustre, H., Ras, J., Barlow, R., Sessions, H., Schlüter, L., Perl, J., Trees, C., Sutuart, V., Head, E. et al., 2005. The second SeaWiFS HPLC analysis round-robin experiment (SeaHARRE-2). TM-2005-212785, NASA Goddard Space Flight Center, Greenbelt, MD.

Houghton, J.T., Ding, Y., Griggs, D.J., Noguer, M., van den Linden, P.J., Dai, X., Maskell, K., Johnson, C.A., 2001. Climate Change 2001: The Scientific Basis. Cambridge University Press, Cambridge, 881 pp.

Iglesias-Rodriguez, M.D., Brown, C.W., Doney, S.C., Kleypas, J., Kolber, D., Kolber, Z., Hayes, P.K., Falkowski, P.G., 2002. Representing key phytoplankton functional groups in ocean carbon cycle models: Coccolithophorids. Global Biogeochemical Cycles 16.

Irigoien, X., Meyer, B., Harris, R., Harbour, D., 2004. Using HPLC pigment analysis to investigate phytoplankton taxonomy: the importance of knowing your species. Helgoland Marine Research 58: 77-82.

Jacques, G., Panouse, M., 1991. Biomass and composition of size fractionated phytoplankton in the Weddell-Scotia confluence zrea. Polar Biology 11: 315-328.

Jeffrey, S.W., 1980. Algal pigment systems. In: P.G. Falkowski (Editor), Primary Productivity in the Sea. Plenum Press, New York, pp. 33-58.

Jeffrey, S.W., 1981. Light Quality And Pigment Adaptations In Micro Algae. Proceedings of the International Botanical Congress: 179.

Jeffrey, S.W., Wright, S.W., Zapata, M., 1999. Recent advances in HPLC pigment analysis of phytoplankton [Review]. Marine & Freshwater Research 50: 879-896.

Kang, S.H., Kang, J.S., Lee, S., Chung, K.H., Kim, D., Park, M.G., 2001. Antarctic phytoplankton assemblages in the marginal ice zone of the northwestern Weddell Sea. Journal of Plankton Research 23: 333-352.

Kang, S.H., Lee, S.H., 1995. Antarctic phytoplankton assemblage in the western Bransfield Strait region, February 1993: composition, biomass, and mesoscale distributions. Marine Ecology-Progress Series 129: 253-267.

Kaplan, A., Kushnir, Y., Cane, M.A., Blumenthal, M.B., 1997. Reduced space optimal analysis for historical data sets: 136 years of Atlantic sea surface temperatures. Journal of Geophysical Research-Oceans 102: 27835-27860.

Knox, G.A., 2007. Biology of the Southern Ocean. Marine Biology. CRC Press, Boca Raton, 621 pp.

Kopczyńska, E.E., Goeyens, L., Semeneh, M., Dehairs, F., 1995. Phytoplankton composition and cell carbon distribution in Prydz Bay, Antarctica - relation to organic particulate matter and its delta-C-13 values. Journal of Plankton Research 17: 685-707.

Kopczyńska, E.E., Savoye, N., Dehairs, F., Cardinal, D., Elskens, M., 2007. Spring phytoplankton assemblages in the Southern Ocean between Australia and Antarctica. Polar Biology 31: 77-88.

Kopczyńska, E.E., Weber, L.H., Elsayed, S.Z., 1986. Phytoplankton species composition and abundance in the indian sector of the Antarctic Ocean. Polar Biology 6: 161-169.

Lance, V.P., Hiscock, M.R., Hilting, A.K., Stuebe, D.A., Bidigare, R.R., Smith, W.O., Barber, R.T., 2007. Primary productivity, differential size fraction and pigment composition responses in two Southern Ocean in situ iron enrichments. Deep-Sea Research I 54: 747-773.

Lancelot, C., Mathot, S., Veth, C., Debaar, H., 1993. Factors controlling phytoplankton iIce-eEdge blooms in the marginal ice-zone of the northwestern Weddell Sea during sea-ice retreat 1988 - field observations and mathematical-modeling. Polar Biology 13: 377-387.

Latasa, M., 2007. Improving estimations of phytoplankton class abundances using CHEMTAX. Marine Ecology Progress Series 329: 13-21.

Latasa, M., Scharek, R., Le Gall, F., Guillou, L., 2004. Pigment suites and taxonomic groups in Prasinophyceae. Journal of Phycology 40: 1149-1155.

Letelier, R.M., Bidigare, R.R., Hebel, D.V., Ondrusek, M., Winn, C.D., Karl, D.M., 1993. Temporal variability of phytoplankton community structure based on pigment analysis. Limnology and Oceanography 38: 1420-1437.

Lewitus, A.J., White, D.L., Tymowski, R.G., Geesey, M.E., Hymel, S.N., Noble, P.A., 2005. Adapting the CHEMTAX method for assessing phytoplankton taxonomic composition in southeastern US estuaries. Estuaries 28: 160-172.

Llewellyn, C.A., Fishwick, J.R., Blackford, J.C., 2005. Phytoplankton community assemblage in the English Channel: a comparison using chlorophyll a derived from HPLC-CHEMTAX and carbon derived from microscopy cell counts. Journal of Plankton Research 27: 103-119.

Lohr, M., Wilhelm, C., 1999. Algae displaying the diadinoxanthin cycle also possess the violaxanthin cycle. Proceedings of the National Academy of Sciences of the United States of America 96: 8784-8789.

Longhurst, A., 1998. Ecological Geography of the Sea. Academic Press, USA, 398 pp.

Mackey, D., Higgins, H., Mackey, M., Holdsworth, D., 1998. Algal class abundances in the western equatorial Pacific: Estimation from HPLC measurements of chloroplast pigments using CHEMTAX. Deep-Sea Research II 45: 1441-1468.

Mackey, M.D., Higgins, H.W., Mackey, D.J., Wright, S.W., 1997. CHEMTAX user's manual: a program for estimating class abundances from chemical markers — application to HPLC measurements of phytoplankton pigments. 229, CSIRO Marine Laboratories, Hobart, Australia.

Mackey, M.D., J.mackey, D., Higgins, H.W., Wright, S.W., 1996. CHEMTAX-a program for estimating class abundances from chemical markers: Application to HPLC measurements of phytoplankton. Marine Ecology Progress Series 144: 265-283.

Mangoni, O., Modigh, M., Conversano, F., Carrada, G.C., Saggiomo, V., 2004. Effects of summer ice coverage on phytoplankton assemblages in the Ross Sea, Antarctica. Deep-Sea Research I 51: 1601-1617.

Martin, J.H., Gordon, R.M., Fitzwater, S.E., 1990. Iron in Antarctic Waters. Nature (London) 345: 156-158.

Martinson, D.G., Iannuzzi, R.A., 1998. Antarctic ocean-ice interaction: implications from ocean bulk property distributions in the Weddell gyre. In: M.O. Jeffries (Editor), Antarctic Sea Ice: Physical Processes, Interactions, and Variability. AGU Antarctic Research Series. American Geological Union, Washington, DC, pp. 243-271.

Martinson, D.G., Iannuzzi, R.A., 2003. Spatial/temporal patterns in Weddell Gyre characteristics and their relationship to global climate. Journal of Geophysical Research-Oceans 108:8083..

Martinson, D.G., Stammerjohn, S., Iannuzzi, R.A., Smith, R.C., Vernet, M., 2008 (accepted). Palmer, Antarctica, Long Term Ecological Research Program first twelve years: physical oceanography, spatio-temporal variability. Deep-Sea Research II.

Massana, R., Balague, V., Guillou, L., Pedros-Alio, C., 2004. Picoeukaryotic diversity in an oligotrophic coastal site studied by molecular and culturing approaches. Fems Microbiology Ecology 50: 231-243.

Medlin, L.K., Lange, M., Nothig, E.M., 2000. Genetic diversity in the marine phytoplankton: a review and a consideration of Antarctic phytoplankton. Antarctic Science 12: 325-333.

Medlin, L.K., Metfies, K., Mehl, H., Wiltshire, K., Valentin, K., 2006. Picoeukaryotic plankton diversity at the Helgoland time series site as assessed by three molecular methods. Microbial Ecology 52: 53-71.

Menden-Deuer, S., Lessard, E.J., Satterberg, J., 2001. Effect of preservation on dinoflagellate and diatom cell volume and consequences for carbon biomass predictions. Marine Ecology Progress Series 222: 41-50.

Mitchell, B.G., Holmhansen, O., 1991. Observations and modeling of the antarctic phytoplankton crop in relation to mixing depth. Deep-Sea Research Part A 38: 981-1007.

Moisan, T.A., Ellisman, M.H., Buitenhuys, C.W., Sosinsky, G.E., 2006. Differences in chloroplast ultrastructure of *Phaeocystis antarctica* in low and high light. Marine Biology 149: 1281-1290.

Moline, M.A., Claustre, H., Frazer, T.K., Schofield, O., Vernet, M., 2004. Alteration of the food web along the Antarctic Peninsula in response to a regional warming trend. Global Change Biology 10: 1973-1980.

Moline, M.A., Prézelin, B.B., 1996. Long-term monitoring and analyses of physical factors regulating variability in coastal Antarctic phytoplankton biomass, in situ productivity and taxonomic composition over subseasonal, seasonal and interannual time scales. Marine Ecology Progress Series 145: 143-160.

Moline, M.A., Prézelin, B.B., 1997. High resolution time-series data for 91/92 primary production and related parameters at a Palmer LTER coastal site: implications for modeling carbon fixation in the Southern Ocean. Polar Biology 17: 39-53.

Montagnes, D.J.S., Berges, J.A., Harrison, P.J., Taylor, F.J.M., 1994. Estimating carbon, nitrogen, protein, and chlorophyll from volume in marine-phytoplankton. Limnology and Oceanography 39: 1578-1578.

Montagnes, D.J.S., Franklin, D.J., 2001. Effect of temperature on diatom volume, growth rate, and carbon and nitrogen content: reconsidering some paradigms. Limnology and Oceanography 46: 2008-2018.

Moore, J.K., Abbott, M.R., 2000. Phytoplankton chlorophyll distributions and primary production in the Southern Ocean. Journal of Geophysical Research-Oceans 105: 28709-28722.

Mullin, M.M., Sloan, P.R., Eppley, R.W., 1966. Relationship between carbon content, cell volume, and Aarea in phytoplankton. Limnology and Oceanography 11: 307-311.

Mura, M.P., Satta, M.P., Agusti, S., 1995. Water-mass influence on summer antarctic phytoplankton biomass and community structure. Polar Biology 15: 15-20.

Olson, R.J., Sosik, H.M., 2007. A submersible imaging-in-flow instrument to analyze nano- and microplankton: Imaging FlowCytobot Limnology and Oceanography Methods 5: 195-203.

Orsi, A.H., Whitworth, T., Nowlin, W.D., 1995. On the meridional extent and fronts of the Antarctic Circumpolar Current. Deep-Sea Research I 42: 641-673.

Padisak, J., Soroczki-Pinter, E., Rezner, Z., 2003. Sinking properties of some phytoplankton shapes and the relation of form resistance to morphological diversity of plankton - an experimental study. Hydrobiologia 500: 243-257.

Parsons, T.R., Maita, Y., Lalli, C.M., 1984. A Manual of Chemical and Biological Methods for Seawater Analysis. Pergamon Press, New York, 173 pp.

Peeken, I., 1997. Photosynthetic pigment fingerprints as indicators of phytoplankton biomass and development in different water masses of the Southern Ocean during austral spring. Deep-Sea Research II 44: 261-282.

Peloquin, J.A., Smith, W.O., 2007. Phytoplankton blooms in the Ross Sea, Antarctica: interannual variability in magnitude, temporal patterns, and composition. Journal of Geophysical Research-Oceans 112.

Pennington, M., 1983. Efficient estimators of abundance, for fish and plankton surveys. Biometrics 39: 281-286.

Perissinotto, R., Rae, C.M.D., Boden, B.P., Allanson, B.R., 1990. Vertical stability as a controlling factor of the marine-phytoplankton production at the Prince-Edward Archipelago (Southern-Ocean). Marine Ecology Progress Series 60: 205-209.

Perrin, R., Lu, P., Marchant, H., 1987. Seasonal variation in marine phytoplankton and ice algae at a shallow antarctic coastal site. Hydrobiologia 146: 33-46.

Popova, E.E., Ryabchenko, V.A., Fasham, M.J.R., 2000. Biological pump and vertical mixing in the Southern Ocean: Their impact on atmospheric CO2. Global Biogeochemical Cycles 14: 477-498.

Prézelin, B.B., Hofmann, E.E., Mengelt, C., Klinck, J.M., 2000. The linkage between Upper Circumpolar Deep Water (UCDW) and phytoplankton assemblages on the west Antarctic Peninsula continental shelf. Journal of Marine Research 58: 165-202.

Prézelin, B.B., Hofmann, E.E., Moline, M., Klinck, J.M., 2004. Physical forcing of phytoplankton community structure and primary production in continental shelf waters of the Western Antarctic Peninsula. Journal of Marine Research 62: 419-460.

Prézelin, B.B., Tilzer, M.M., Schofield, O., Haese, C., 1991. The control of the production process of phytoplankton by the physical structure of the aquatic environment with special reference to its optical-properties. Aquatic Sciences 53: 136-186.

Priddle, J., Smetacek, V., Bathmann, U., 1992. Antarctic marine primary production, biogeochemical carbon cycles and climatic-change. Philosophical Transactions of the Royal Society of London Series B-Biological Sciences 338: 289-297.

Quetin, L.B., Ross, R.M., Frazer, T.K., Amsler, M.O., Wyatt-Evens, C., Oakes, S.A., 2003. Growth of larval krill, *Euphausia superba*, in fall and winter west of the Antarctic Peninsula. Marine Biology 143: 833-843.

Quetin, L.B., Ross, R.M., Fritsen, C.H., Vernet, M., 2007. Ecological responses of Antarctic krill to environmental variability: can we predict the future? Antarctic Science 19: 253-266.

Raven, J.A., Falkowski, P.G., 1999. Oceanic sinks for atmospheric CO2. Plant Cell Environment 22: 741-755.

Riegman, R., Kraay, G.W., 2001. Phytoplankton community structure derived from HPLC analysis of pigments in the Faroe-Shetland channel during summer 1999: the distribution of taxonomic groups in relation to physical/chemical conditions in the photic zone. Journal of Plankton Research 23: 191-205.

Rodriguez, F., Varela, M., Zapata, M., 2002. Phytoplankton assemblages in the Gerlache and Bransfield Straits (Antarctic Peninsula) determined by light microscopy and CHEMTAX analysis of HPLC pigment data. Deep-Sea Research II 49: 723-747.

Rodríguez, J., Jimenez-Gomez, F., Blanco, J.M., Figueroa, M.L., 2002. Physical gradients and spatial variability of the size structure and composition of phytoplankton in the Gerlache Strait (Antarctica). Deep-Sea Research II 49: 693-706.

Ross, R., Prézelin, B., Smith, R., Quetin, L., 1990. Palmer, Antarctica LTER: Long-Term Ecological Research on the Antarctic Marine Ecosystem: An Ice-Dominated Environment. Palmer Station Antarctica Long Term Ecological Research, Retrieved 21 April 2008 from: http://pal.lternet.edu/docs/publications/proposals/9096proposal.

Ross, R.M., Quetin, L.B., Martinson, D.G., Iannuzzi, R., Stammerjohn, S., Smith, R.C., 2008 (accepted). Patterns of distribution of five dominant zooplankton species in the epipelagic zone West of the Antarctic Peninsula, 1993 – 2004. Deep-Sea Research II.

Ross, R.M., Quetin, L.B., Newberger, T., Oakes, S.A., 2004. Growth and behavior of larval krill (Euphausia superba) under the ice in late winter 2001 west of the Antarctic Peninsula. Deep-Sea Research II 51: 2169-2184.

Sakshaug, E., Johnsen, G., Andresen, K., Vernet, M., 1991. Modeling of light-dependent algal photosynthesis and growth experiments with the Barents Sea diatoms *Thalassiosira-Nordenskioldii* and *Chaetoceros-Furcellatus*. Deep-Sea Research A 38: 415-430.

Sakshaug, E., Skjoldal, H.R., 1989. Life at the ice edge. Ambio 18: 60-67.

Sarmiento, J.L., Gruber, N., Brzezinski, M.A., Dunne, J.P., 2004. High-latitude controls of thermocline nutrients and low latitude biological productivity. Nature 427: 56-60.

Sarmiento, J.L., Toggweiler, J.R., 1984. A new model for the role of the oceans in determining atmospheric pCO2. Nature 308: 621-624.

Savidge, G., Harbour, D.S., Gilpin, L.C., Boyd, P.W., 1995. Phytoplankton distributions and production in the Bellingshausen Sea, Austral spring 1992. Deep-Sea Research II 42: 1201-1224.

Schlüter, L., Møhlenberg, F., 2003. Detecting presence of phytoplankton groups with non-specific pigment signatures. Journal Of Applied Phycology 15: 465-476.

Schlüter, L., Møhlenberg, F., Havskum, H., Larsen, S., 2000. The use of phytoplankton pigments for identifying and quantifying phytoplankton groups in coastal areas: testing the influence of light and nutrients on pigment/chlorophyll a ratios. Marine Ecology Progress Series 192: 49-63.

See, J.H., Campbell, L., Richardson, T.L., Pinckney, J.L., Shen, R., 2005. Combining new technologies for determination of phytoplankton community structure in the northern Gulf of Mexico. Journal of Phycology 41.

Smetacek, V., 1999. Diatoms and the ocean carbon cycle. Protist 150: 25-32.

Smetacek, V., Scharek, R., Gordon, L.I., Eicken, H., Fahrbach, E., Rohardt, G., Moore, S., 1992. Early spring phytoplankton blooms in ice platelet layers of the southern Weddell Sea, Antarctica. Deep-Sea Research 39: 153-168.

Smith, D.A., Hofmann, E.E., Lascara, C.M., Klinck, J.M., 1999. Hydrography and circulation of the west Antarctic Peninsula continental shelf. Deep-Sea Research I 46: 925-949.

Smith, K.L., Robison, B.H., Helly, J.J., Kaufmann, R.S., Ruhl, H.A., Shaw, T.J., Twining, B.S., Vernet, M., 2007. Free-drifting icebergs: Hot spots of chemical and biological enrichment in the Weddell Sea. Science 317: 478-482.

Smith, R.C., Baker, K.S., Byers, M.L., Stammerjohn, S.E., 1998. Primary productivity of the palmer long term ecological research area and the Southern Ocean. Journal of Marine Systems 17: 245-259.

Smith, R.C., Baker, K.S., Dierssen, H.M., Stammerjohn, S.E., Vernet, M., 2001. Variability of primary production in an Antarctic marine ecosystem as estimated using a multi-scale sampling strategy. American Zoologist 41: 40-56.

Smith, R.C., Baker, K.S., Fraser, W.R., Hofmann, E.E., Karl, D.M., Klinck, J.M., Quetin, L.B., Prezelin, B.B., Ross, R.M., Trivelpiece, W.Z., Vernet, M., 1995. The Palmer LTER: A long-term ecological research program at Palmer Station, Antarctica. Oceanography 8: 77-86.

Smith, R.C., Domack, E.W., Emslie, S.D., Fraser, W.R., Ainley, D.G., Baker, K.S., Kennett, J., Leventer, A., Mosley-Thompson, E., Stammerjohn, S.E., Vernet, M., 1999. Marine ecosystems sensitivity to historical climate change: Antarctic Peninsula. BioScience 49: 393-404.

Smith, R.C., Martinson, D.G., Stammerjohn, S.E., Iannuzzi, R.A., Ireson, K., 2008 (accepted). Bellingshausen and western Antarctic Peninsula region: pigment biomass and sea ice spatial/temporal distribution and interannual variability. Deep-Sea Research II.

Smith, W.O., Asper, V.L., 2001. The influence of phytoplankton assemblage composition on biogeochemical characteristics and cycles in the southern Ross Sea, Antarctica. Deep Sea Research I 48: 137-161.

Smith, W.O., Marra, J., Hiscock, M.R., Barber, R.T., 2000. The seasonal cycle of phytoplankton biomass and primary productivity in the Ross Sea, Antarctica. Deep-Sea Research II 47: 3119-3140.

Smith, W.O., Nelson, D.M., 1985. Phytoplankton bloom produced by a receding ece edge in the Ross Sea: spatial coherence with the density rield. Science 227: 163-166.

Smith, W.O., Nelson, D.M., 1986. Importance of ece edge phytoplankton production in the Southern-Ocean. Bioscience 36: 251-257.

Sosik, H.M., Olson, R.J., 2002. Phytoplankton and iron limitation of photosynthetic efficiency in the Southern Ocean during late summer. Deep-Sea Research I 49: 1195-1216.

Sosik, H.M., Olson, R.J., 2007. Automated taxonomic classification of phytoplankton sampled with imaging-in-flow cytometry. Limnology and Oceanography-Methods 5: 204-216.

Stammerjohn, S.E., Martinson, D.G., Smith, R.C., Iannuzzi, R.A., 2008 (accepted). Sea ice in the western Antarctic Peninsula region: spatio-temporal variability from ecological and climate change perspectives. Deep-Sea Research II.

Steeman-Nielsen, E., 1952. The use of radio-active carbon (C14) for measuring organic production in the sea. Journal du conseil international pour l'exploration de la mar 18: 117-140.

Stolte, W., Kraay, G.W., Noordeloos, A.A.M., Riegman, R., 2000. Genetic and physiological variation in pigment composition of *Emiliania huxleyi* (Prymnesiophyceae) and the potential use of its pigment ratios as a quantitative physiological marker. Journal of Phycology 36: 529-539.

Sullivan, B., Matlick, H.A., Prezelin, B.B., 1994. Palmer LTER: Patterns of distribution of inorganic macronutrients, phytoplankton pigmentation, and photosynthetic activity in an ice-dominated ecosystem in austral winter 1993. Antarctic Journal of the United States 29: 207-211.

Suzuki, K., Hinuma, A., Saito, H., Kiyosawa, H., Liu, H.B., Saino, T., Tsuda, A., 2005. Responses of phytoplankton and heterotrophic bacteria in the northwest subarctic Pacific to in situ iron fertilization as estimated by HPLC pigment analysis and flow cytometry. Progress in Oceanography 64: 167-187.

Tarantola, A., 1987. Inverse Problem Theory: Methods for Data Fitting and Parameter Estimation. Elsevier, New York, 613 pp.

Tréguer, P., Jacques, G., 1992. Dynamics of nutrients and phytoplankton, and fluxes of carbon, nitrogen, and silicon in the Antarctic Ocean. Polar Biology 12: 149-162.

Utermöhl, H., 1931. Neue Wege in der quantitativen Erfassung des Planktons. (Mit besonderer Berücksichtigung des Ultraplanktons.). Verh. Int. Verein. Limnol. 5: 567-596.

Utermöhl, H., 1958. Zur Vervollkommnung der quantitativen Phytopolankton-Methodik. Mitt. int. Ver. theor. angew. Limnol. 9: 1-38.

van Leeuwe, M.A., de Baar, H.J.W., Veldhuis, M.J.W., 1998. Pigment distribution in the Pacific region of the Southern Ocean (autumn 1995). Polar Biology 19: 348-353.

van Leeuwe, M.A., van Sikkelerus, B., Gieskes, W.W.C., Stefels, J., 2005. Taxon specific differences in photoacclimation to fluctuating irradiance in an Atarctic diatom and a green flagellate. Marine Ecology Progress Series 288: 9-19.

van Oijen, T., van Leeuwe, M.A., Granum, E., Weissing, F.J., Bellerby, R.G.J., Gieskes, W.W.C., de Baar, H.J.W., 2004. Light rather than iron controls photosynthate production and allocation in Southern Ocean phytoplankton populations during austral autumn. Journal of Plankton Research 26: 885-900.

Varela, M., Fernandez, E., Serret, P., 2002. Size-fractionated phytoplankton biomass and primary production in the Gerlache and south Bransfield Straits (Antarctic Peninsula) in Austral summer 1995-1996. Deep-Sea Research II 49: 749-768.

Vaughan, D.G., Marshall, G.J., Connolley, W.M., Parkinson, C., Mulvaney, R., Hodgson, D.A., King, J.C., Pudsey, C.J., Turner, J., 2003. Recent rapid regional climate warming on the Antarctic Peninsula. Climatic Change 60: 243-274.

Vernet, M., Martinson, D., Iannuzzi, R., Stammerjohn, S., Kozlowski, W., Sines, K., Smith, R., Garibotti, I., 2008 (accepted). Primary production within the sea ice zone west of the Antarctic Peninsula: sea ice, summer mixed layer and irradiance. Deep-Sea Research II.

Vernet, M., Smith, R.C., 2007. Measuring and modelling primary production in marine pelagic ecosystems. In: T.J. Fahey and A.K. Knapp (Editors), Principles and Standards for Measuring Primary Production. Long Term Ecological Research Network Series. Oxford University Press, New York, pp. 142-174.

Villafañe, V.E., Helbling, E.W., Holmhansen, O., 1995. Spatial and temporal variability of phytoplankton biomass and taxonomic composition around Elephant-Island, Antarctica, during the summers of 1990-1993. Marine Biology 123: 677-686.

Volk, T., Hoffert, M., 1985. Ocean carbon pumps: Analysis of relative strengths and efficiencies in ocean-driven atmospheric CO2 changes. In: E. Sundquist and W. Broeker (Editors), The Carbon Cycle and Atmospheric CO2: Natural Variations, Archean to Present. Geophysical Monograph Series, pp. 99-110.

Walsh, J.J., Dieterle, D.A., Lenes, J., 2001. A numerical analysis of carbon dynamics of the Southern Ocean phytoplankton community: the roles of light and grazing in effecting both sequestration of atmospheric CO2 and food availability to krill. Deep-Sea Research I 48: 1-48.

Waters, K., Smith, R.C., 1992. Palmer LTER: A sampling grid for the Palmer LTER program. Antarctic Journal of the United States 27: 236-239.

Wilmotte, A., Demonceau, C., Goffart, A., Hecq, J.H., Demoulin, V., Crossley, A.C., 2002. Molecular and pigment studies of the picophytoplankton in a region of the Southern Ocean (42-54 degrees S, 141-144 degrees E) in March 1998. Deep-Sea Research II 49: 3351-3363.

Wright, S.W., Jeffrey, S.W., 1987. Fucoxanthin pigment markers of marine-phytoplankton analyzed by HPLC and HPTLC. Marine Ecology-Progress Series 38: 259-266.

Wright, S.W., Jeffrey, S.W., Mantoura, R.F.C., Llewellyn, C.A., Bjørnland, T., Repeta, D., Welschmeyer, N., 1991. Improved HPLC method for the analysis of chlorophylls and carotenoids from marine phytoplankton. Marine Ecology Progress Series 77: 183-196.

Wright, S.W., Thomas, D.P., Marchant, H.J., Higgins, H.W., Mackey, M.D., Mackey, D.J., 1996. Analysis of phytoplankton of the Australian sector of the Southern Ocean: comparisons of microscopy and size frequency data with interpretations of pigment HPLC data using the 'CHEMTAX' matrix factorisation program. Marine Ecology Progress Series 144: 285-298.

Wright, S.W., van den Enden, R.L., 2000. Phytoplankton community structure and stocks in the East Antarctic marginal ice zone (BROKE survey, January-March 1996) determined by CHEMTAX analysis of HPLC pigment signatures. Deep-Sea Research II 47: 2363-2400.

Wulff, A., Wängberg, S.A., 2004. Spatial and vertical distribution of phytoplankton pigments in the eastern Atlantic sector of the Southern Ocean. Deep-Sea Research II 51: 2701-2713.

Zapata, M., Jeffrey, S.W., Wright, S.W., Rodriguez, F., Garrido, J.L., Clementson, L., 2004. Photosynthetic pigments in 37 species (65 strains) of Haptophyta: implications for oceanography and chemotaxonomy. Marine Ecology Progress Series 270: 83-102.

Zapata, M., Rodríguez, F., Garrido, J.L., 2000. Separation of chlorophylls and carotenoids from marine phytoplankton: a new HPLC method using a reversed phase C-8 column and pyridine-containing mobile phases. Marine Ecology Progress Series 195: 29-45.

Zar, J.H., 1999. Biostatistical Analysis. Prentice Hall, Inc., Upper Saddle River, NJ, 663 pp.

APPENDIX A

LITERATURE REVIEW

Literature review of Southern Ocean composition work and studies in various regions specifically employing CHEMTAX for determination of composition.

Author	Year Pub.	Study Region	Study Time Frame	Method(s) Employed	Relevant Findings / Conclusions
Kopczyńska et al.	1986	40-60°S, South of Africa	Mar 1980	microscopy	data reported as cell counts only; flagellates most abundant north of the Polar Front;
Fryxell and Kendrick	1988	Weddell Sea ice edge	Jun 1995	microscopy	diatom and haptophyte dominance
Buma et al.	1990	Drake Passage, Bransfield Strait, Scotia Sea, Northern Weddell	Mar - Apr 1987	pigments, linear regression	prymnesiophytes as common as diatoms in Atlantic sector
Jacques and Panouse	1991	Weddell-Scotia Confluence	Nov 1988 – Jan 1989	microscopy	large diatoms dominated Scotia Sea; mixed small diatom, dinoflagellates, crytophytes, haptophytes community in Weddell MIZ; suggests community impacted by krill grazing
Letelier et al.	1993	Hawaii	Feb 1998 - Oct 1991	pigments (inverse least squares regression algorithm)	
Kang and Lee	1995	Drake Passage, Bransfield Strait	Dec 1993	microscopy	*Cryptomonas sp.* and *Phaeocystis antarctica* dominated (83%) in the Bransfield, diatoms dominated (84%) in the Drake
Kopczyńska et al.	1995	Prydz Bay (SW of Australia)	Jan - Feb 1991	microscopy	diatom dominance (~80%) with flagellates also present
Mura et al.	1995	Gerlache, Bransfield Straits, Weddell/Bellingshausen Confluence	Jan - Feb 1993	Microscopy	cryptophyte dominance (~90%); low biomass associated with strong mixing; high biomass at confluences; associates community structure with mesoscale water masses
Andersen et al.	1996	Bermuda, Hawaii	Jul 1992, Apr 1993	pigments (Letelier 1993 algorithms), microscopy	generally good agreement between methods but increasing disparity with depth; hypothesize this due to depth-dependent accessory pigment changes
Mackey et al.	1996	Southern Ocean and Equatorial Pacific		CHEMTAX	methods paper; used synthesized data sets

(continued)

Author	Year Pub.	Study Region	Study Time Frame	Method(s) Employed	Relevant Findings / Conclusions
Wright et al.	1996	east Antarctica (South of Australia)	Mar 1987	CHEMTAX, microscopy	methods correlated strongly; CHEMTAX detected crytophytes when missed by microscopy
Peeken	1997	SW of Africa, from 47 - 60° S	Oct - Nov 1992	pigments, regression	found diatoms at polar front, flagellates at ACC; no cryptophytes theorized due to salp grazing
Barlow et al.	1998	Bellingshausen Sea	Nov - Dec 1992	pigments; fixed ratios	diatoms dominant in and near ice edge; combination of other flagellates greater than diatoms at open water stations
Ferrario et al.	1998	Gerlache, Southern Bransfield Straits	Nov 1989	microscopy	found diatom (*Chatoceros*) resting spores
Mackey	1998	western Equatorial Pacific	Oct 1990	CHEMTAX	
van Leeuwe et al.	1998	Pacific region transect, along 90°W, 51 – 70°S	Mar-May 1995	pigments, fixed ratios	diatoms dominant S of Polar Front
Arrigo et al.	1999	Ross Sea	1996-1997	pigments, 3 groups associated with 3 marker pigments	diatoms dominated in stratified waters; *Phaeocystis antarctica* in more deeply mixed waters
Jeffrey et al.	1999				review of advances in HPLC and chemotaxonomic techniques
Schlüter et al.	2000	laboratory, cultures from coastal/estuarine waters	Jun 1996	CHEMTAX, microscopy	good agreement between methods except in presence of small microflagellates, which lead to high subjectivity in microscopic counts
Wright and van den Enden	2000	East Antarctica (South of Australia)	Jan - Mar 1996	CHEMTAX	stratified waters associated with diatoms, well mixed regions with mix of prasinophytes and haptophytes
Kang et al.	2001	northern Weddell	Jan 1995	microscopy	*Phaeocystis* and diatom dominance
Riegman and Kraay	2001	Equatorial Pacific (Faroe-Shetland Channel)	1999	CHEMTAX	
Henrikson et al.	2002	laboratory; cultures from Danish fjords	1997, 1998	CHEMTAX	

(continued)

Author	Year Pub.	Study Region	Study Time Frame	Method(s) Employed	Relevant Findings / Conclusions
Rodriguez et al.	2002	Gerlache and Bransfield Straits, wAP	Dec 1995 - Jan 1996	CHEMTAX, microscopy	diatoms, *Phaeocystis*, cryptomonads and flagellates dominant; some discrepancies between methods for small flagellates
Suzuki et al.	2002	Bering Sea	Jun 1995	CHEMTAX	
Carreto et al.	2003	Río del Plato estuary, Argentina	Nov 1999	CHEMTAX, microscopy	
DiTullio et al.	2003	South Pacific, South of New Zealand	Jan – Mar 1996	CHEMTAX	diatoms, cryptophytes and crysophytes dominant above 1% light depth; haptophytes and prasinophytes dominant at or below 1% light depth (results for stations > 60°S)
Furaya et al.	2003	East China Sea	Apr 1996	CHEMTAX	
Schlüter and Møhlenberg	2003	Danish Estuaries	Mar - Dec 1988	CHEMTAX	method development for determination on input matrices; suggests size fractionation of samples for improved results
Irigoien et al.	2004	English Channel	Jul 1997, Jun 1998	CHEMTAX	stresses need to know input groups for proper CHEMTAX estimates
Havskum et al.	2004	laboratory	Jun 1998	CHEMTAX, microscopy, flow-cytometry	CHEMTAX recommended with microscopy and flow cytometry for screening of dominant species
Wulff and Wänberg	2004	South of South Africa, to 60.5° S	Jan 1998	CHEMTAX	sampled "winter ice edge", "spring ice edge" and "Antarctic Polar front"; diatoms and haptophytes dominant; surface / deep differences seen only in South
Lewitus et al.	2005	southeastern US Estuaries	Aug 1998 – Aug 1999	CHEMTAX, microscopy	
Llewellyn et al.	2005	English Channel	Mar 1999 - Oct 2002	CHEMTAX, microscopy	technique comparison; strong relationship for diatoms, weak for others

(continued)

Author	Year Pub.	Study Region	Study Time Frame	Method(s) Employed	Relevant Findings / Conclusions
See et al.	2005	Texas gulf coast	Mar 2004	Fluoroprobe, Flow-CAM, CHEMTAX, microscopy	goal was to evaluate usefulness of Flow-CAM; good agreement between methods except in presence of green algae and cryptophytes
Delizo et al.	2007	Sub-Antarctic, South of New Zealand	2000, 2001	CHEMTAX, using DiTullio et al. ratios	nanoflagellate and diatom dominance; assemblages controlled by both top-down and bottom-up processes
Gomi	2007	Eastern India Section of Southern Ocean	Nov 01 - Mar 02	microscopy	diatom dominance with weak stability, Phaeocystis with strong
Latasa	2007	laboratory		CHEMTAX	tested for methodological improvements to CHEMTAX estimations; suggests applying output ratio as input of successive runs
Peloquin and Smith	2007	Ross Sea	Dec 2001, Feb 2002, Dec 2003, Feb 2004	not described	haptophyte and diatom dominance; diatoms hypothesized to be associated with modified circumpolar deep water

APPENDIX B

FIGURES

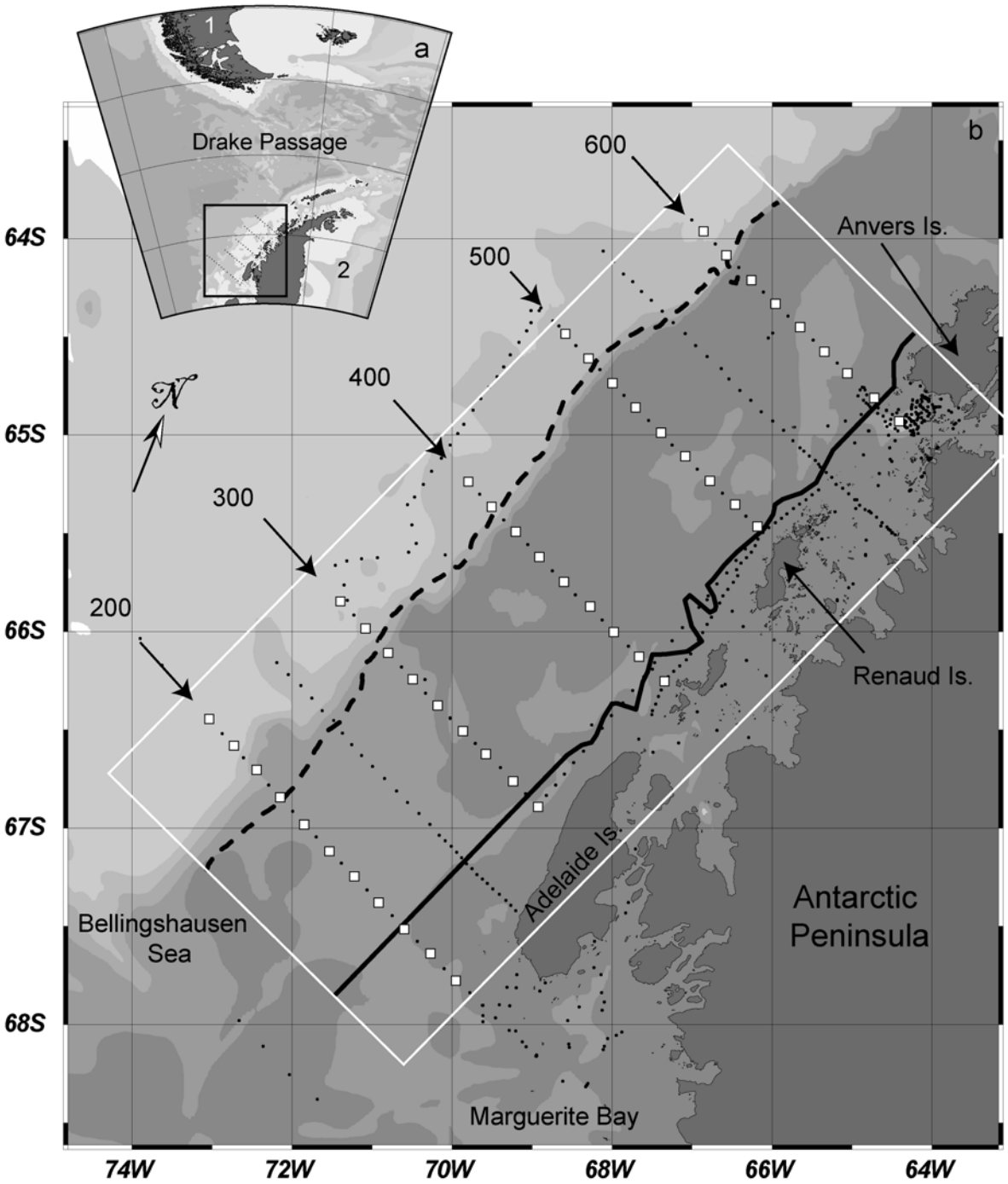

Figure 1. Map of sampling region. Inset map (a) includes the southern tip of South America (1) and the Weddell Sea (2), and the black box marks the region blown up in main map (b). Cardinal lines 200-400 are marked and cardinal stations (sampled 8-12 years) are indicated by white boxes; stations visited fewer than seven years indicated by black circles. Solid and dotted black lines demark outer limits of shelf and slope regions, respectively, and the white box indicates region included in time series analysis. Note inset map (a) is South Polar Orthographic projection while main map (b) is Mercator projection. Arrow indicates north for main map only.

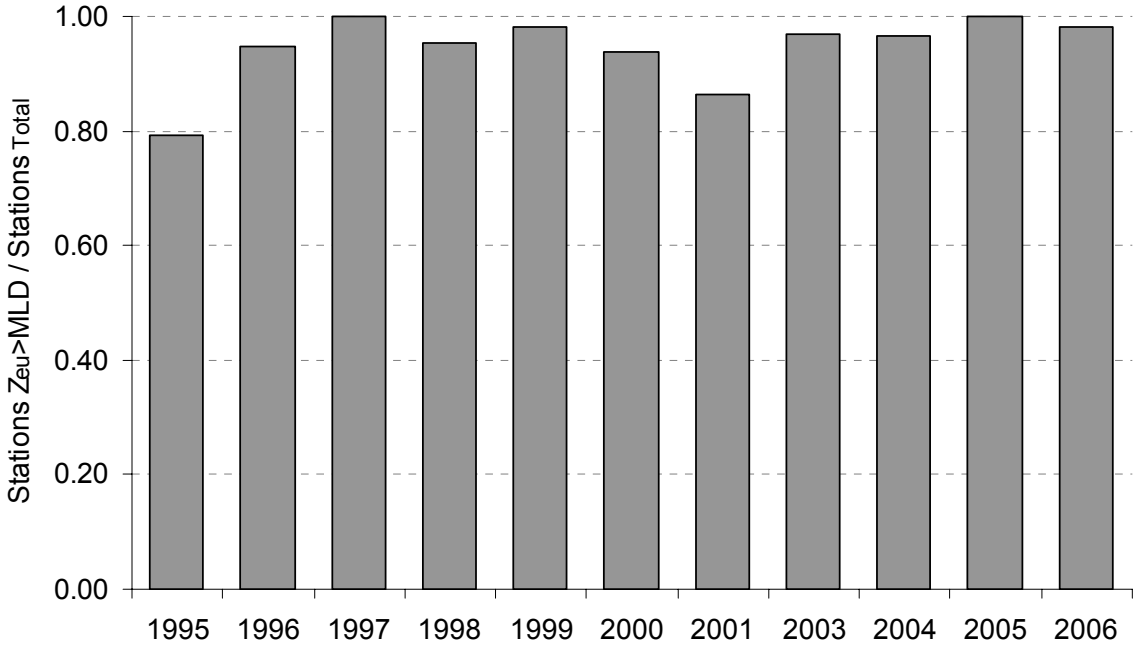

Figure 2. Euphotic zone vs. mixed layer depth comparison by year, 1995-2006. Bars indicate proportion of total stations sampled where the eupotic zone depth (Z_{eu}) was deeper than the mixed layer depth (MLD).

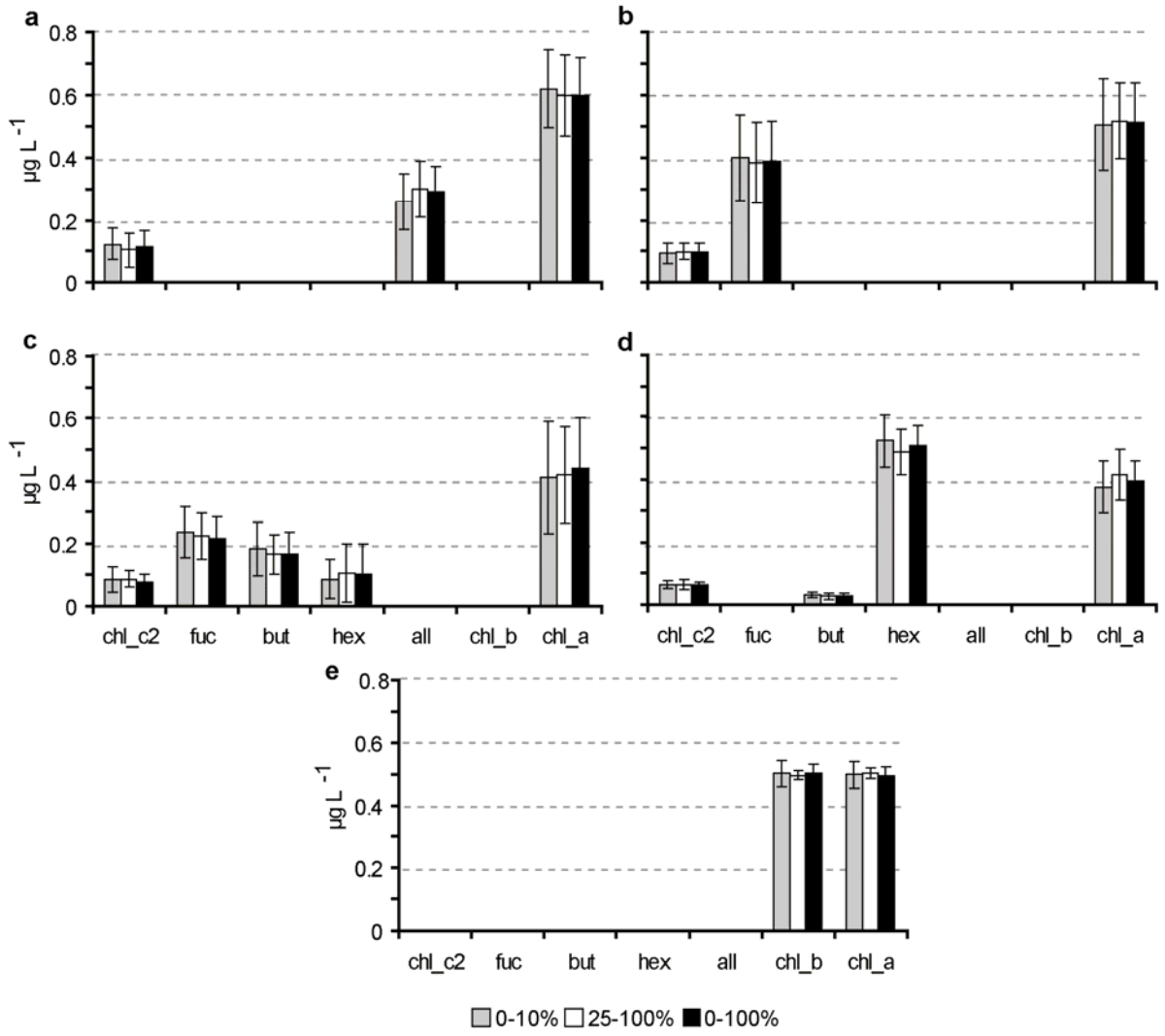

Figure 3. Final pigment ratios based on light bins. Subplots are: (a) cryptophytes, (b) diatoms, (c) mixed flagellates, (d) type 4 haptophytes, (e) prasinophytes. All units are in terms of µg L^{-1} chl_a and error bars represent one standard deviation between individual years.

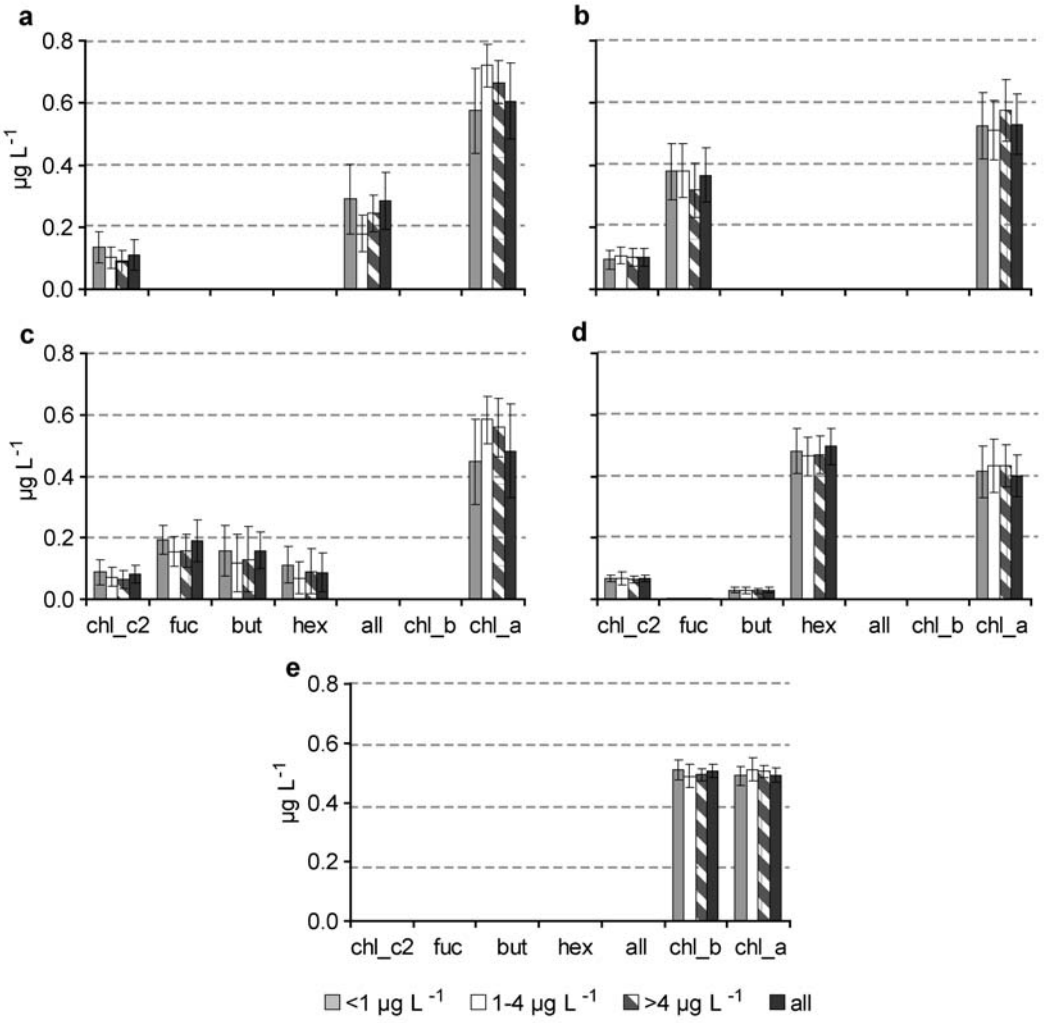

Figure 4. Final pigment ratios based on µg L^{-1} chl_a. Subplots are: (a) cryptophytes, (b) diatoms, (c) mixed flagellates, (d) type 4 haptophytes, (e) prasinophytes. All units are in terms of µg L^{-1} chl_a and error bars represent one standard deviation between individual years.

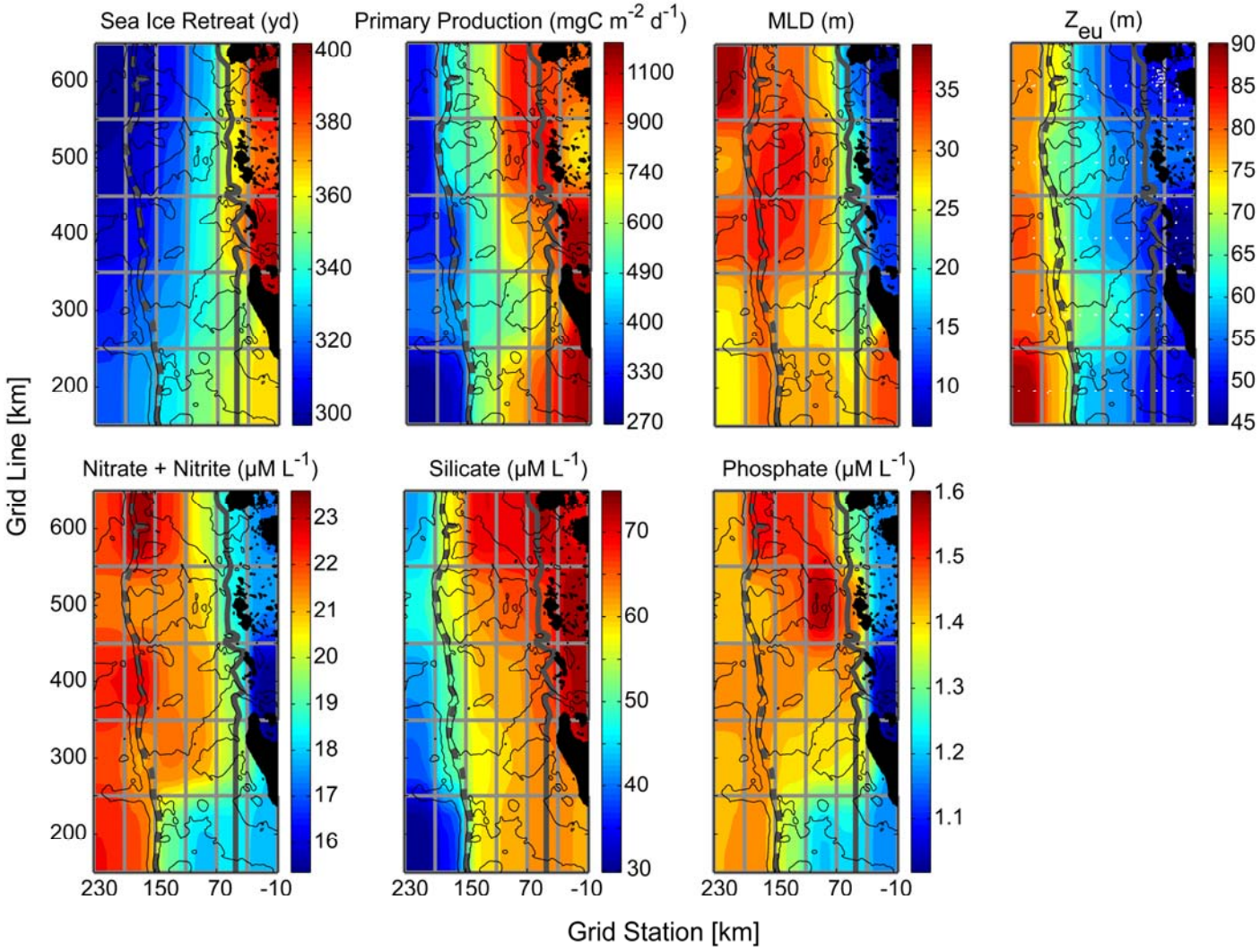

Figure 5. Climatologies of primary physical and biologal variables influencing phytoplankton along the wAP. Note each plot has an independent color bar.

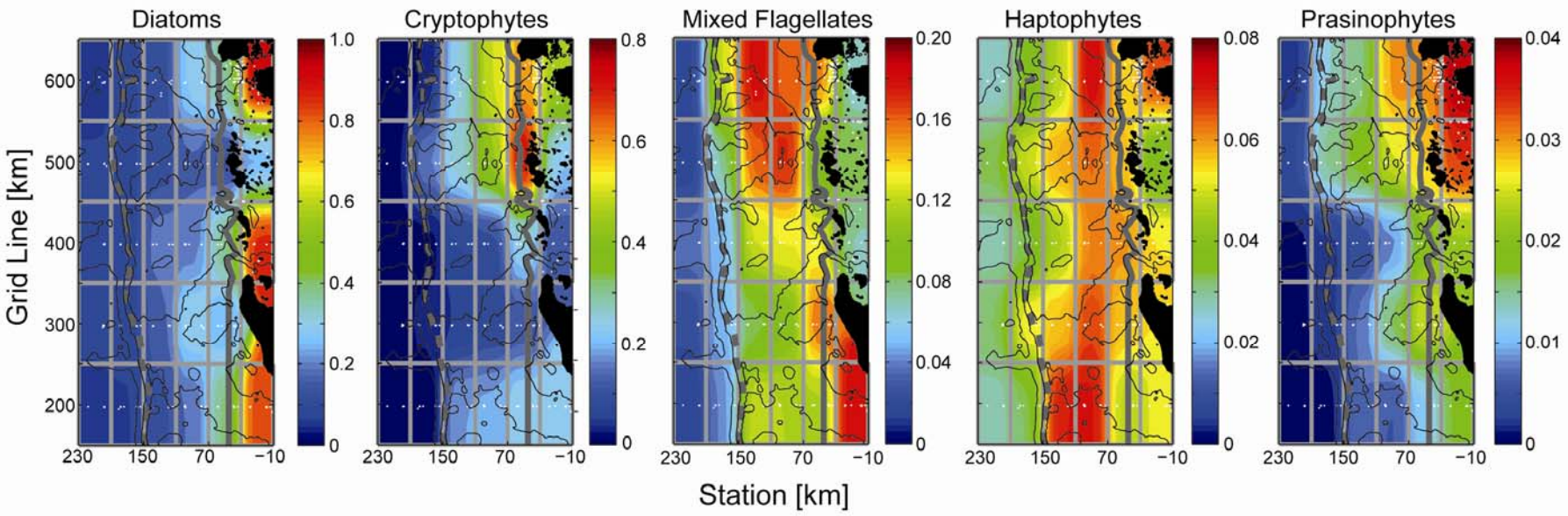

Figure 6. 50% Light depth climatologies, in µg L^{-1} chl_a. Note each group has independent colorbar.

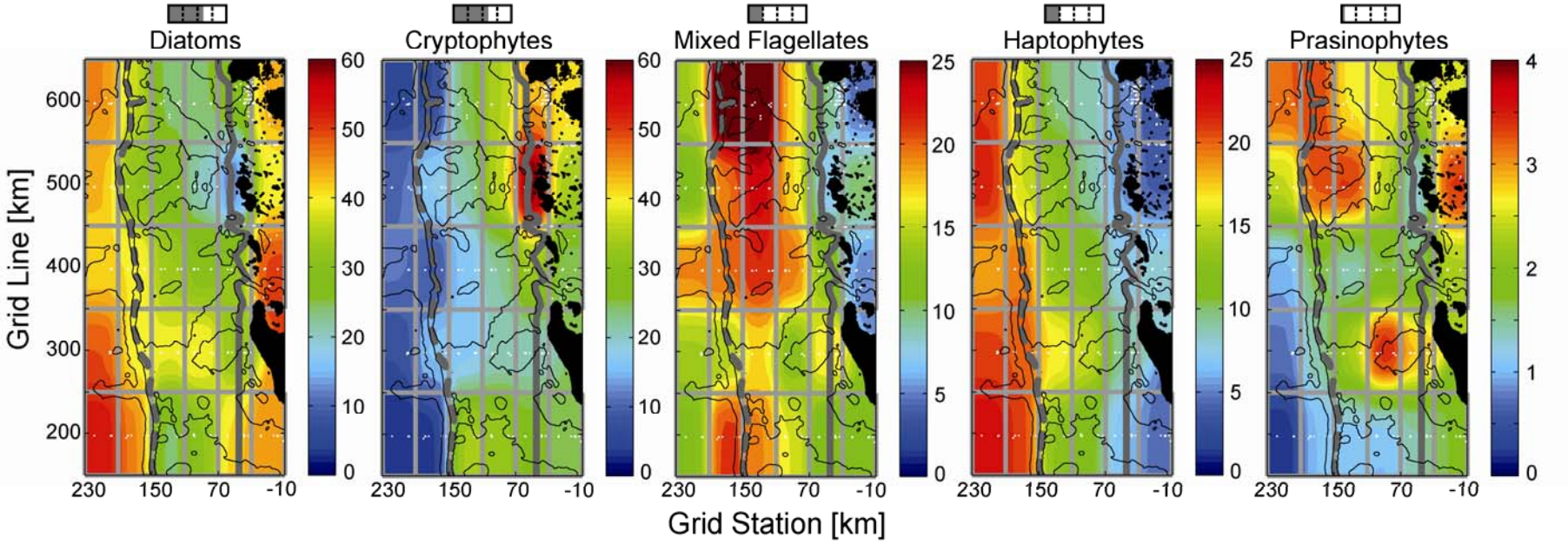

Figure 7. 50% Light depth climatologies, as a ratio of group contribution to total chl_a. Note differing colorbars; battery indicator at top of each plot represents maximum percentage accounted for by each group.

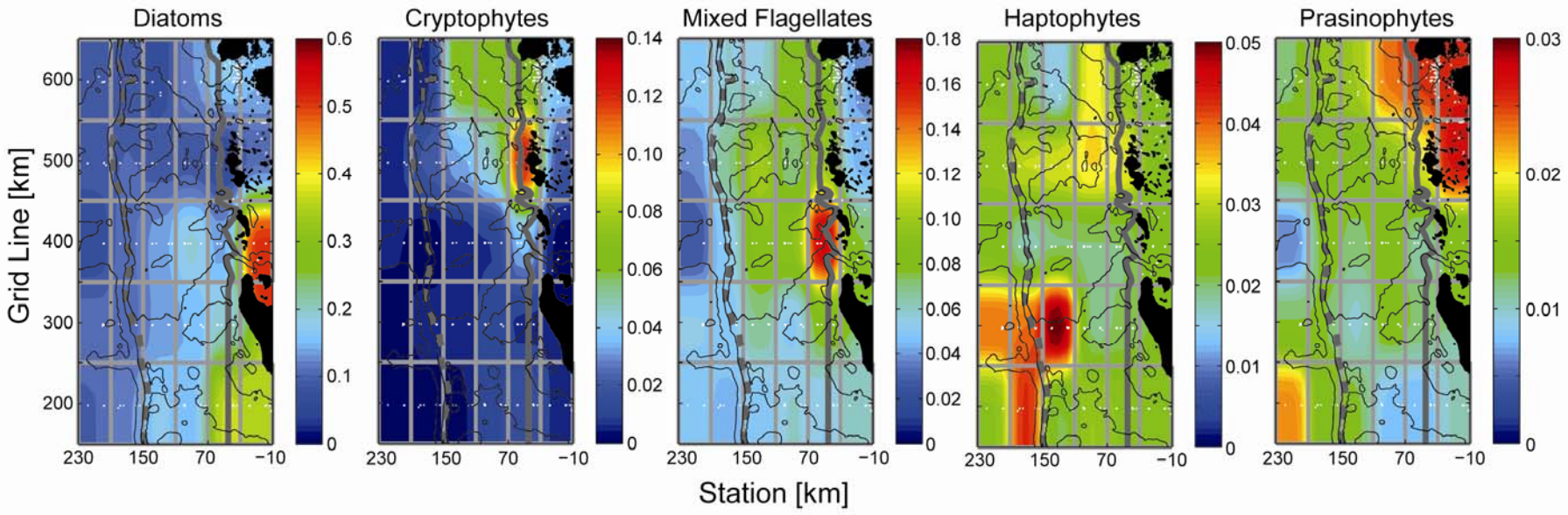

Figure 8. 1% Light depth climatologies, in µg L^{-1} chl_a. Note each group has independent color bar.

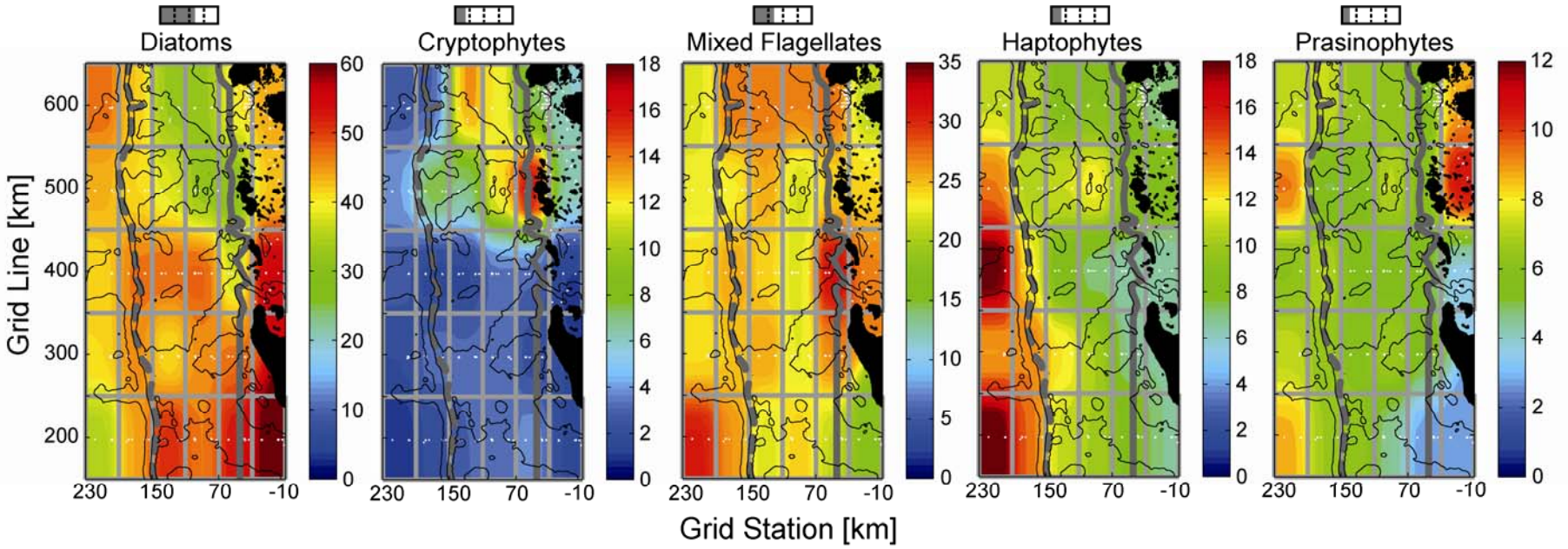

Figure 9. 1% Light depth climatologies, as a percentage of group contribution to total chl_a. Note differing colorbars.

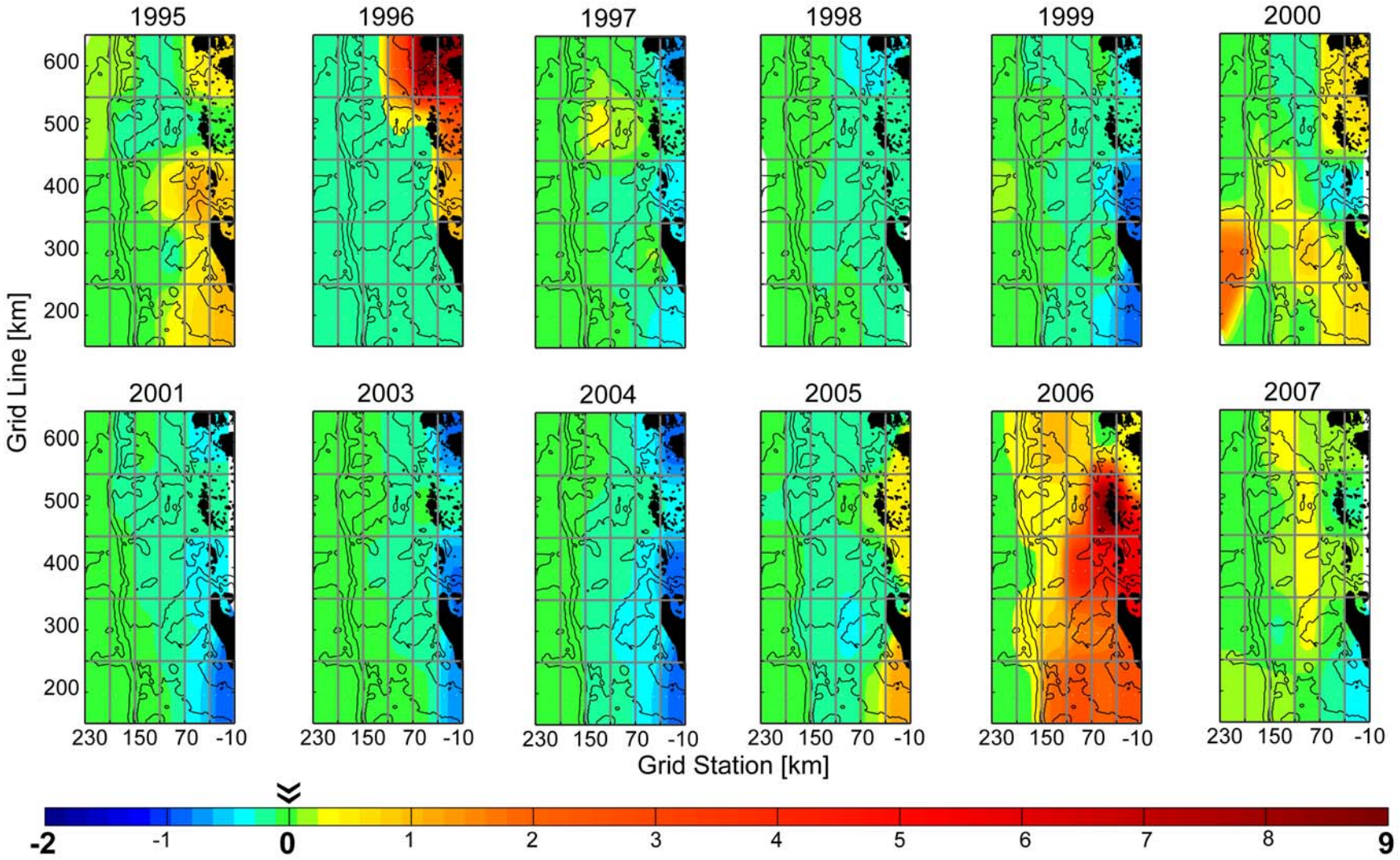

Figure 10. 50% Light depth diatom anomalies, in µg L^{-1} chl_a.

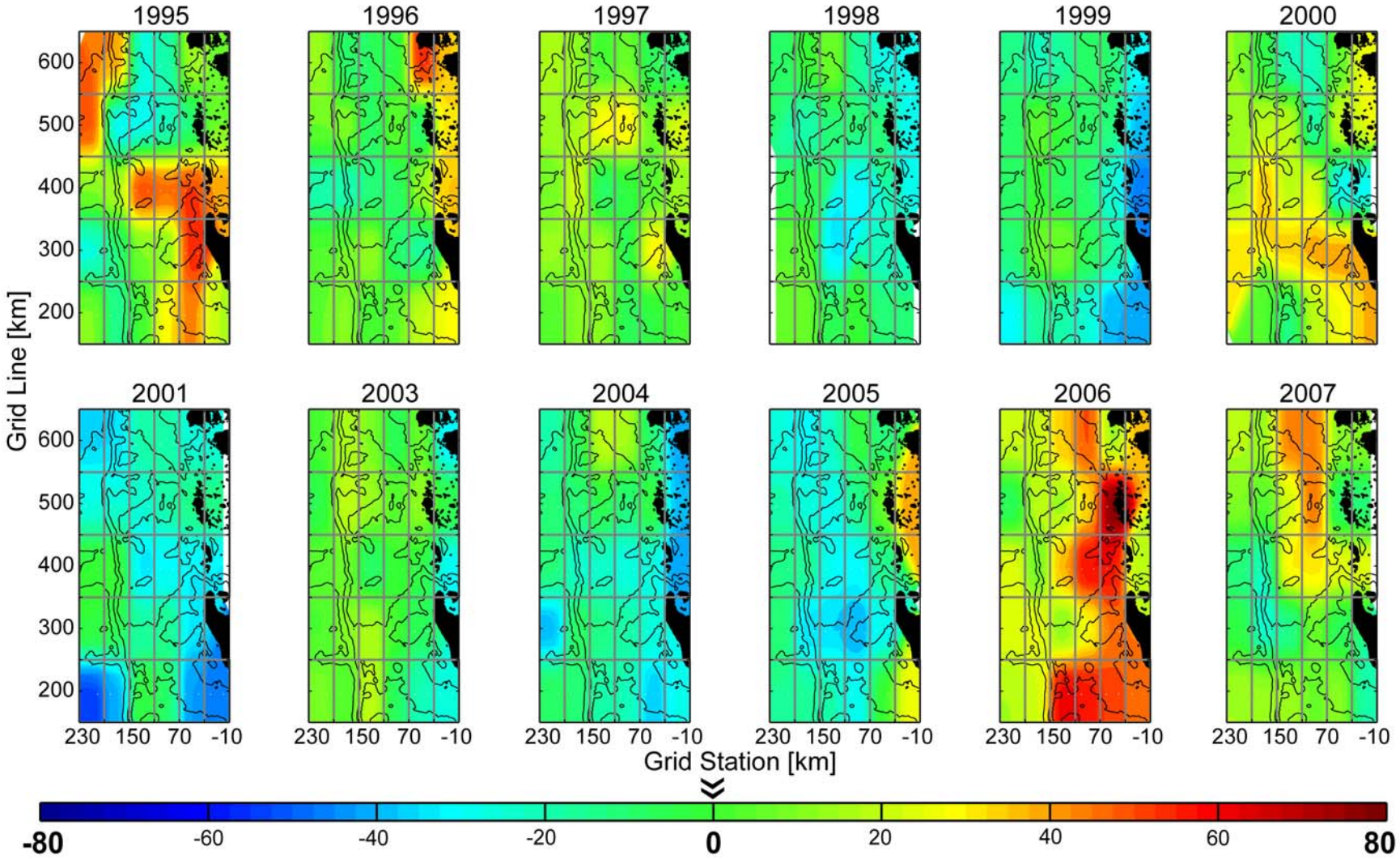

Figure 11. 50% Light depth diatom anomalies, as a percentage of group contribution to total chl_a.

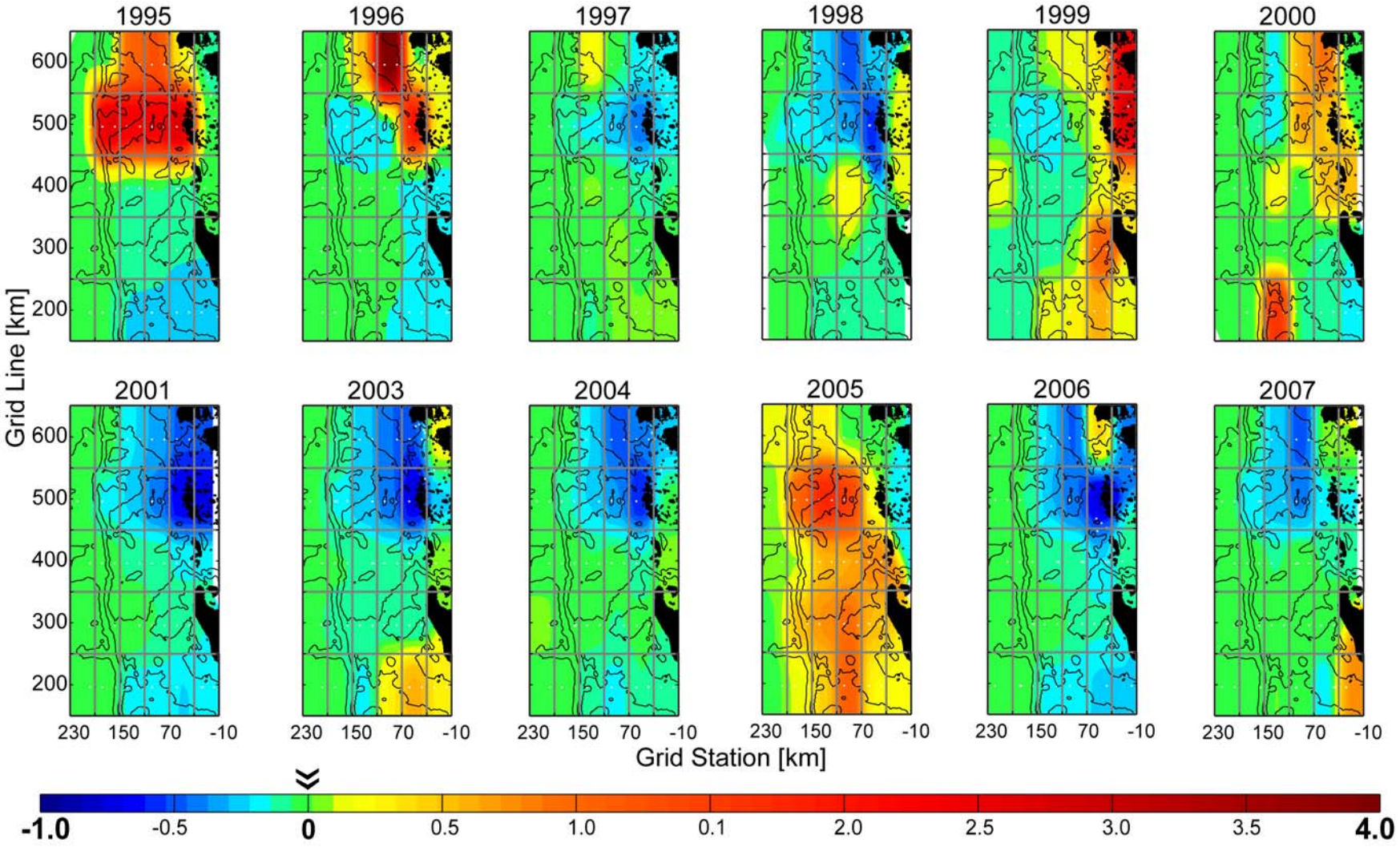

Figure 12. 50% Light depth cryptophyte anomalies, in µg L^{-1} chl_a.

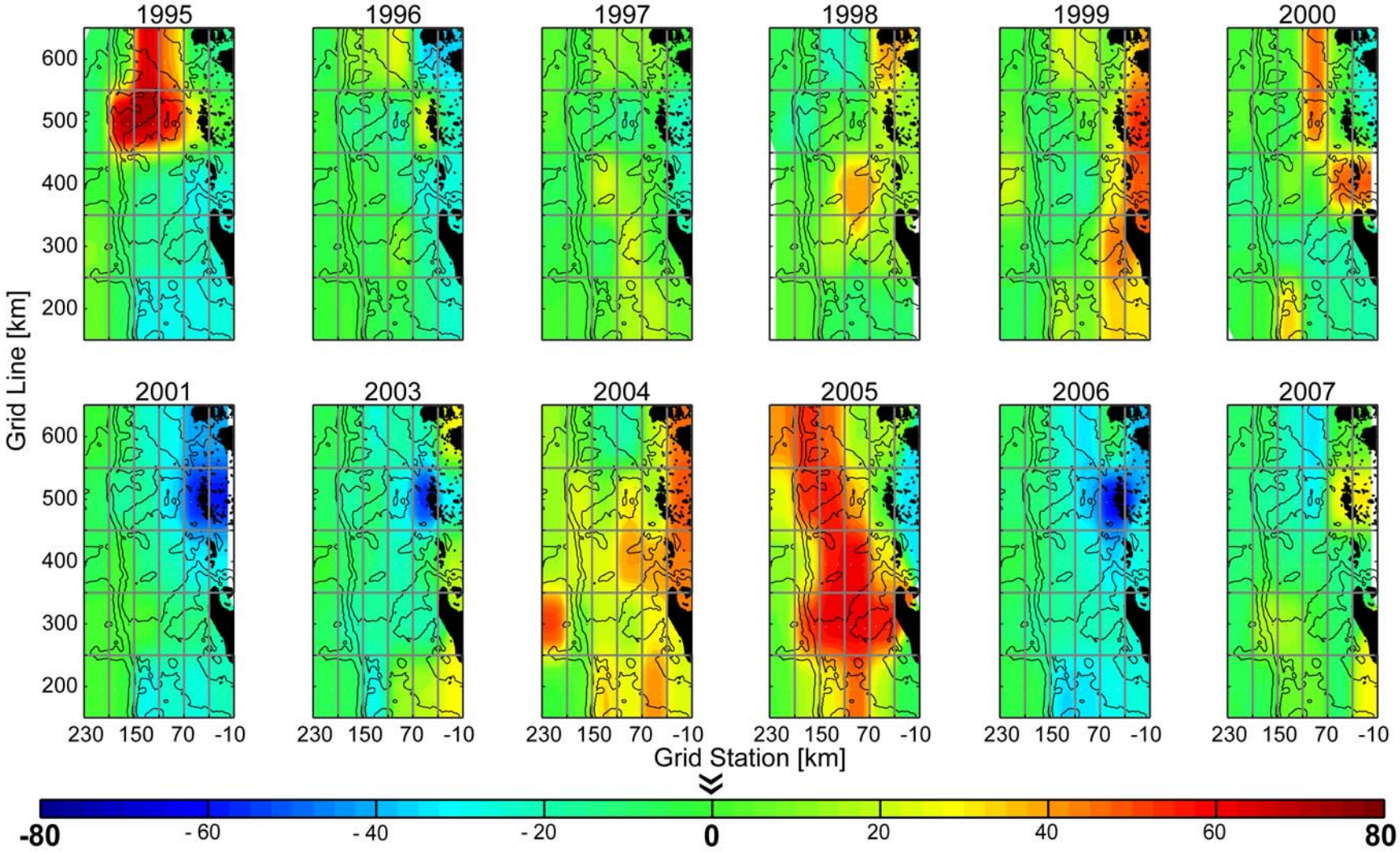

Figure 13. 50% Light depth cryptophyte anomalies, as a percentage of group contribution to total chl_a.

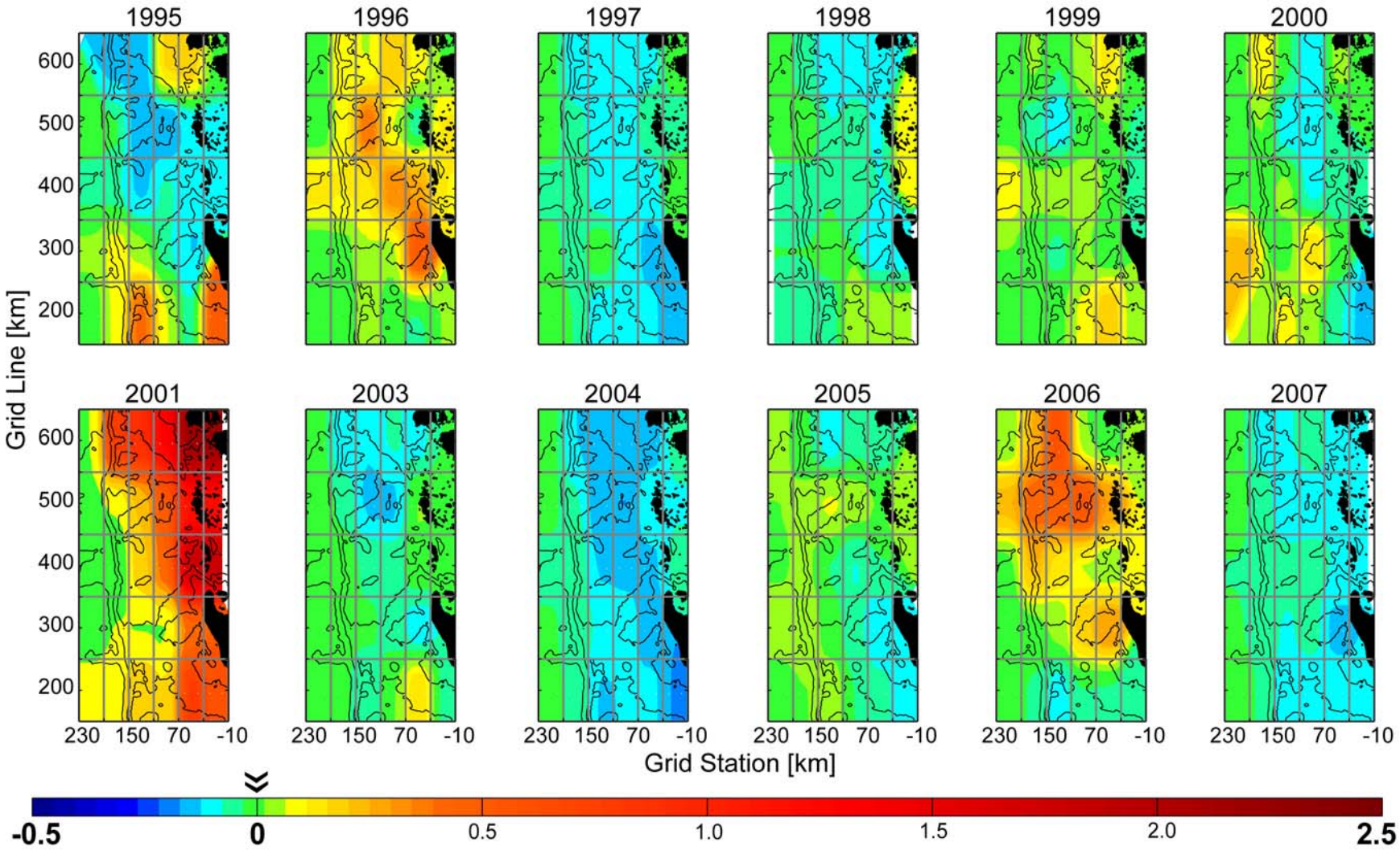

Figure 14. 50% Light depth mixed flagellate anomalies, in µg L^{-1} chl_a.

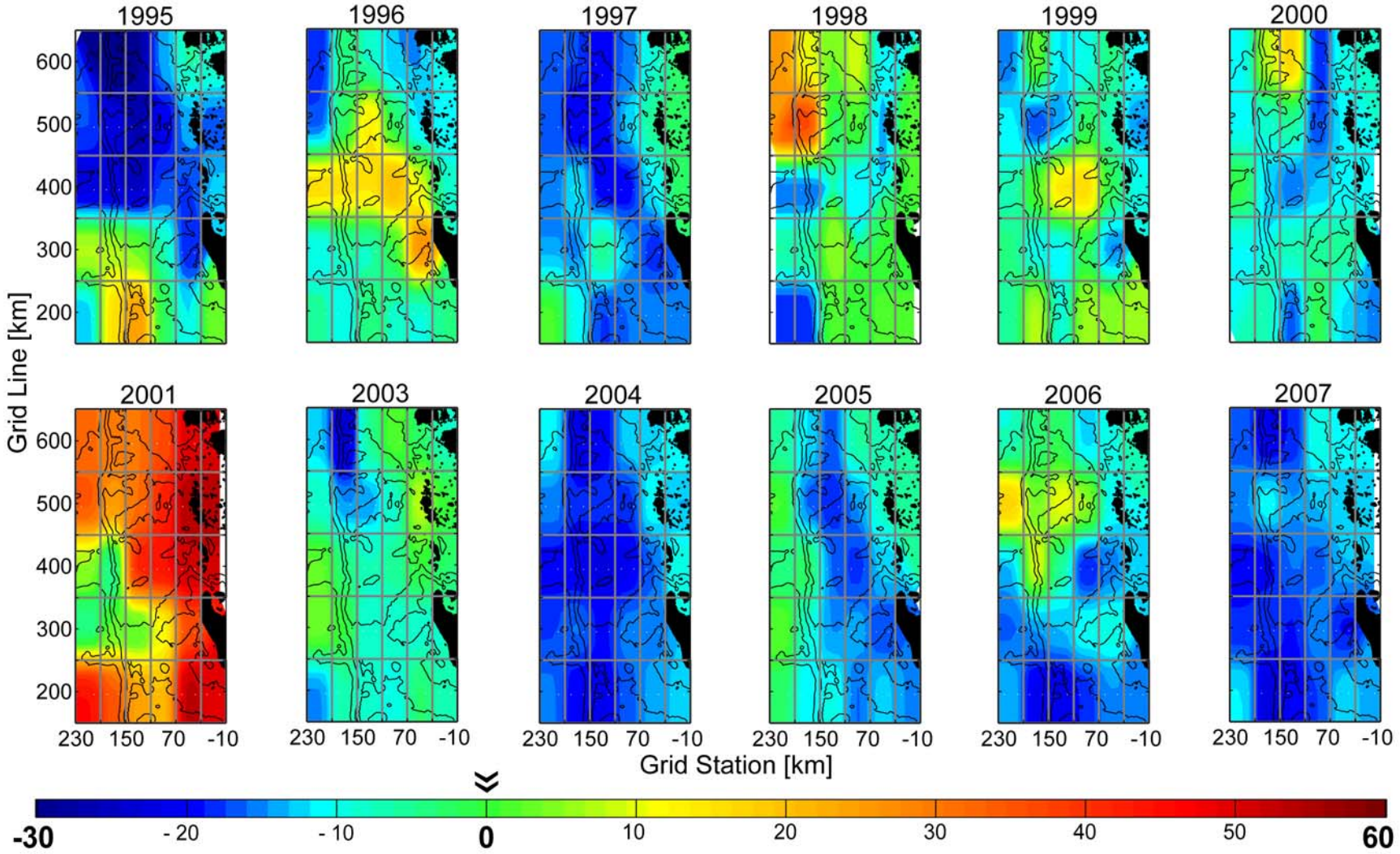

Figure 15. 50% Light depth mixed flagellate anomalies, as a percentage of group contribution to total chl_a.

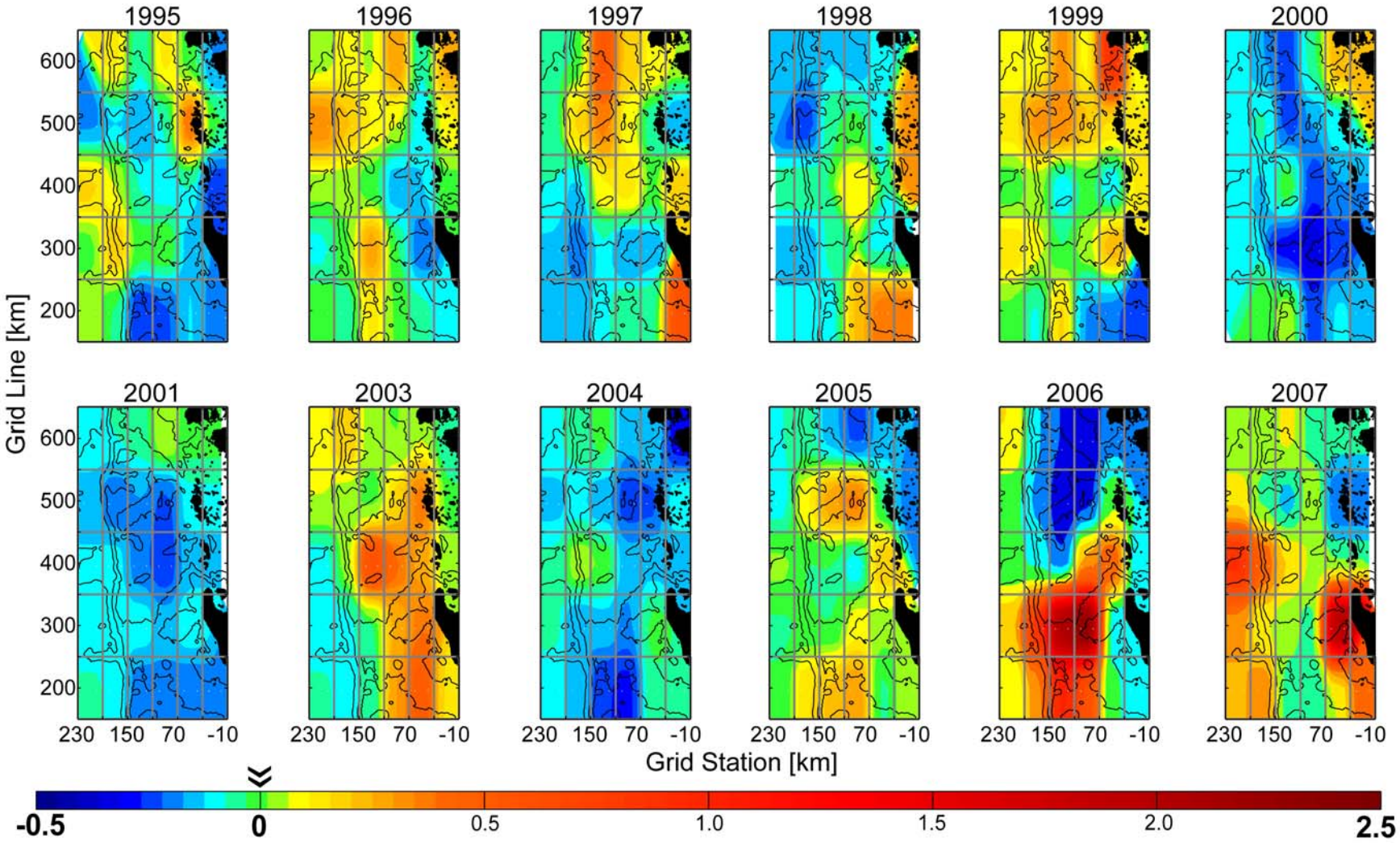

Figure 16. 50% Light depth haptophyte anomalies, in µg L^{-1} chl_a.

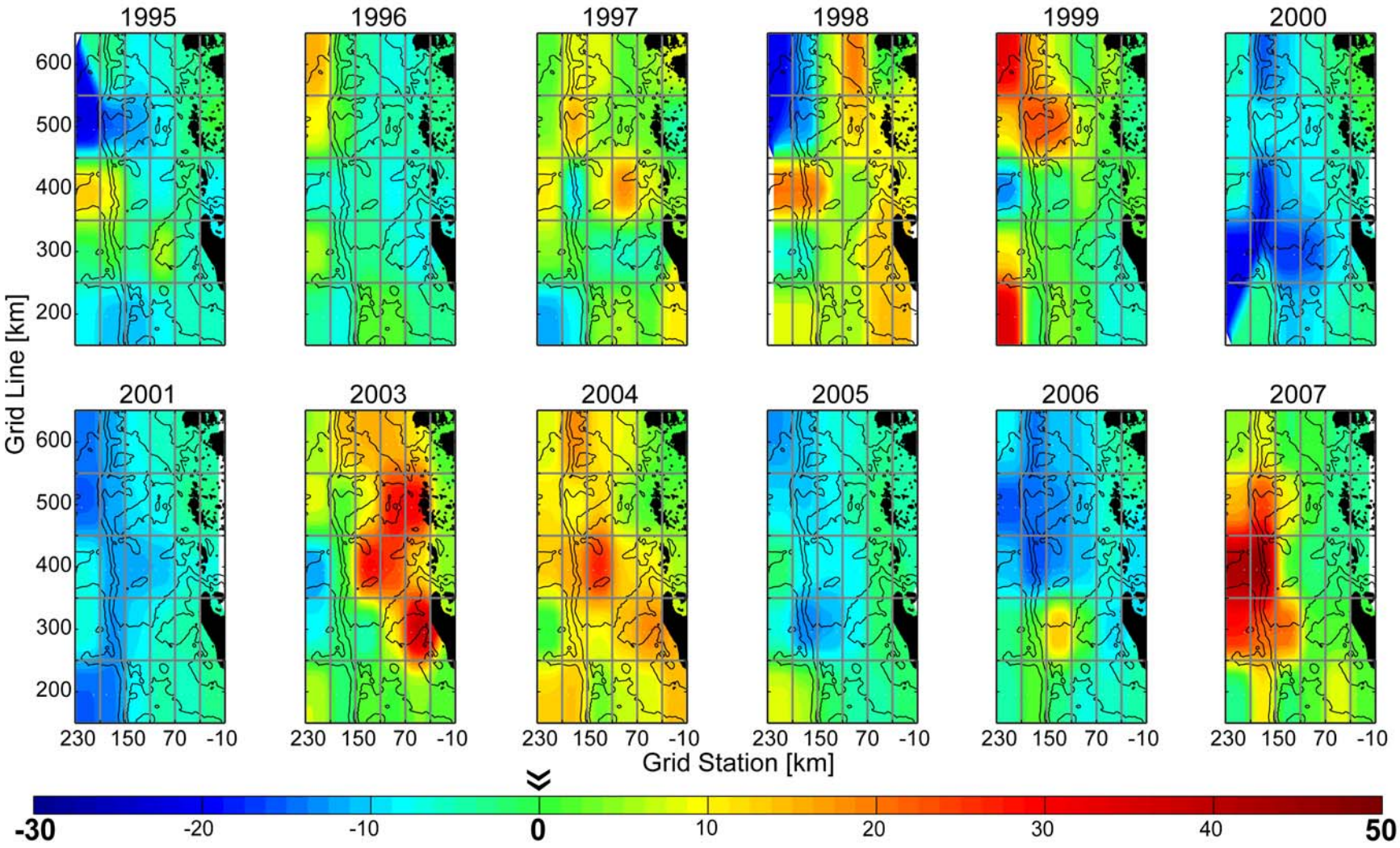

Figure 17. 50% Light depth haptophyte anomalies, as a percentage of group contribution to total chl_a.

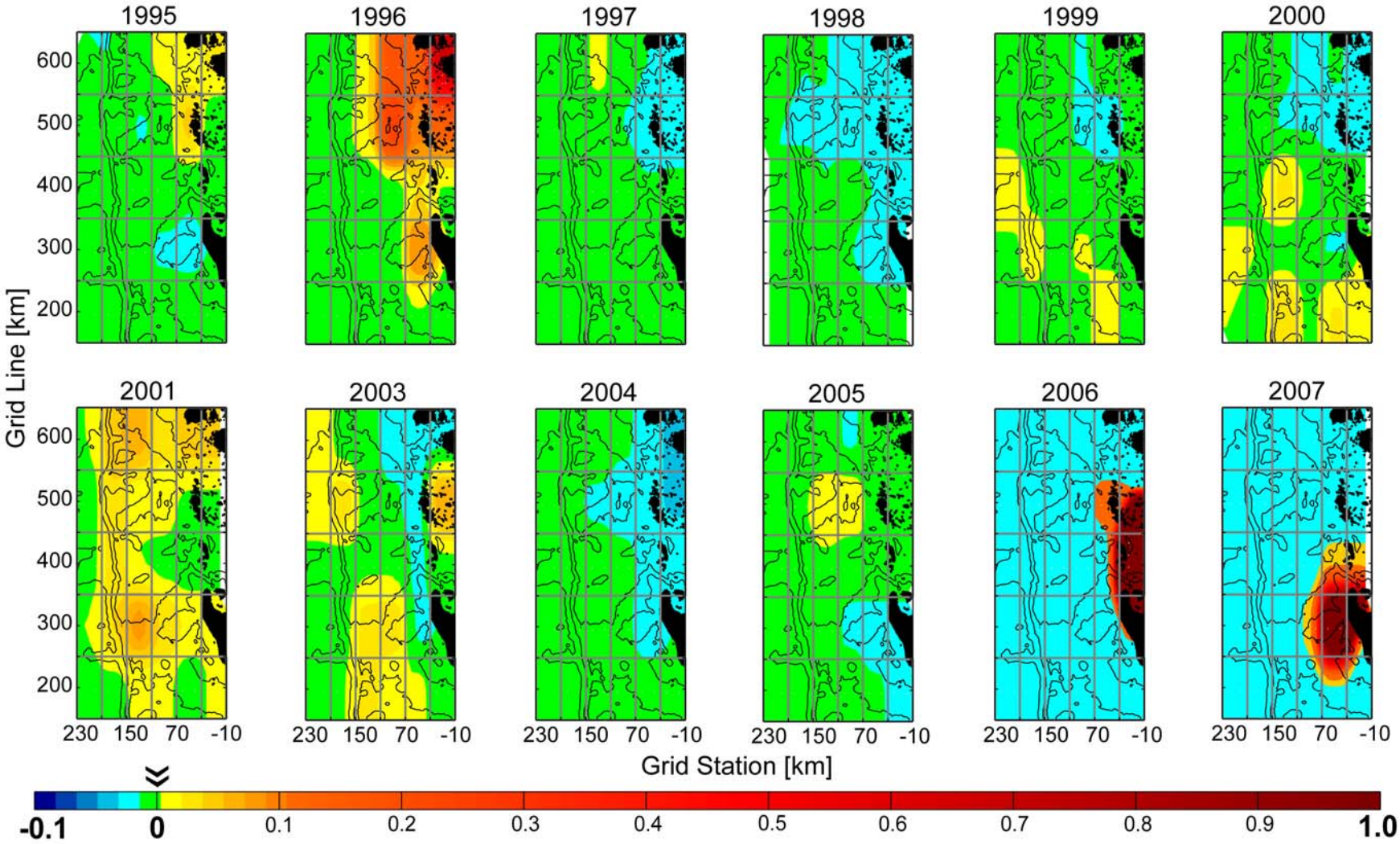

Figure 18. 50% Light depth prasinophyte anomalies, in µg L^{-1} chl_a.

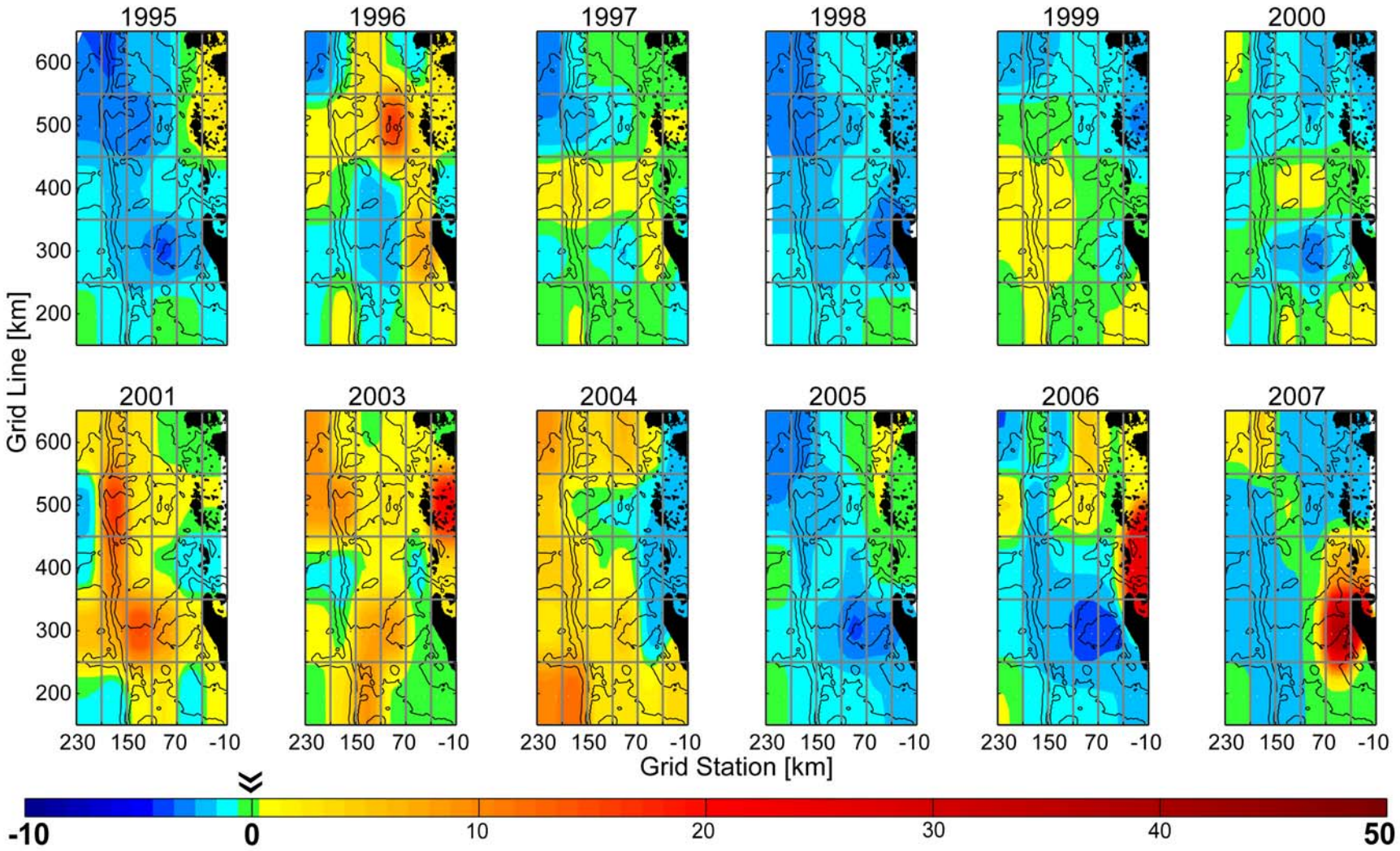

Figure 19. 50% Light depth prasinophyte anomalies, as a ratio of group contribution to total chl_a.

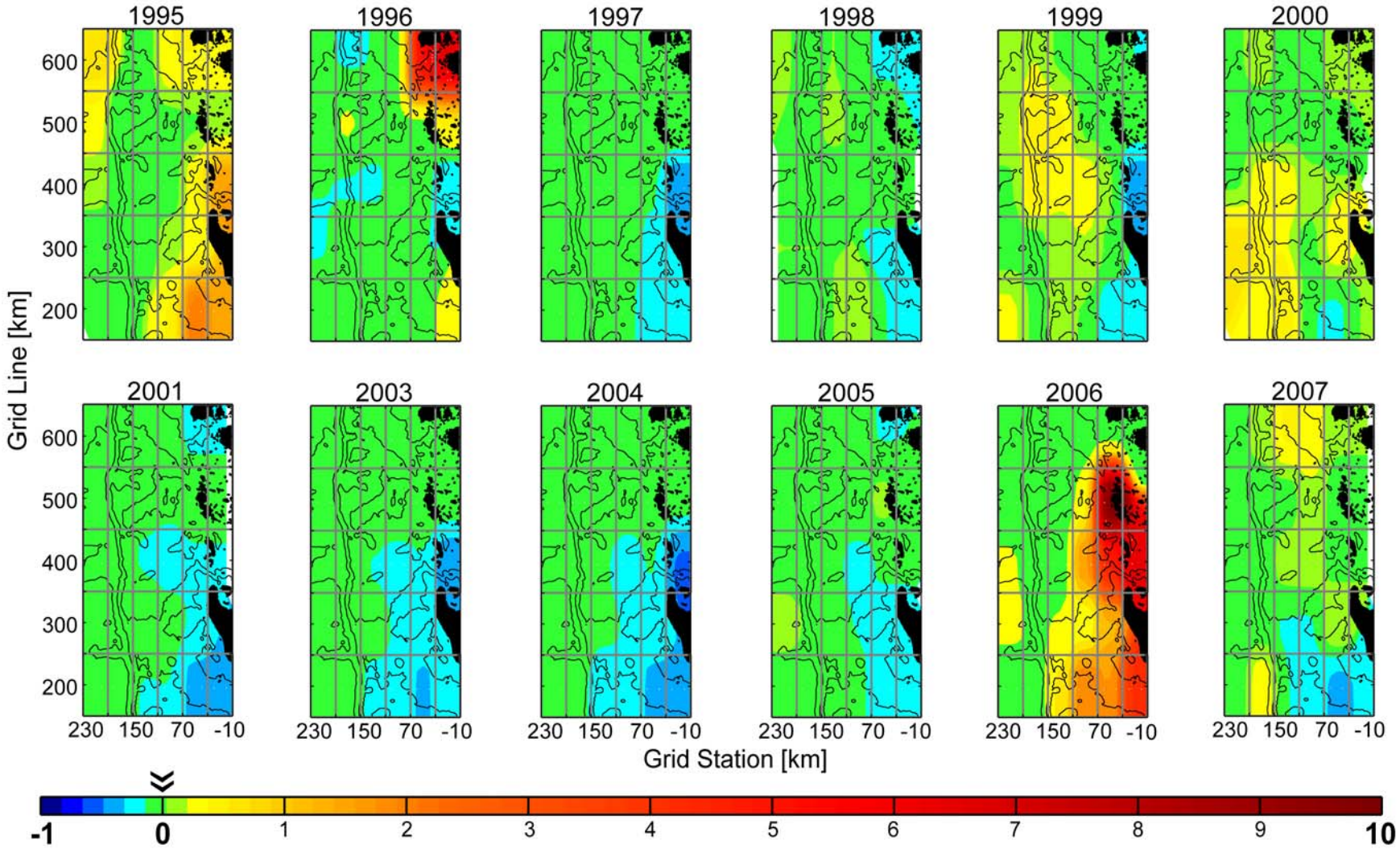

Figure 20. 1% Light depth diatom anomalies, in µg L^{-1} chl_a.

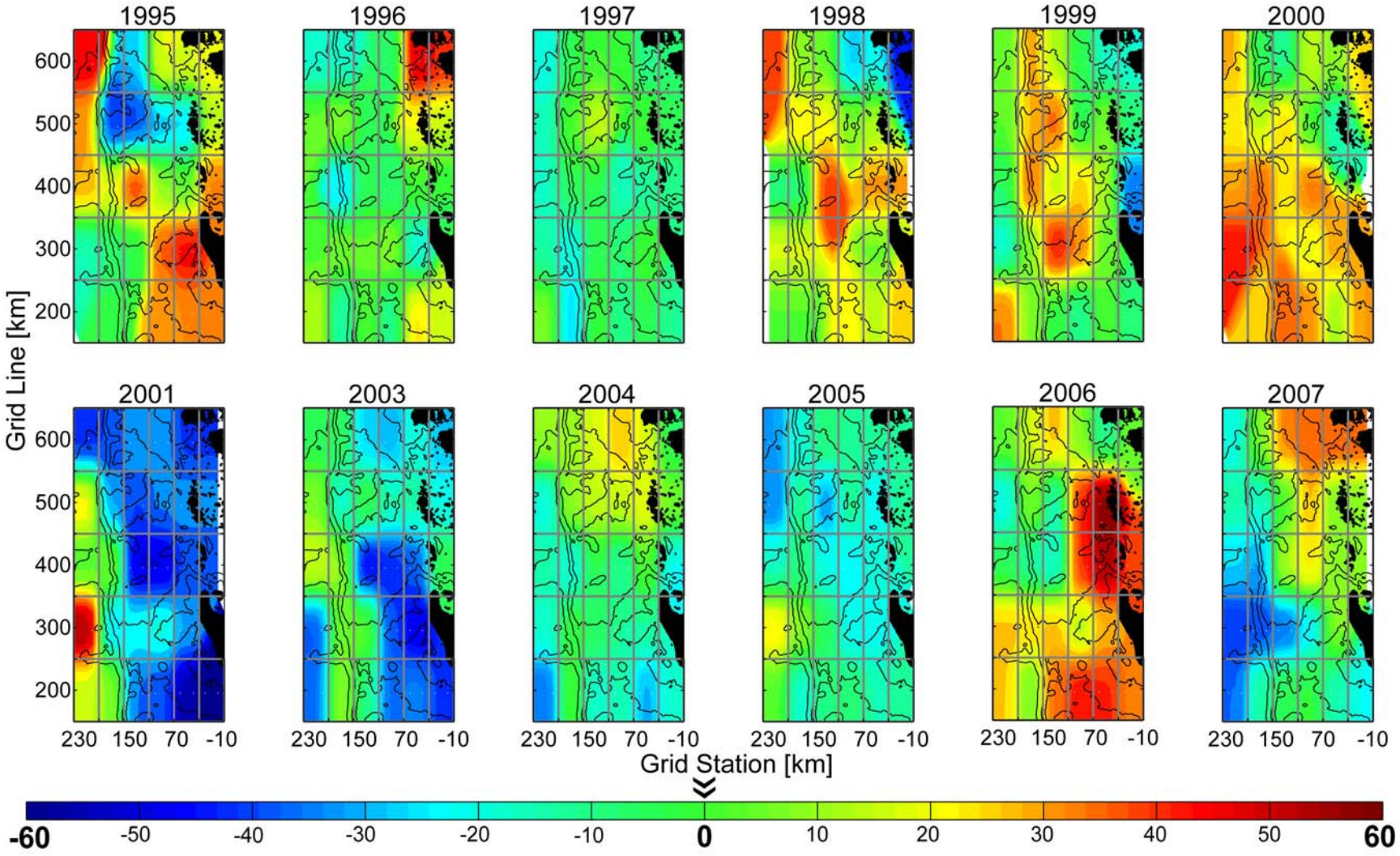

Figure 21. 1% Light depth diatom anomalies, as a ratio of group contribution to total chl_a.

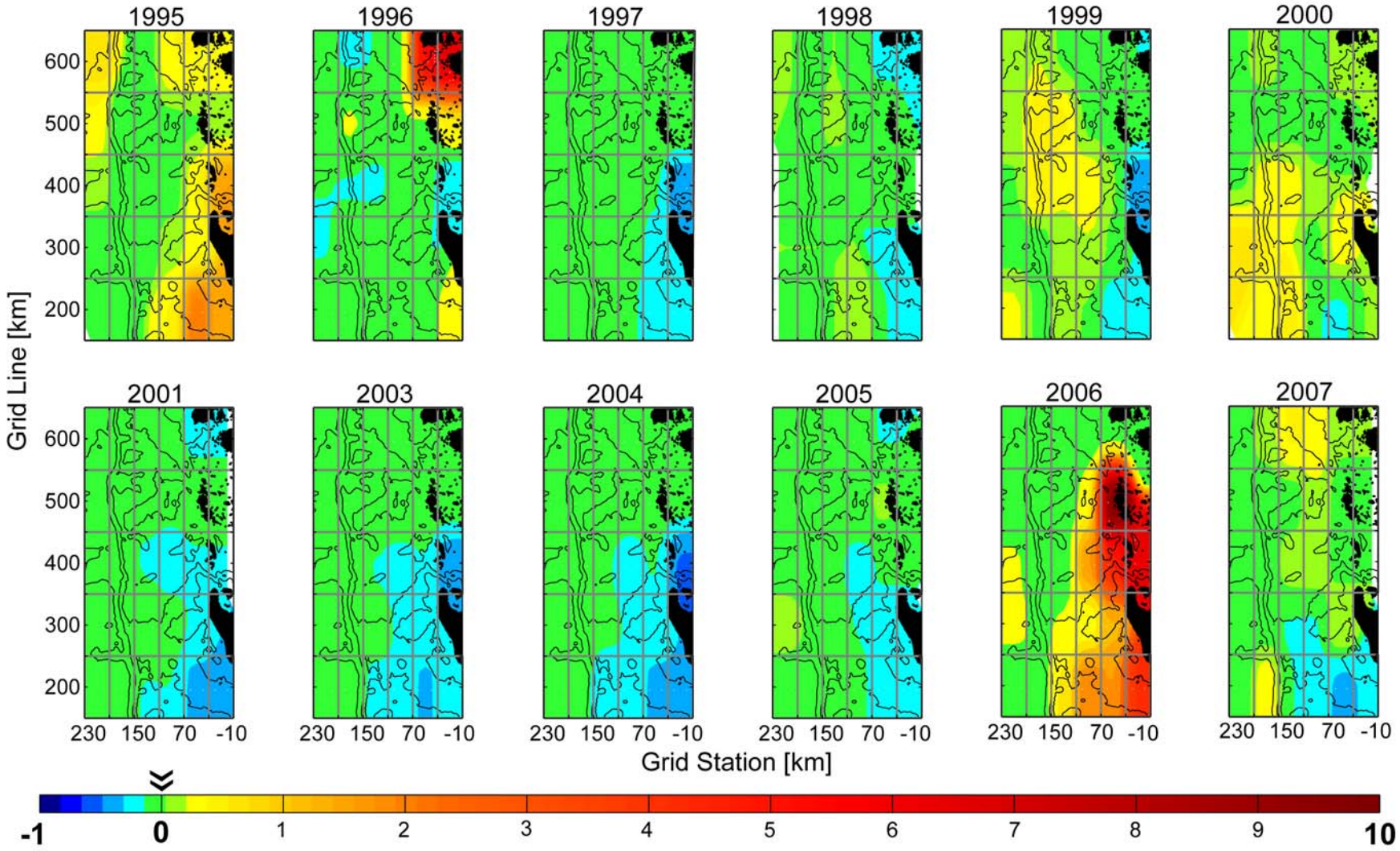

Figure 22. 1% Light depth mixed flagellate anomalies, in µg L^{-1} chl_a.

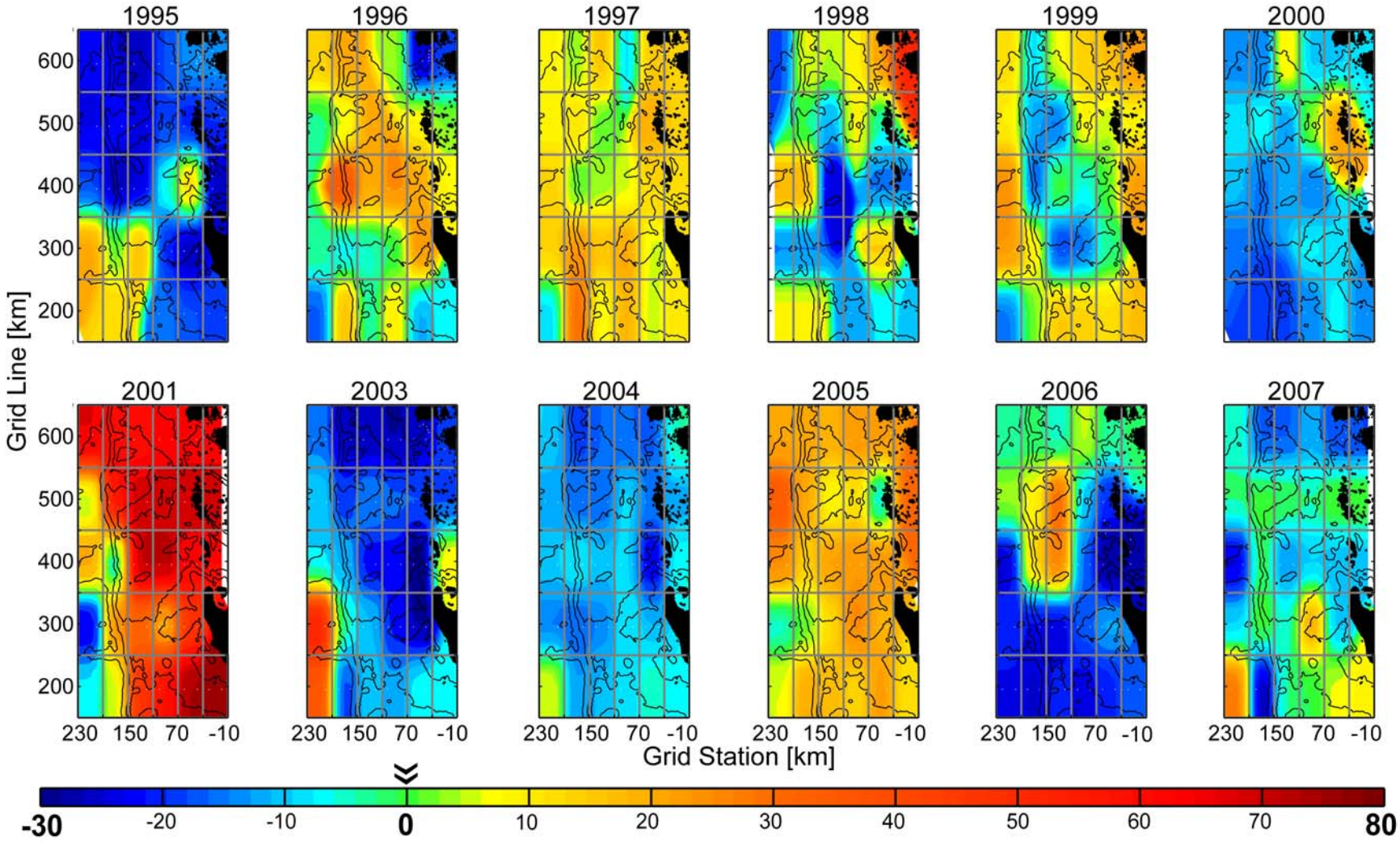

Figure 23. 1% Light depth mixed flagellate anomalies, as a ratio of group contribution to total chl_a.

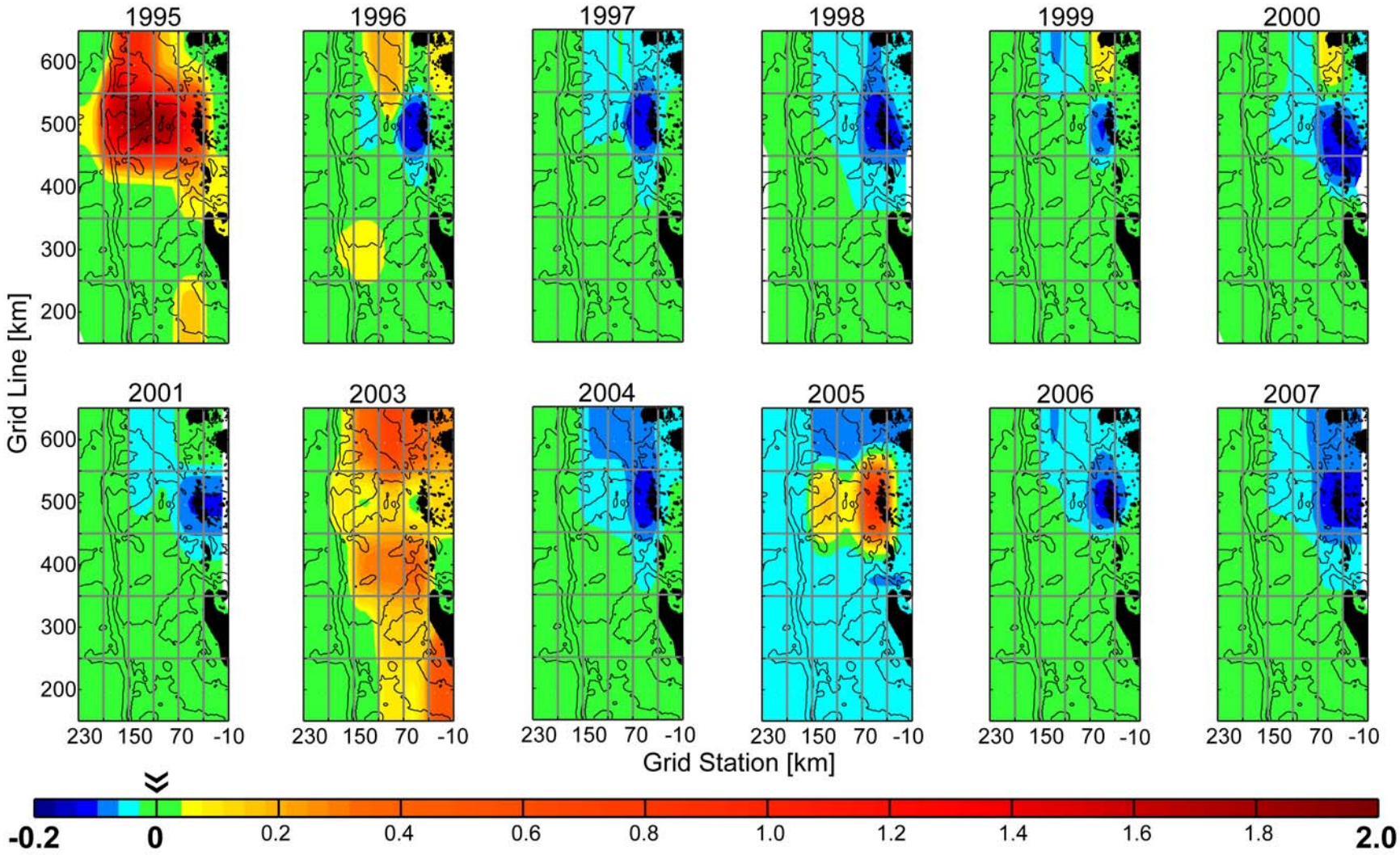

Figure 24. 1% Light depth cryptophyte anomalies, in µg L^{-1} chl_a.

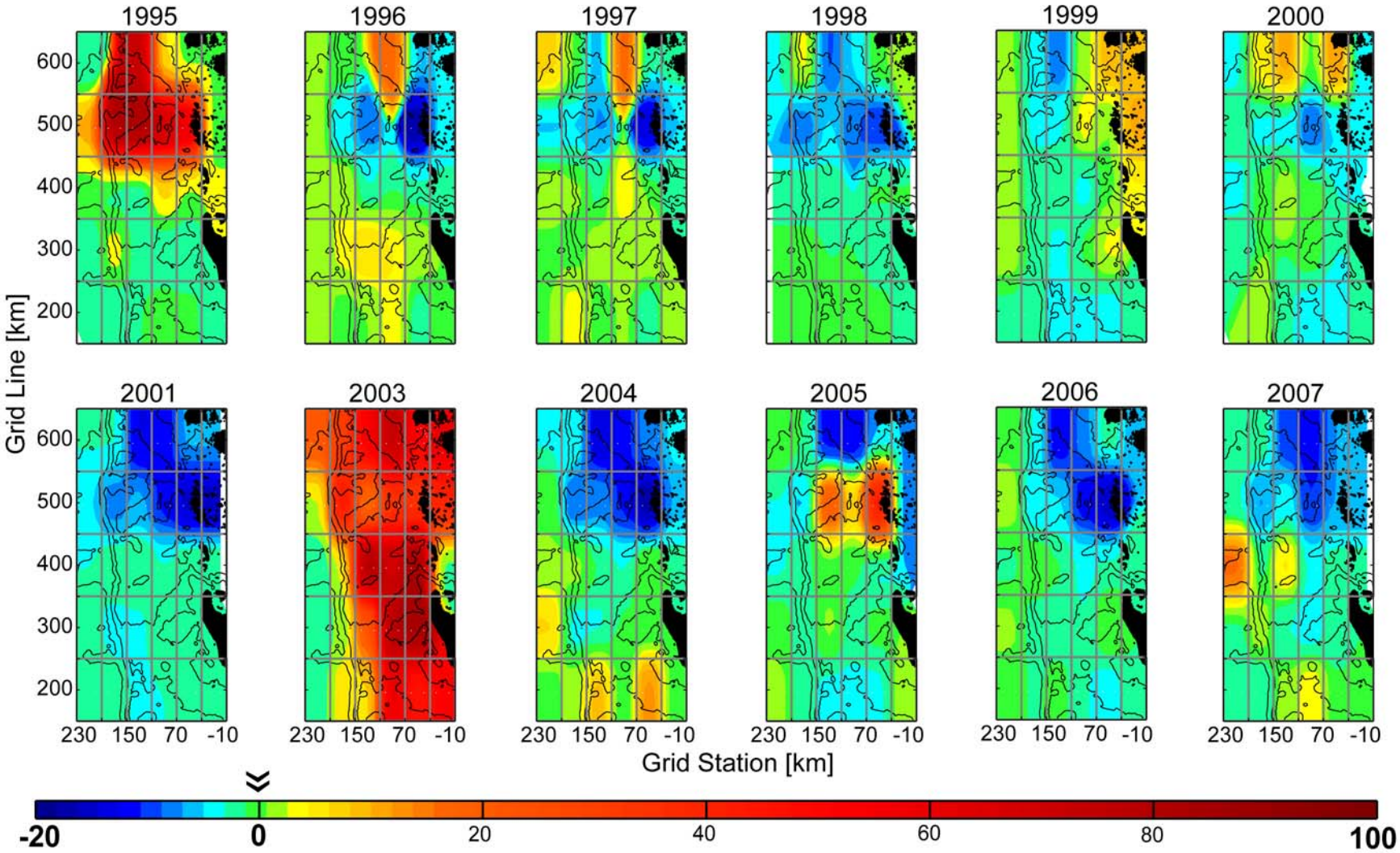

Figure 25. 1% Light depth cryptophyte anomalies, as a ratio of group contribution to total chl_a.

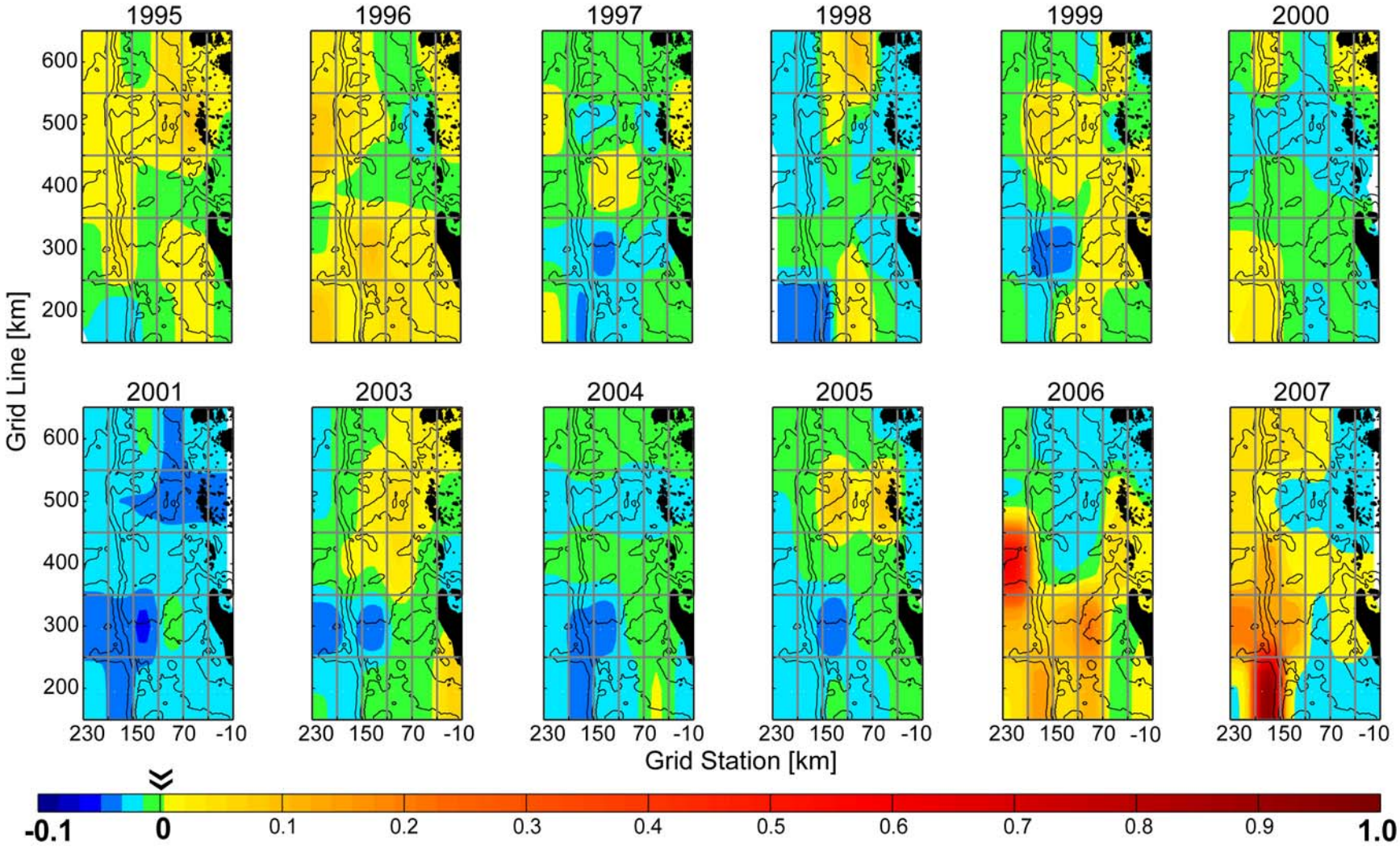

Figure 26. 1% Light depth haptophyte anomalies, in µg L^{-1} chl_a.

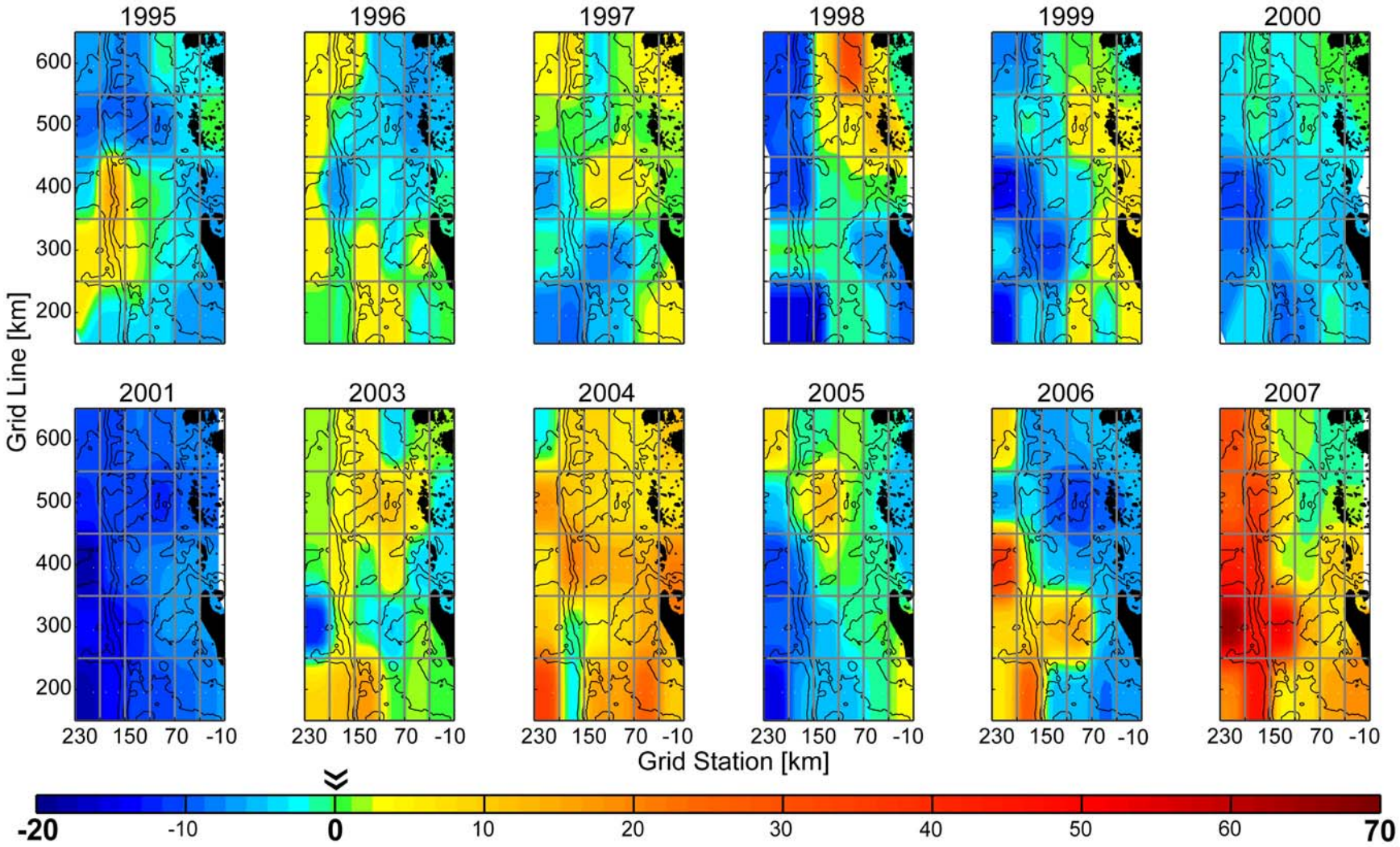

Figure 27. 1% Light depth haptophyte anomalies, as a ratio of group contribution to total chl_a.

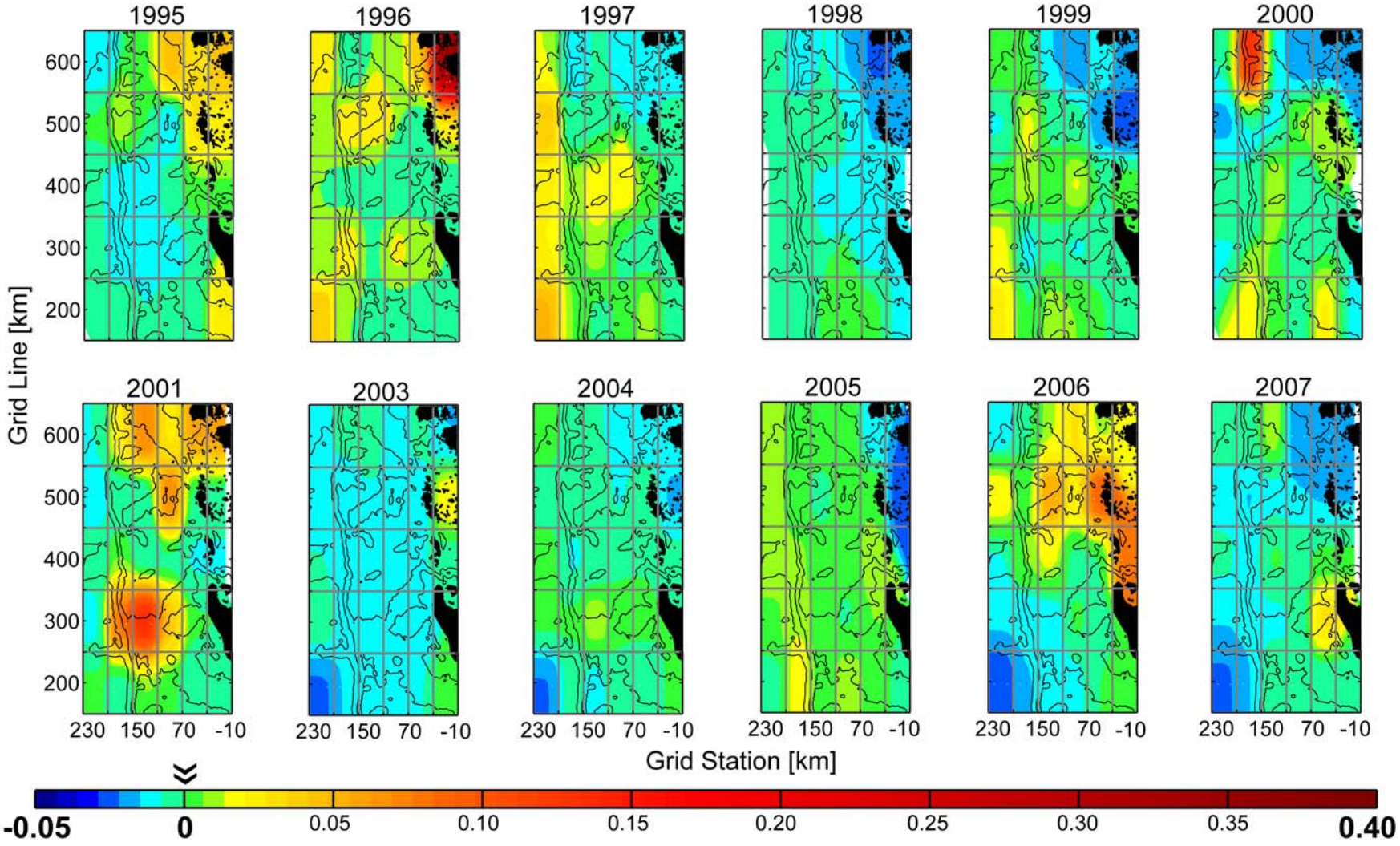

Figure 28. 1% Light depth prasinophyte anomalies, in µg L^{-1} chl_a.

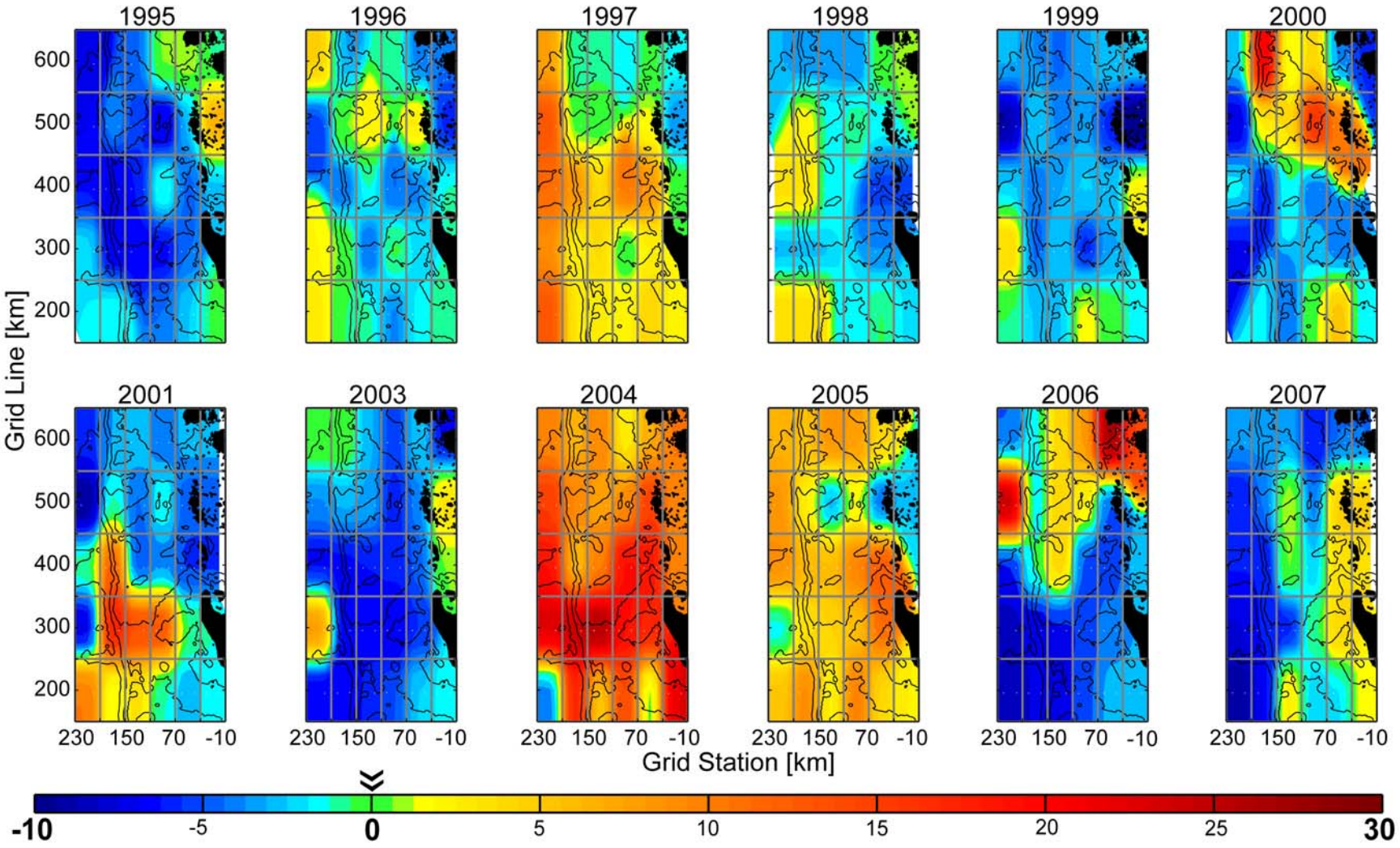

Figure 29. 1% Light depth prasinophyte anomalies, as a ratio of group contribution to total chl_a.

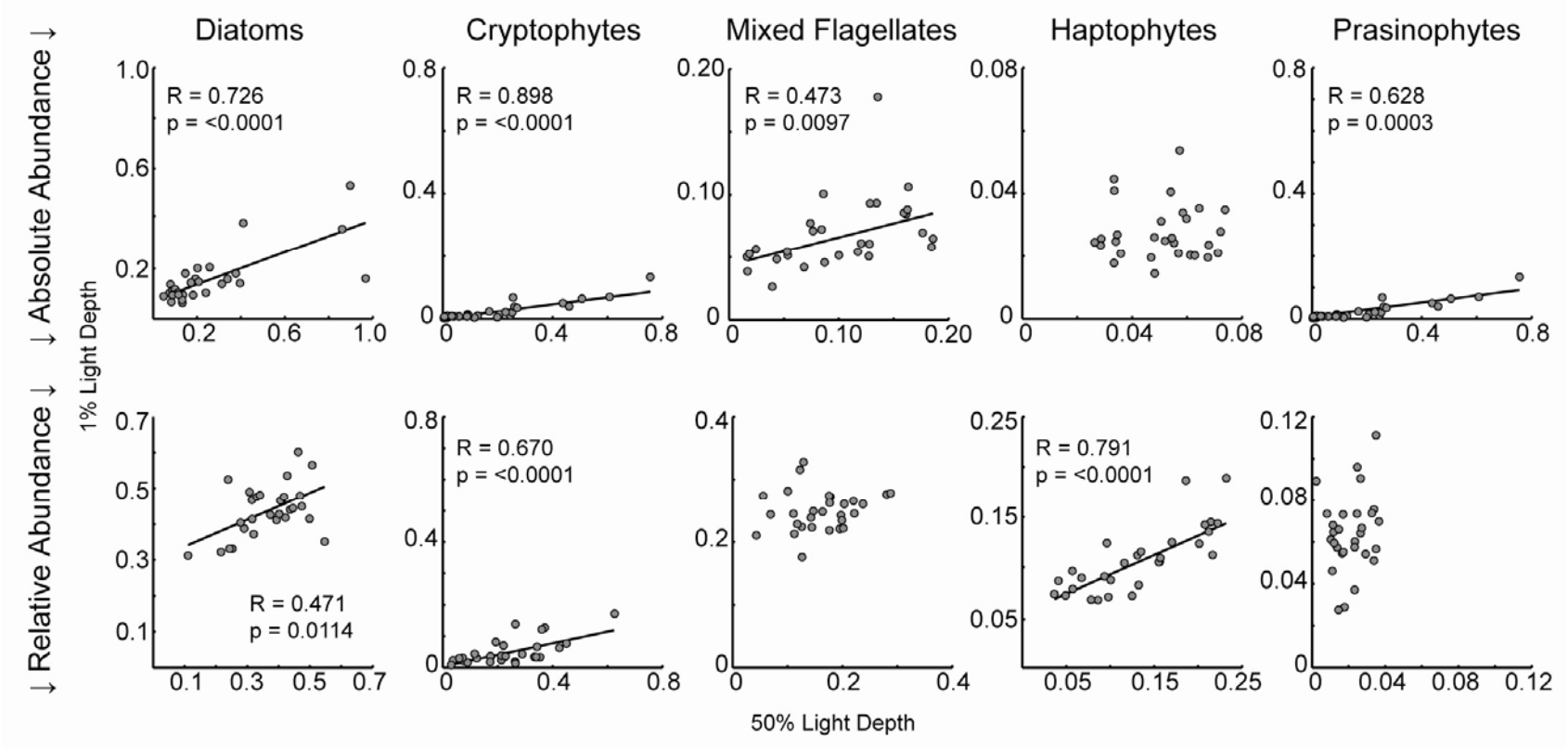

Figure 30. 50% vs 1% light depth climatology correlation plots, for both relative and absolute abundance. 50% light depth abundance on the X axis and 1% light depth abundance on the Y axis in all plots. The top row of plots are in terms of μg $_{[chl\_a]}$ L^{-1} associated with the group; the bottom row is in terms of the ratio of μg $_{[chl\_a]}$ L^{-1} associated with the group to total μg $_{[chl\_a]}$ L^{-1}. Significant Spearman correlations additionally show a robust regression line (Huber weighting, tuning constant 1.7), correlation coefficient (R) and associated p-values.

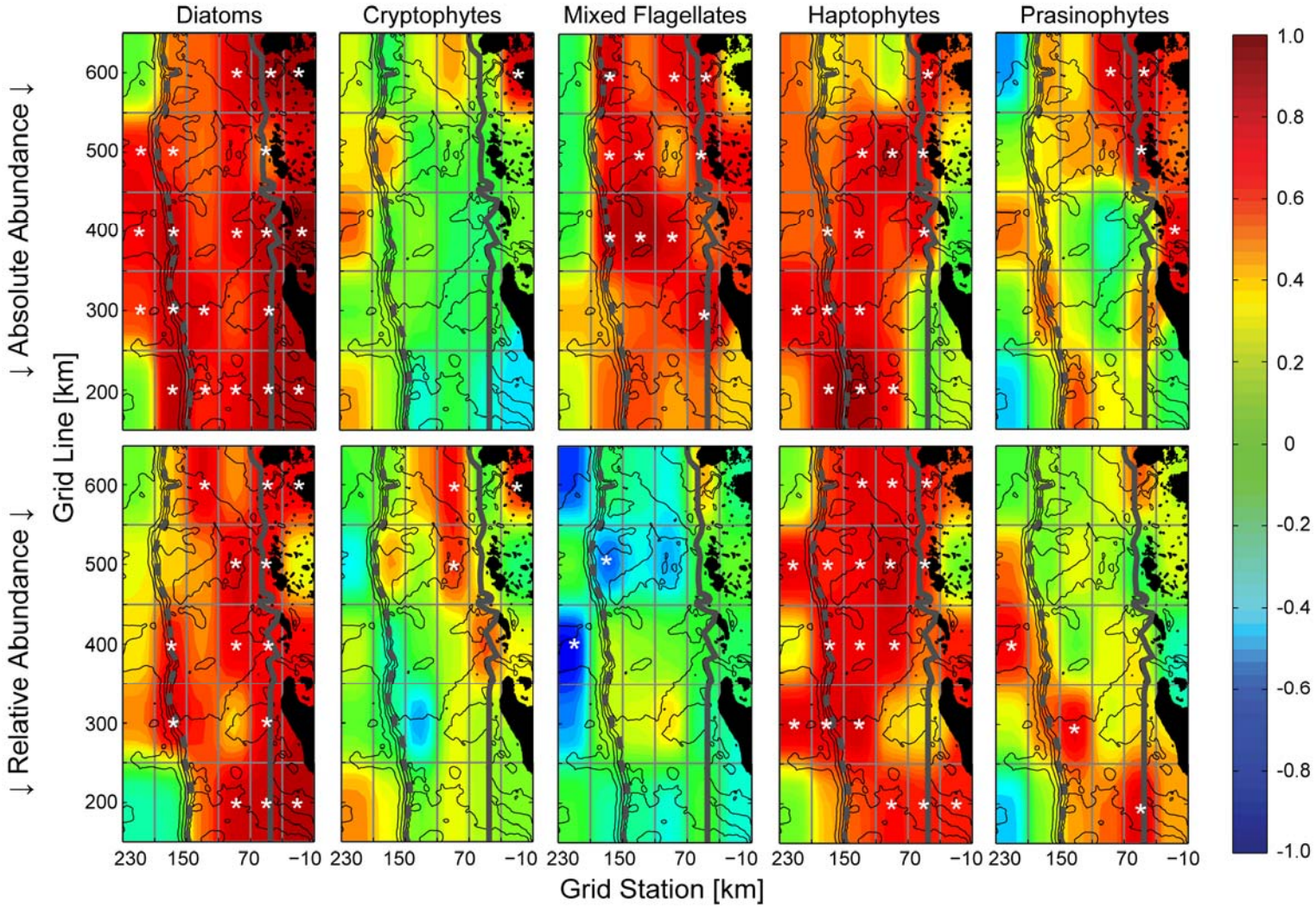

Figure 31. 50% vs 1% light depth anomaly correlation plots, by grid cell for both relative and absolute abundance. Statistically significant cells are marked with a white asterisk (*).

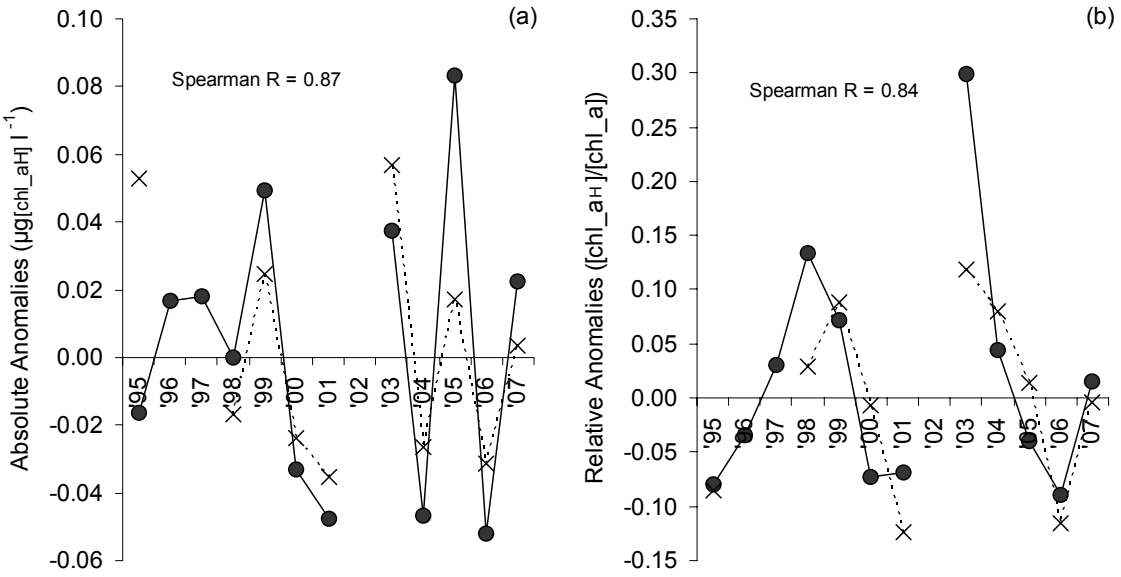

Figure 32. Haptophyte anomalies in grid cell 20 (strong correlation) at 50% (•) and 1% (x) light depths. Subplots are: (a) absolute anomaly values in terms of µg $_{[chl\_aH]}$ l-1 and (b) relative anomaly values in terms of the ratio of [chl_a_H] to total [chl_a].

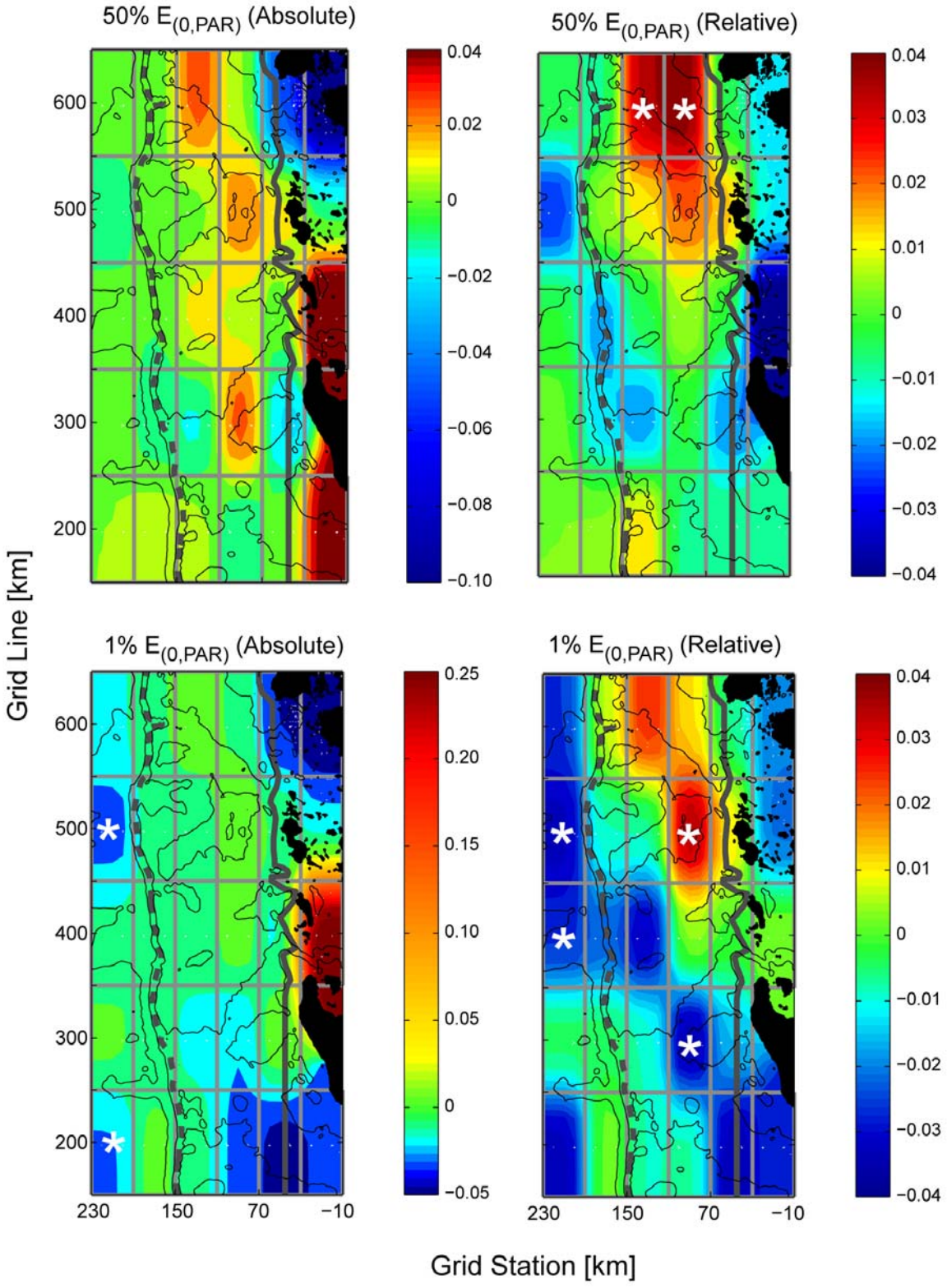

Figure 33. Diatom trends at 50% and 1% light depths, as the slopes of grid cell anomalies. Slopes significantly different from zero marked with white asterisk (*).

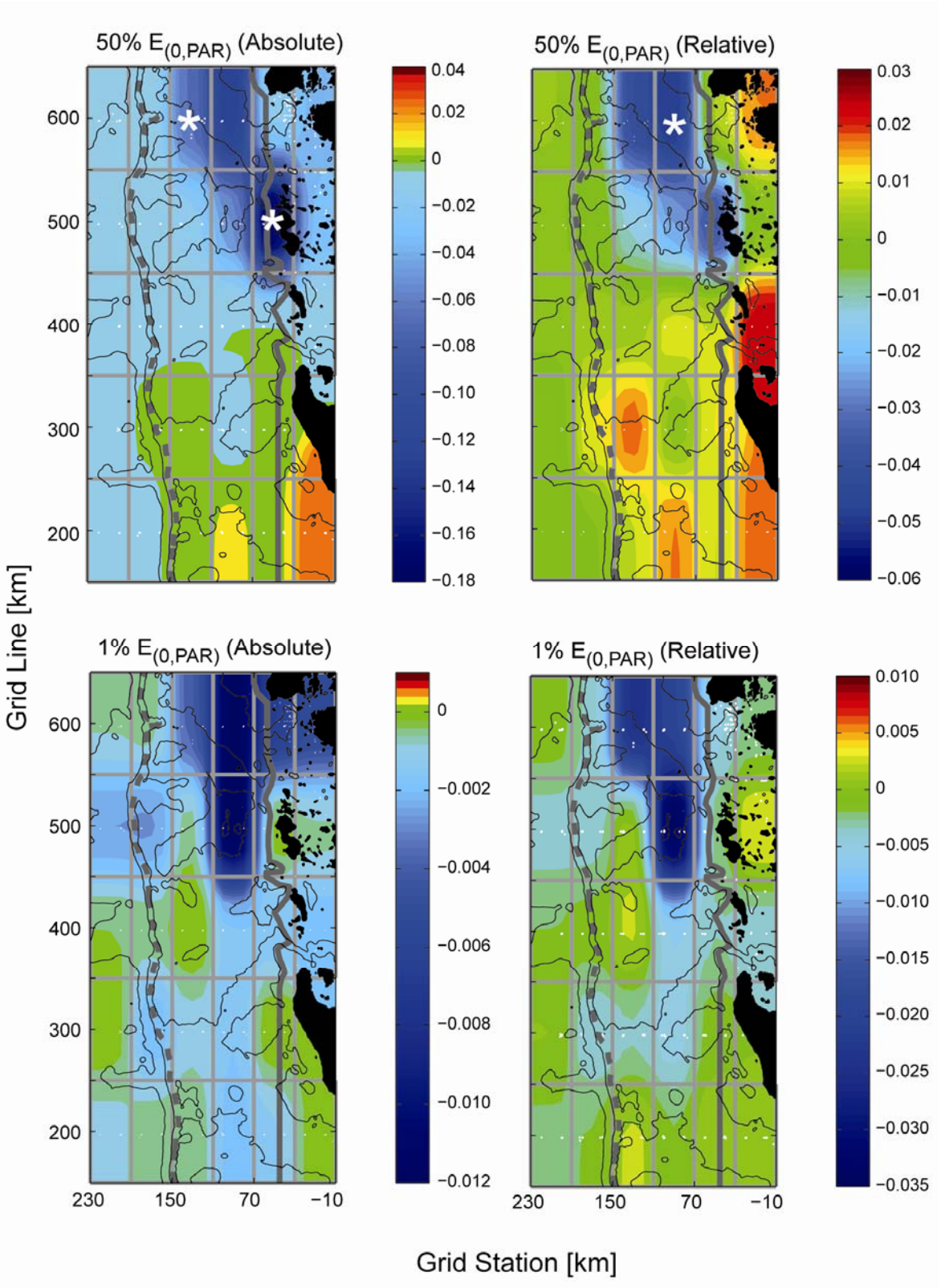

Figure 34. Cryptophyte trends at 50% and 1% light depths, as the slope of grid cell anomalies. Slopes significantly different from zero marked with white asterisk (*).

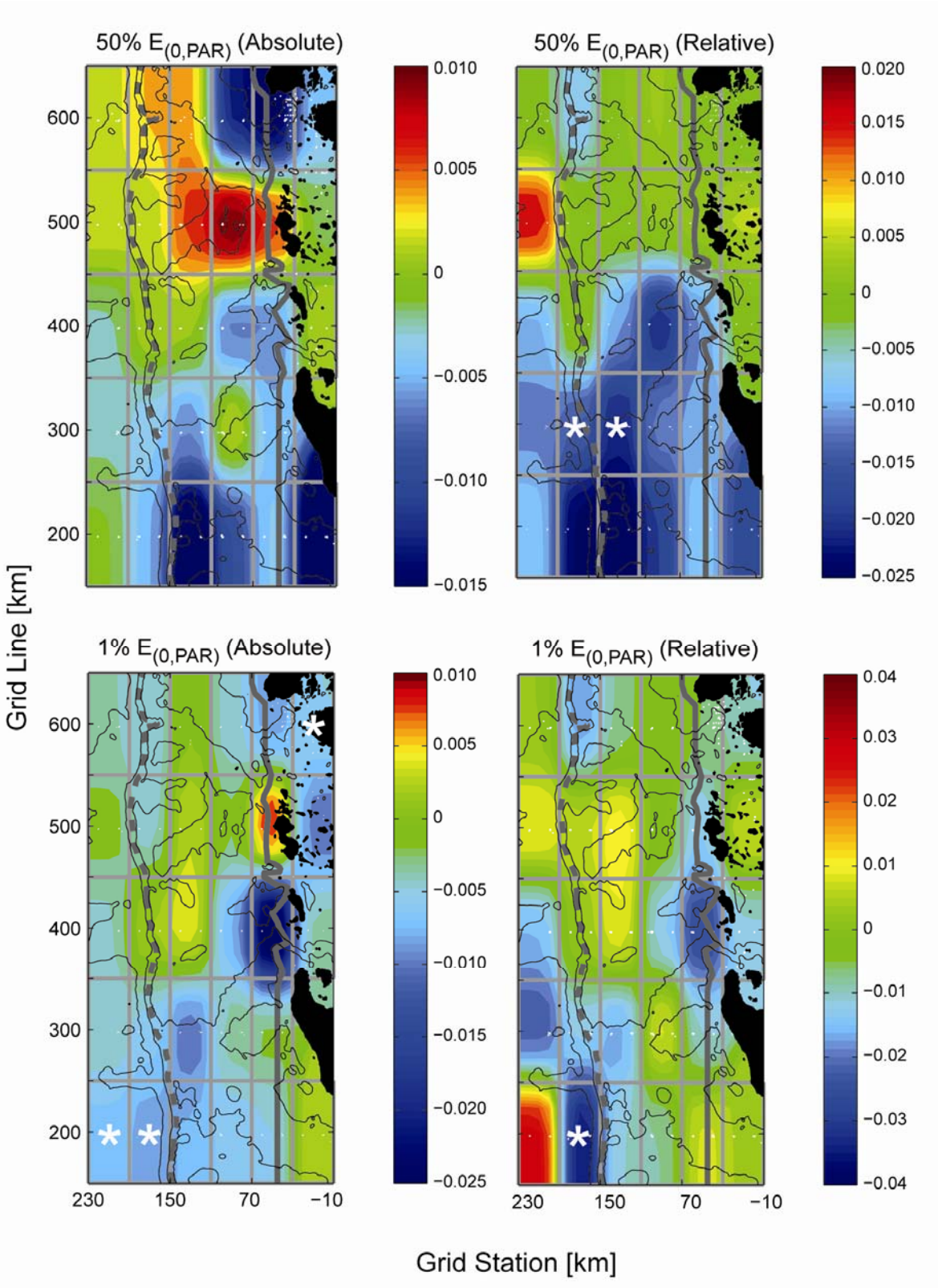

Figure 35. Mixed flagellate trends at 50% and 1% light depths, as the slope of grid cell anomalies. Slopes significantly different from zero marked with white asterisk (*).

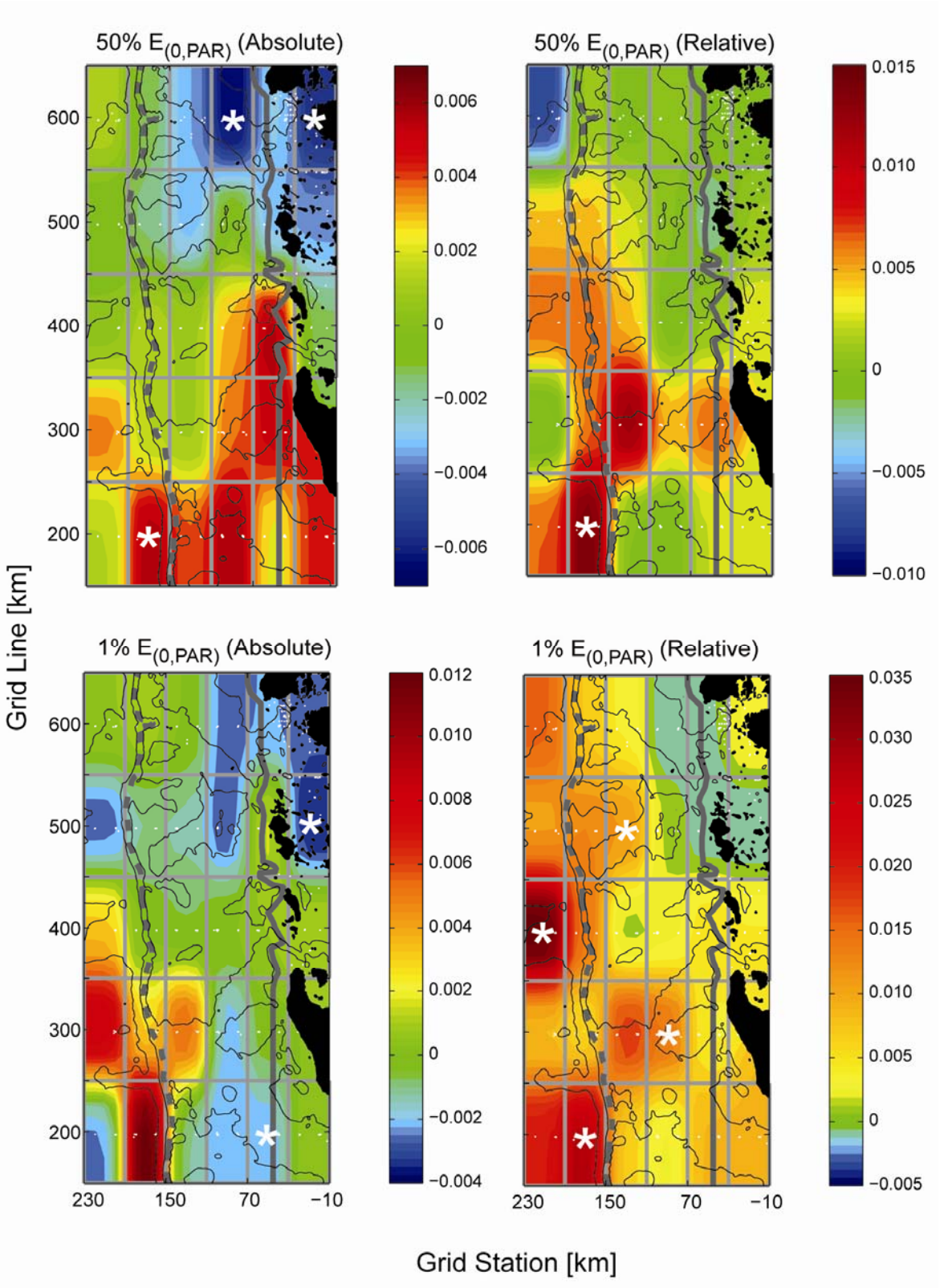

Figure 36. Type 4 Haptophyte trends at 50% and 1% light depths, as the slope of grid cell anomalies. Slopes significantly different from zero marked with white asterisk (*).

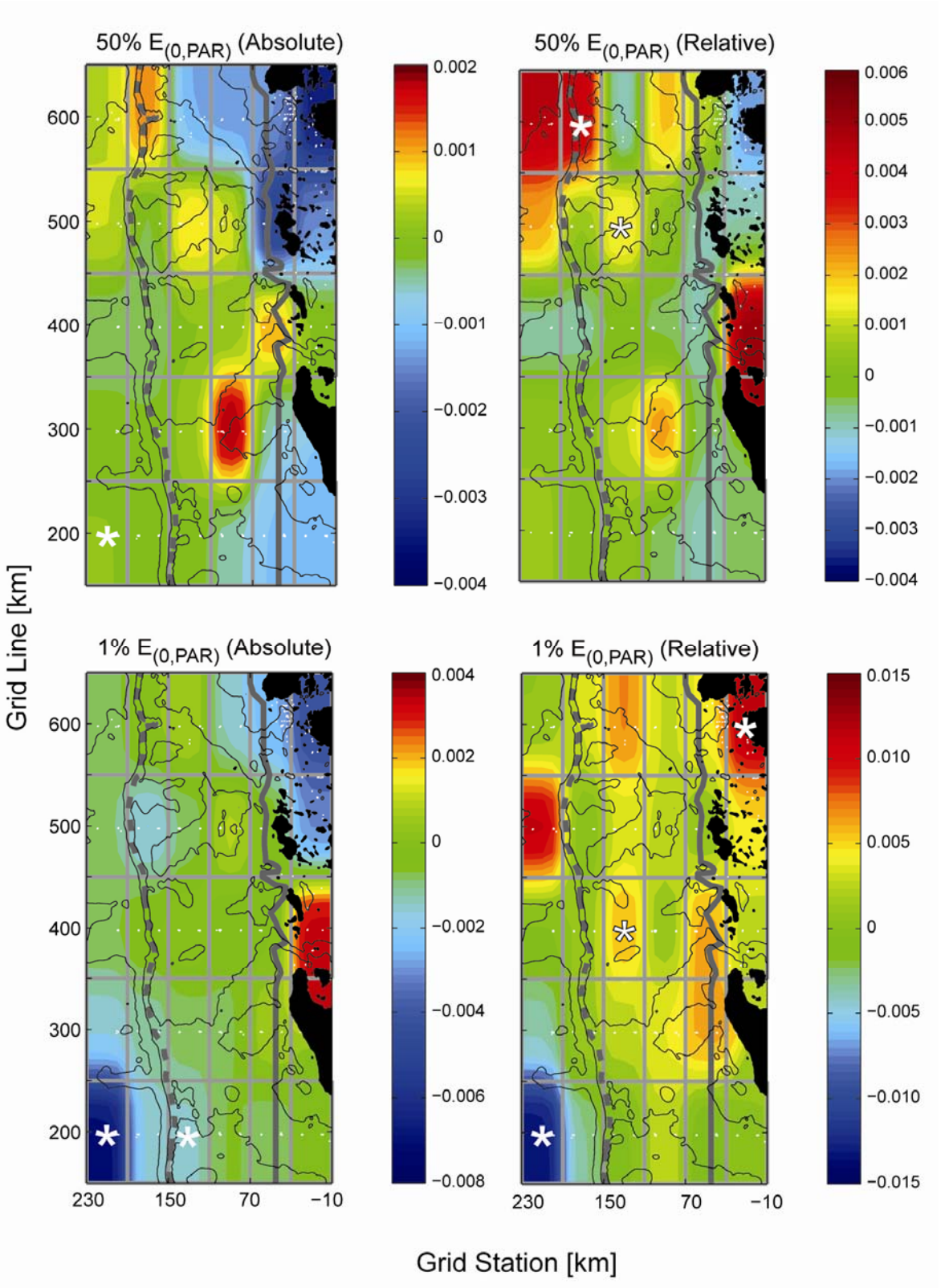

Figure 37. Prasinophyte trends at 50% and 1% light depths, as the slope of grid cell anomalies. Slopes significantly different from zero marked with white asterisk (*).

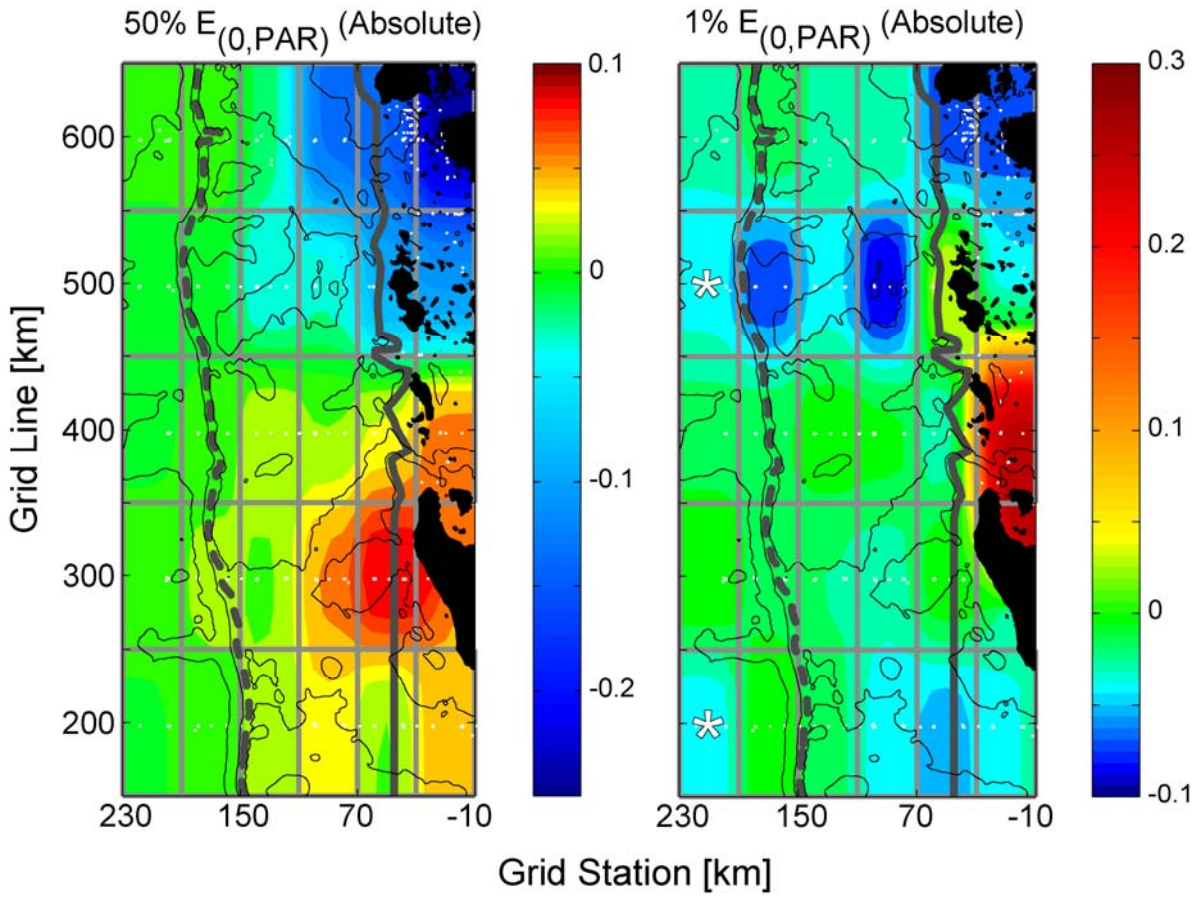

Figure 38. Chlorophyll a (µg L^{-1}) trends at 50% and 1% light depths, as the slope of grid cell anomalies. Slopes significantly different from zero marked with white asterisk (*). Note: no slopes significantly different from zero were detected at the 50% light depth.

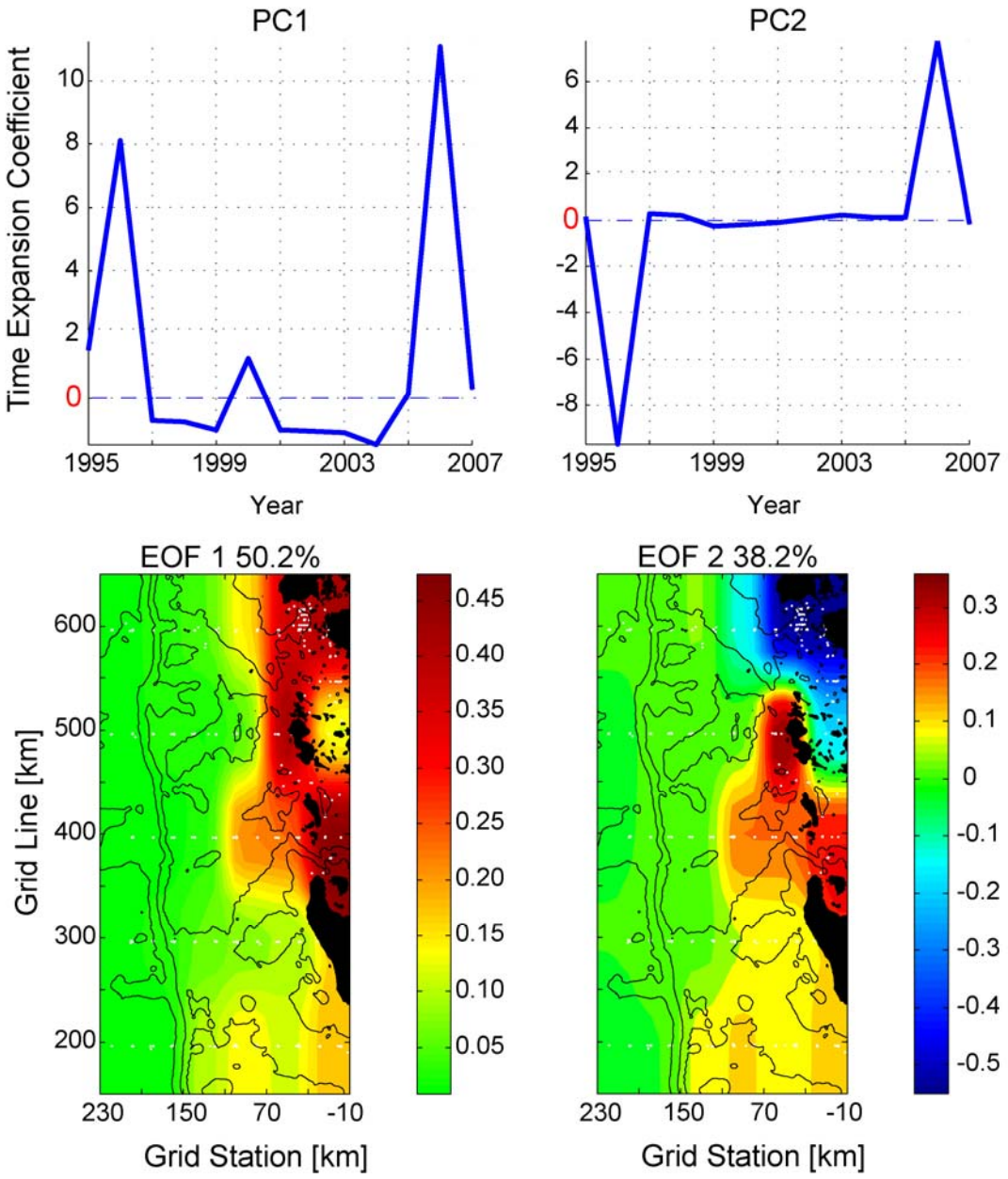

Figure 39. First two principle components (PCs) and empirical orthogonal functions (EOFs) of the Diatoms at 50% light depth.

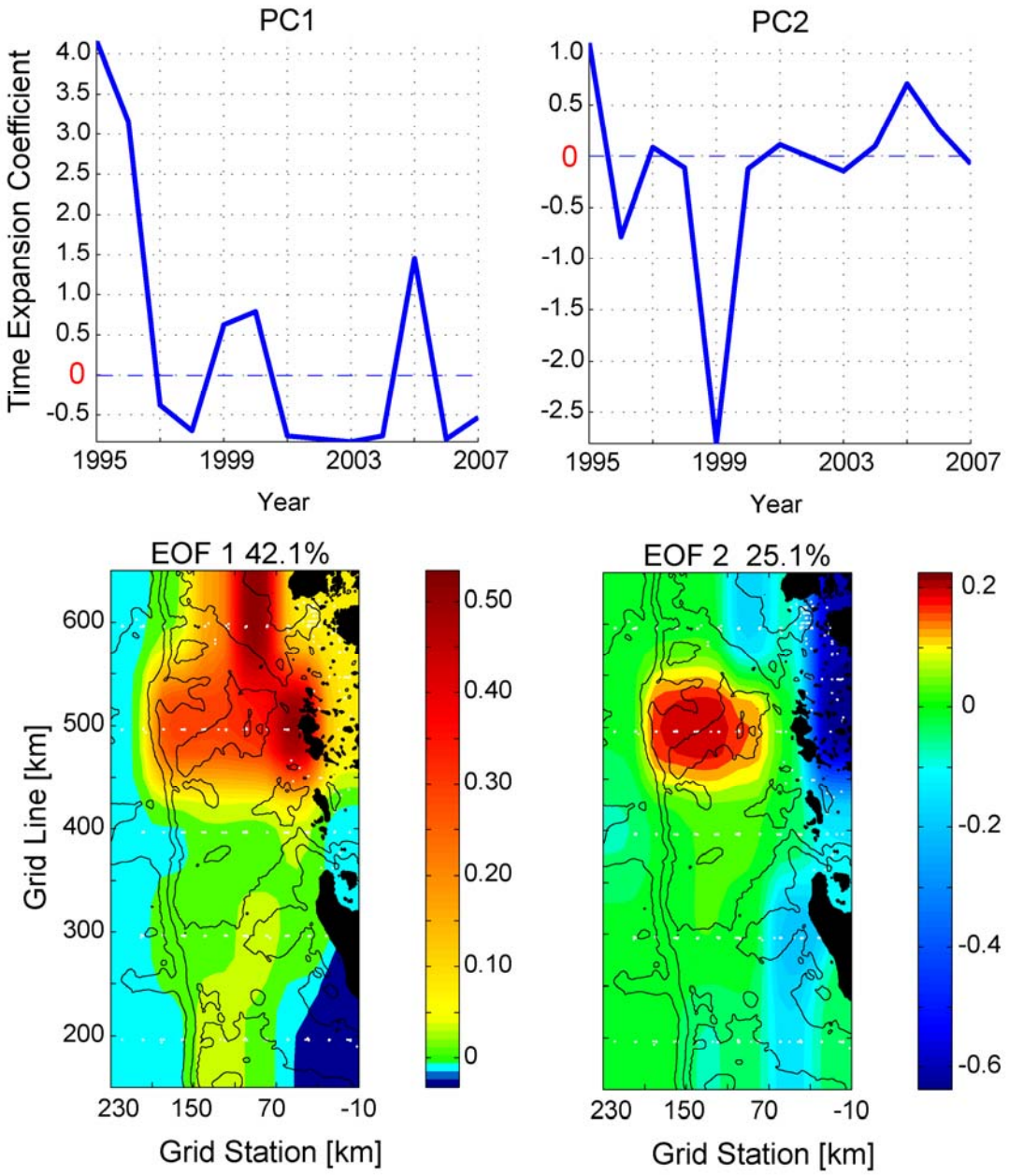

Figure 40. First two principle components (PCs) and empirical orthogonal functions (EOFs) of the Cryptophytes at 50% light depth.

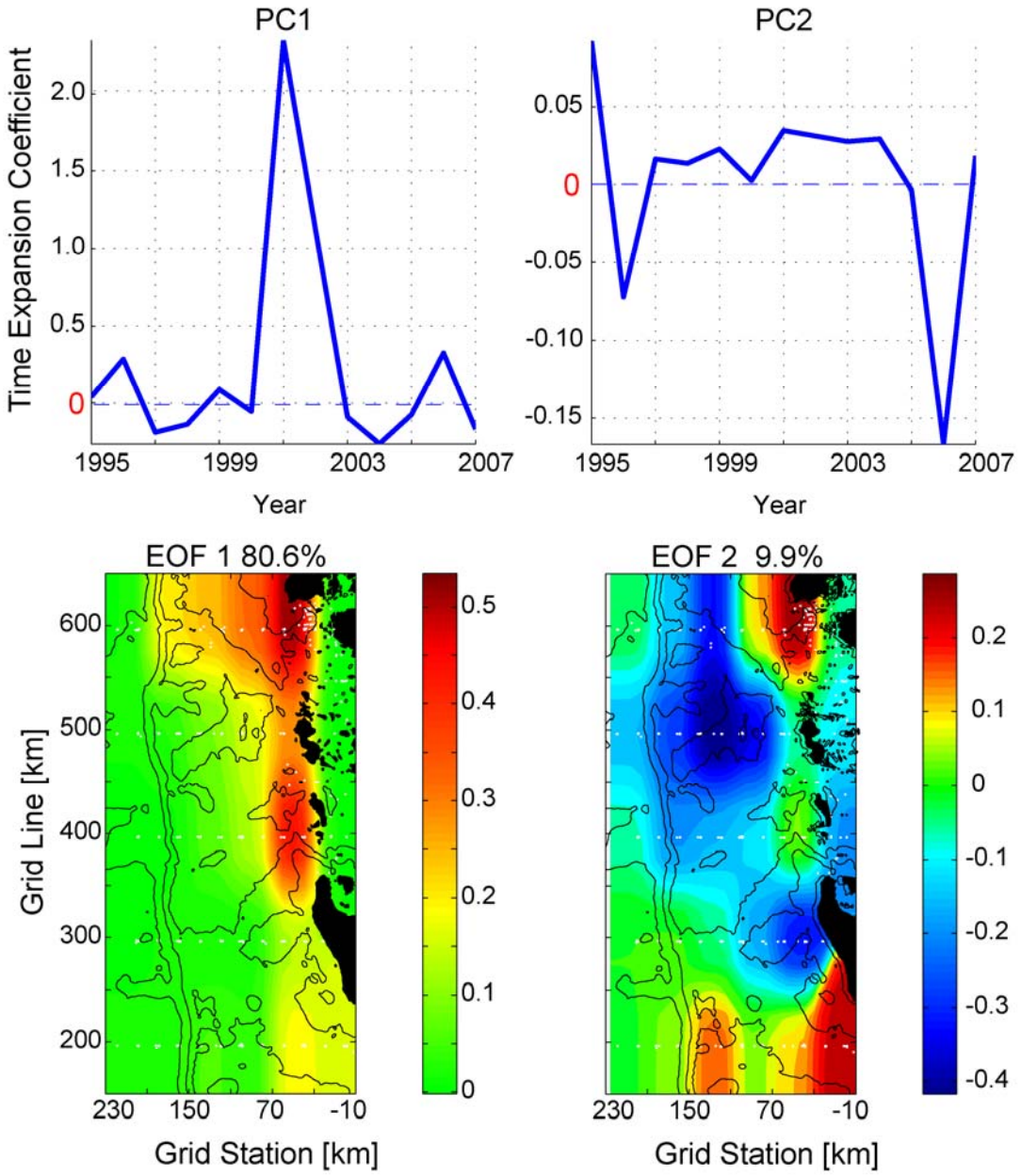

Figure 41. First two principle components (PCs) and empirical orthogonal functions (EOFs) of the Mixed Flagellates at 50% light depth.

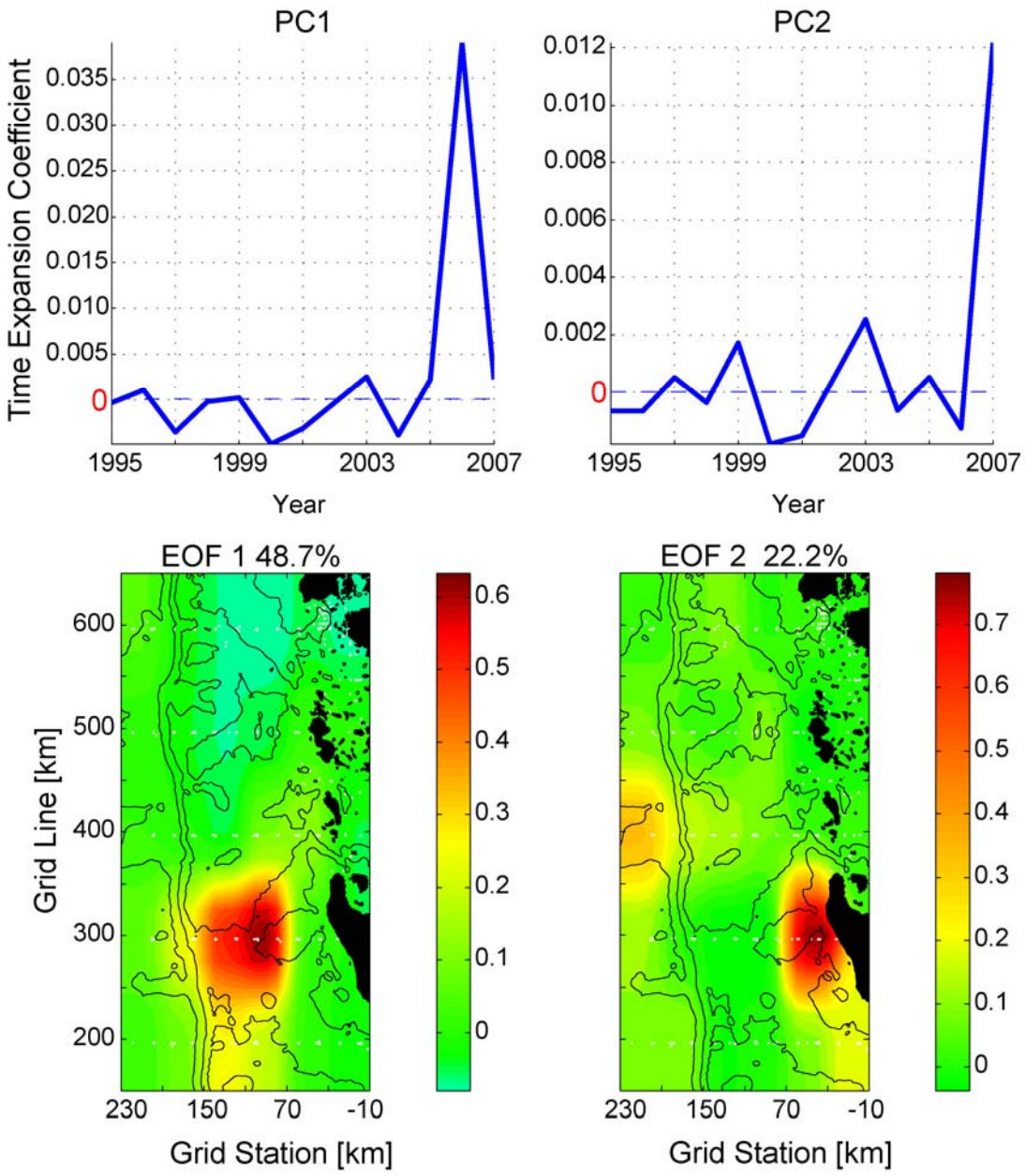

Figure 42. First two principle components (PCs) and empirical orthogonal functions (EOFs) of the Haptophytes at 50% light depth.

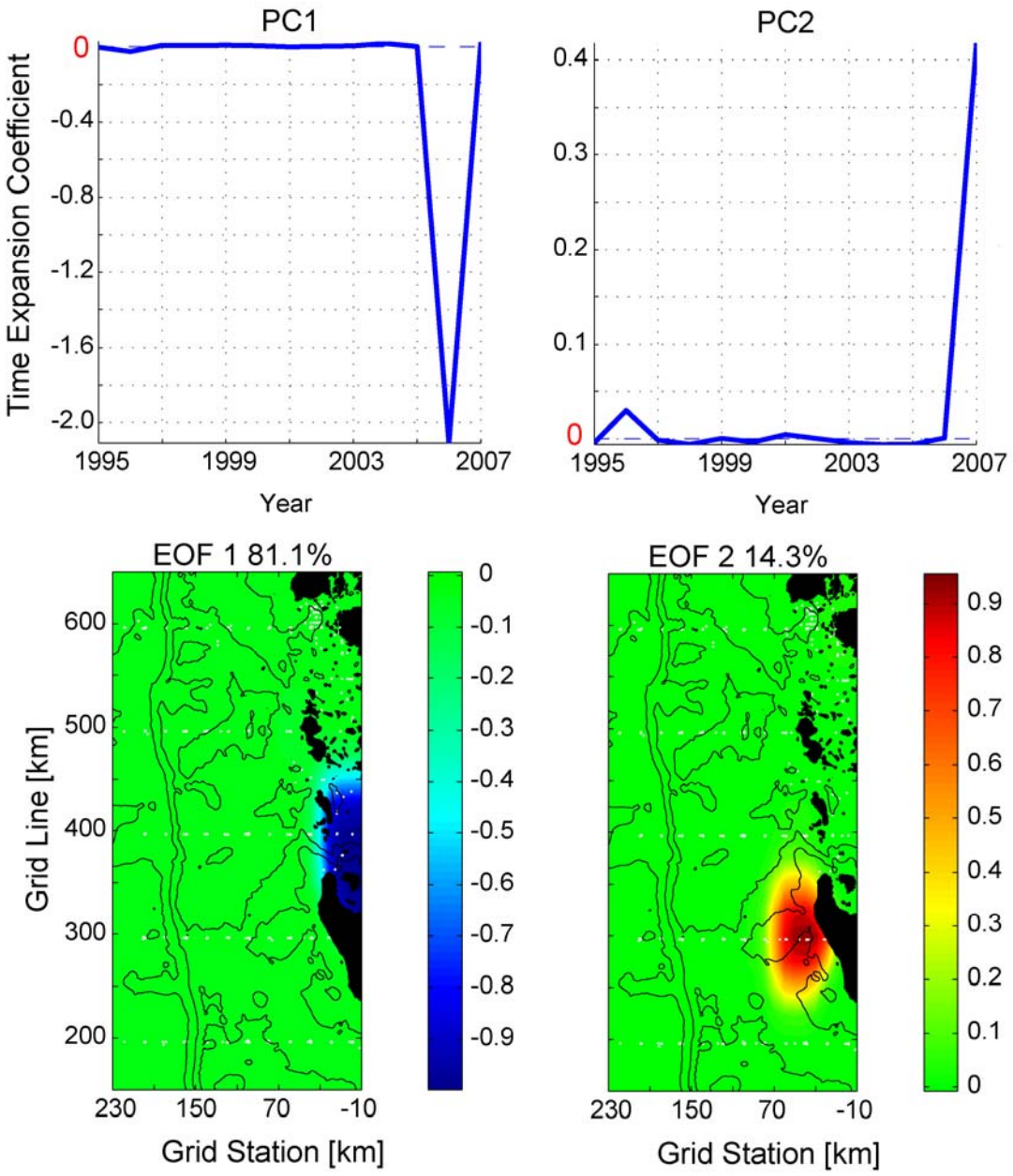

Figure 43. First two principle components (PCs) and empirical orthogonal functions (EOFs) of the Prasinophytes at 50% light depth.

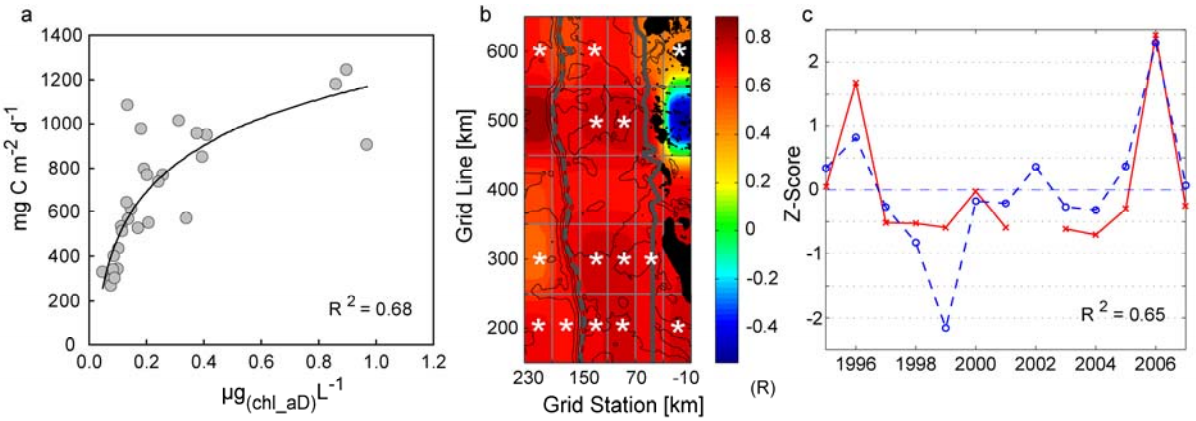

Figure 44. Climatology (a), anomaly (b) and principle component (c) correlation figures between 50% light depth diatoms (μg $_{[chl\_aD]}$ L^{-1} and primary production (μg C m^{-2} d^{-1}). Regression line reflects a non-linear robust fit line on the climatological value in each of the grid cells (a). Statistically significant grid cell correlations are marked with a white asterisk (*)(b). Solid red line with crosses (-x-) is PC1 of the diatoms; dashed blue line with circles (-o-) is PC1 of primary production(c).

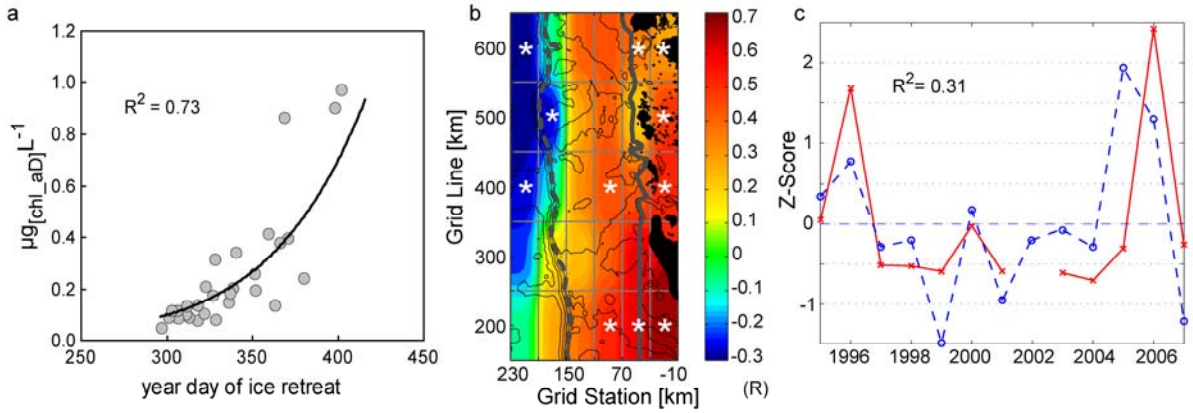

Figure 45. Climatology (a), anomaly (b) and principle component (c) correlation figures between 50% light depth diatoms (μg $_{[chl\_aD]}$ L^{-1}) and sea ice retreat (yd). Regression line reflects the robust fit line on the climatological value in each of the grid cells (a). Statistically significant grid cell anomaly correlations are marked with a white asterisk (*)(b). Solid red line with crosses (-x-) is PC1 of the diatoms; dashed blue line with circles (-o-) is PC1 of sea ice retreat; note ice data has been "pushed" ahead by one year to temporally match the yearly composition data which it influenced (c).

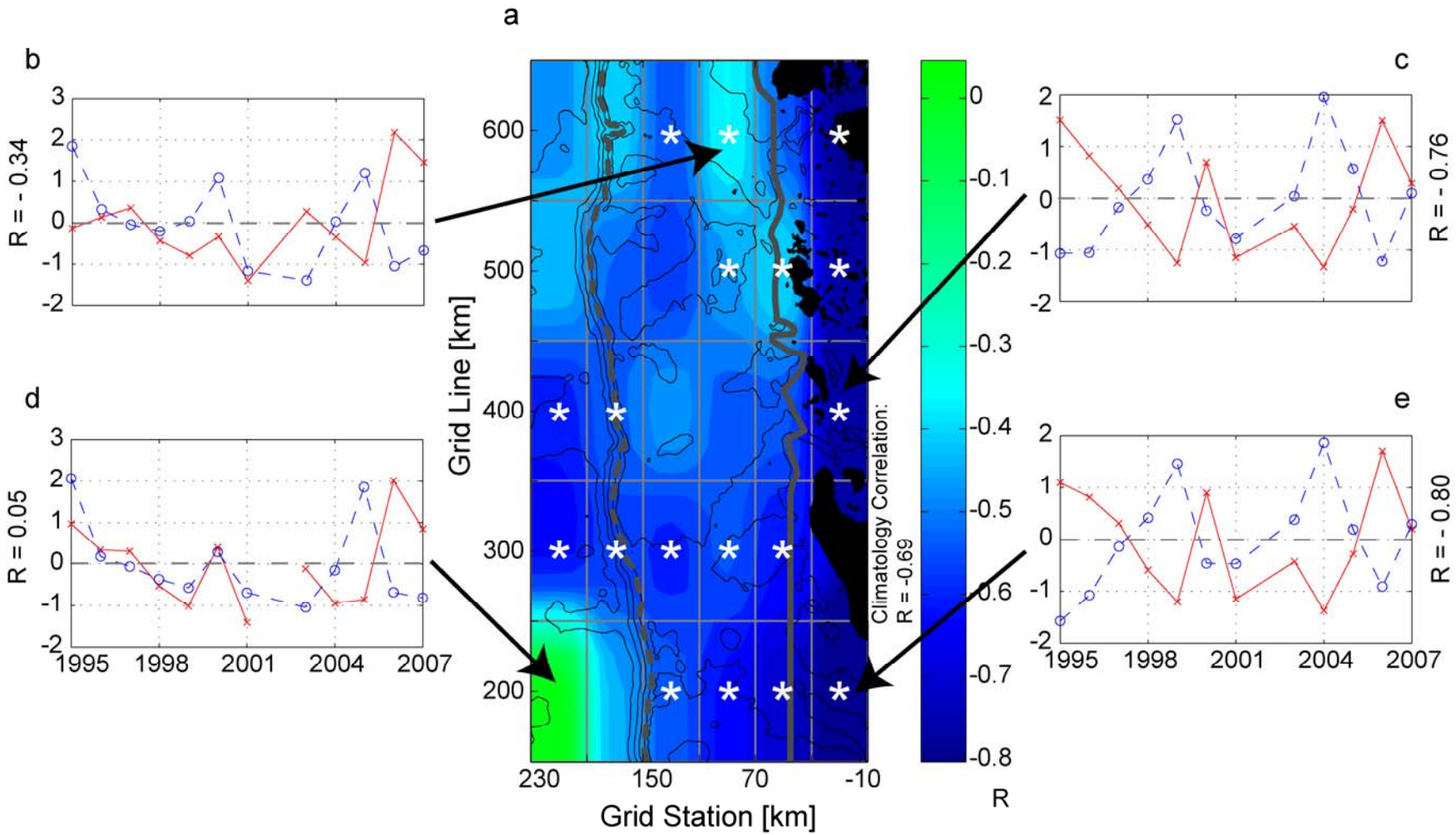

Figure 46. Correlation of diatom and cryptophyte anomalies at the 50% light depth. Subplots are: (a) spatial correlation, (b) grid cell 600.090, (c) 400.010, (d) 200.210, and (e) and 200.010. Solid red lines with crosses (-x-) are diatom anomalies, dashed blue lines with circles (-o-) are cryptophytes. Cells which show statistically significant correlation are marked with a white asterisk (*).

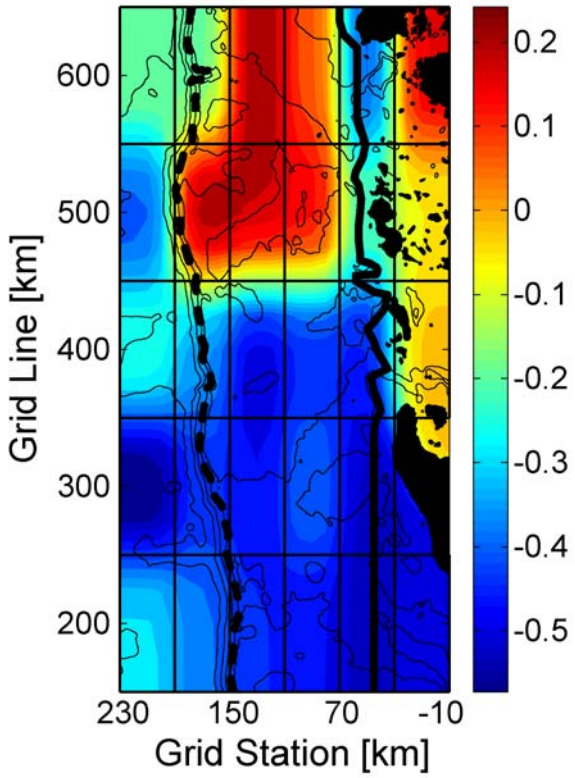

Figure 47. Anomaly correlation map between the ratio of diatoms to cryptophyes and the abundance of mixed flagellates at the 50% light depth. No significant correlations were found.

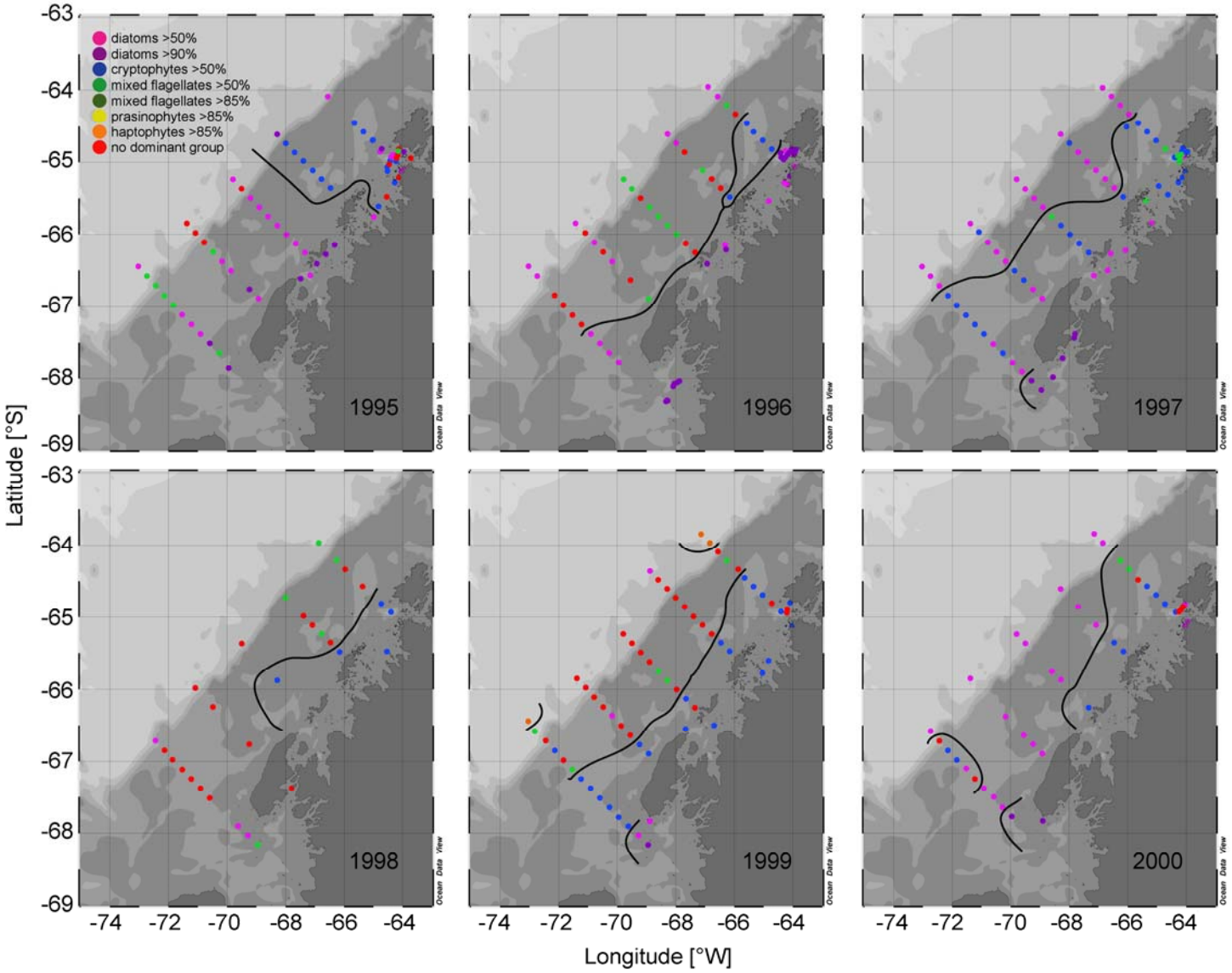

Figure 48. Assemblage maps 1995-2000. Colors refer to assemblages at each station; black lines mark qualitative locations of primary assemblages.

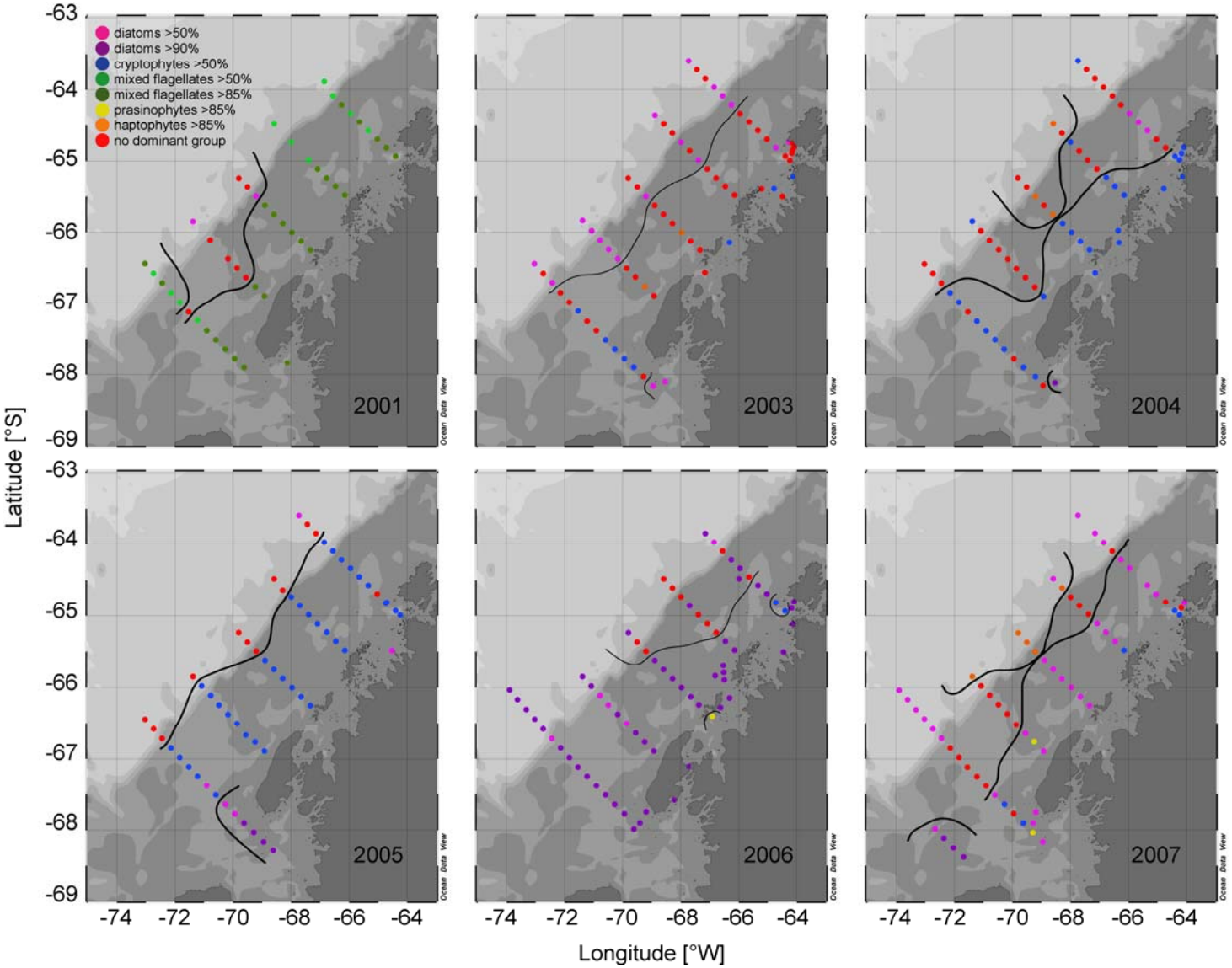

Figure 49. Assemblage maps 2001-2007. Colors refer to assemblages at each station; black lines mark qualitative locations of primary assemblages.

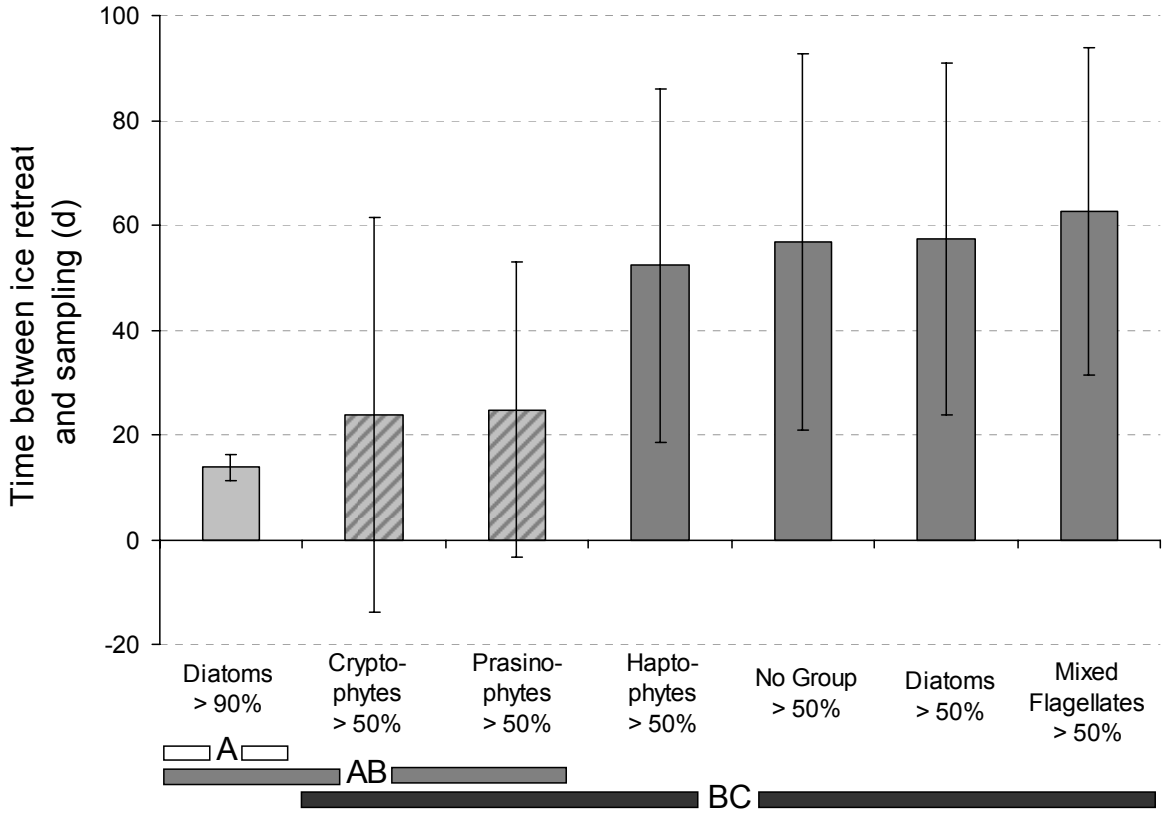

Figure 50. Average time between last ice and presence of assemblages. Error bars represent one standard deviation from the mean. Grouping bars indicate possible seasonal succession order, with Cryptophytes > 50% and Prasinophytes > 50% (group AB) assemblages occurring with either the Diatoms >90% (group A) or the remainder of the common assemblages (group BC).

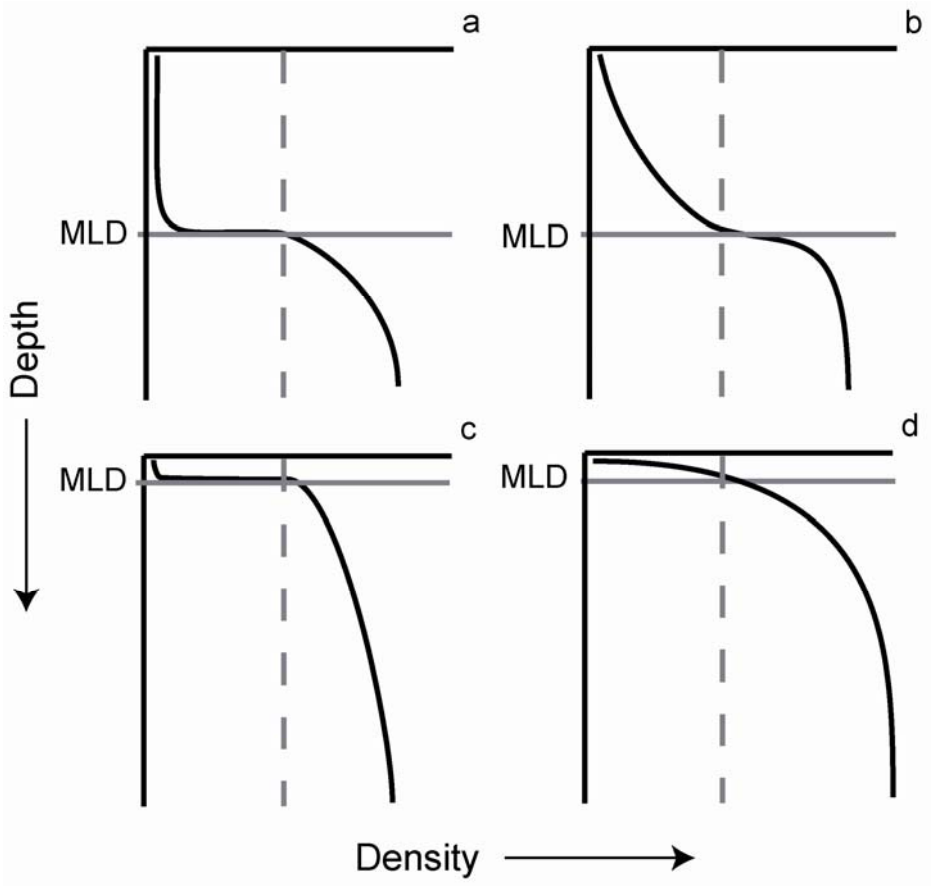

Figure 51. Schematics of possible mixing regimes and their impact on the depth and strength of the mixed layer. Solid black lines represent density gradients, dashed grey lines represent the point at which the defined change in density occurred (here in identical locations because the surface density in all figures is the same) and solid grey lines represent the depth of the resulting mixed layer. Plots are: (a) deep MLD, strong gradient,(b) deep MLD, weak gradient, (c) shallow MLD, strong gradient and (d) shallow MLD, weak gradient.

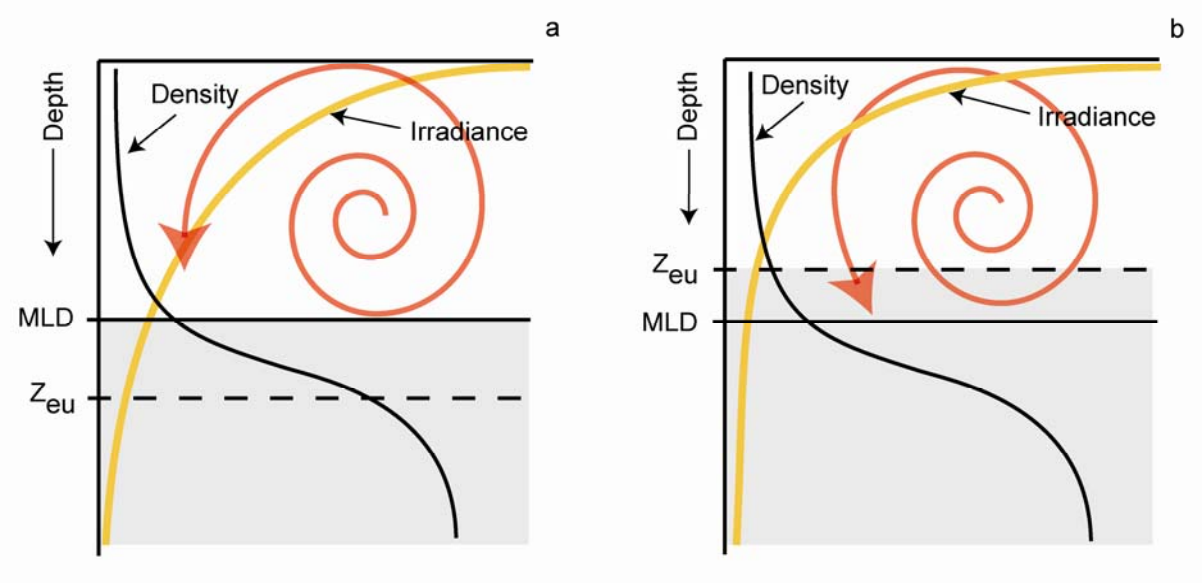

Figure 52. Schematic of mixed layer depth (MLD) and euphotic zone depth (Z_{eu}) comparison. Density gradients (shown here as the black salinity line) form stratified water columns; when MLD is shallower than the Z_{eu}, phytoplankton to the 1% light depth is never exposed to extreme low-light stress (a); this regime is representative of 94.5% of the stations included in this study. When the SML is deeper the the Z_{eu}, phytoplankton is exposed to a more variable irradiance regime, including stress-inducing low-light levels (b) which can lead to short term changes in cellular pigment content. Red arrow represents range of vertical mixing in both figures.

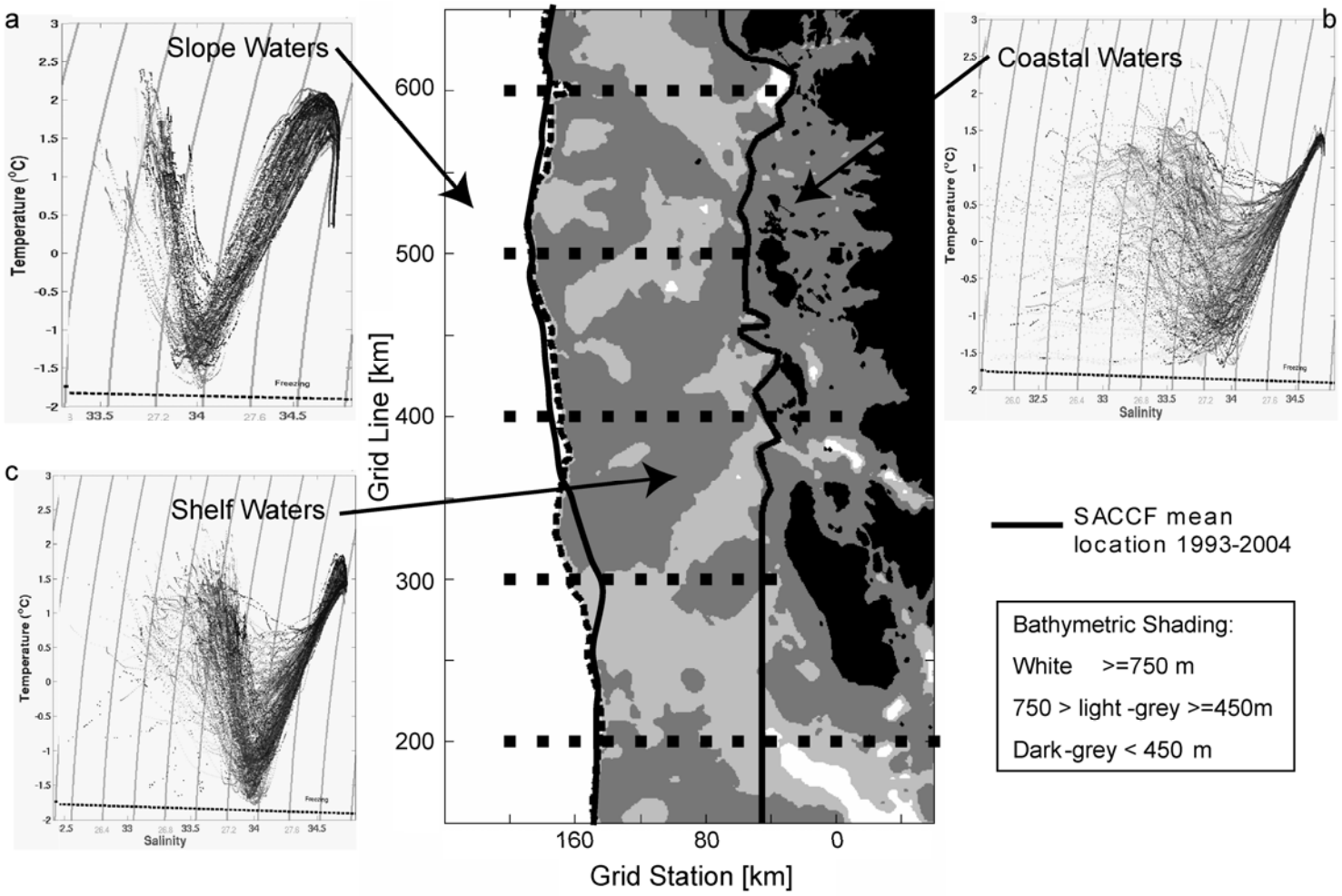

Figure 53. Primary water mass sub-regions within the Pal LTER sampling grid. Slope temperature-salinity diagrams show a steep, V-shaped curve (a), representative of water frequently refreshed by the Antarctic Circumpolar Current (ACC). Coastal waters show a much broader, U-shaped curve, suggesting less frequent renewal by the ACC. The shelf region (c) exhibit characteristics of both and can be considered transitional waters. It is hypothesized that the renewal is bathymetrically controlled (Martinson et al., 2008). Figure from Doug Martinson.

APPENDIX C

TABLES

Table 1. Palmer LTER Cruise Sampling Summary

Year	Cruise Dates	Cruise Duration (days)	Stations (n)	Total Samples (n)	50% Samples (n)	1% Samples (n)
1995	07 Jan – 06 Feb	31	73	427	73	69
1996	08 Jan – 10 Feb	34	74	447	73	74
1997	11 Jan – 12 Feb	33	78	545	77	73
1998	28 Jan – 13 Feb	17	29	175	29	26
1999	08 Jan – 12 Feb	36	61	359	61	60
2000	09 Jan – 26 Jan	18	41	238	41	39
2001	09 Jan – 26 Jan	18	45	268	45	44
2003	05 Jan – 02 Feb	29	68	406	68	68
2004	07 Jan – 01 Feb	26	64	383	64	64
2005	04 Jan – 01 Feb	29	61	355	59	61
2006	07 Jan – 02 Feb	27	69	412	69	69
2007	07 Jan – 04 Feb	29	64	383	63	64

Palmer LTER cruise timing, duration and sampling stations included in study, total number of pigment samples used as input data to CHEMTAX for composition determination, and number of samples at the 50% and 1% light depths.

Table 2. HPLC Gradient Protocols

HPLC System	Time (min)	% Solvent A	% Solvent B	% Solvent C
Hitachi	0	100	0	0
	0.5	0	100	0
	7	0	75	25
	17	0	30	70
	24	0	20	80
	26	0	100	0
	29	100	0	0
	35	100	0	0
Waters†/Agilent*	0	100	0	n/a
	18	60	40	n/a
	22	0	100	n/a
	35	0	100	n/a
	38	100	0	n/a
	40*	100	0	n/a
	42*	100	0	n/a
	45†	100	0	n/a

† * A modification of the Zapata et al., 2000 method was used for both the Waters and Agilent systems; minor adjustments were made based on system configuration to minimize total run time while allowing adequate post-run equilibration.

Table 3. HPLC Pigment Information

Pigment	Abbreviation	Retention Time Wright	Retention Time Zapata	Extinction Coefficient (L g^{-1} cm^{-1})	Wavelength (nm)
chlorophyll c3	chl_c3	6.2	7.7		
chlorophyll c2†‡	chl_c2	7.1	10.8		
chlorophyllide a	chlide-a	n/a	10.9		
peridinin‡	per	9.1	13.2		
19' butanoyloxyfucoxanthin†‡	but	9.3	17.7		
fucoxanthin†‡	fuc	10.1	18.6		
19' hexanoyloxyfucoxanthin†‡	hex	10.4	21.2		
neoxanthin	neox	10.8	19.1		
prasinoxanthin	pras	11.3	19.9		
diadinoxanthin‡	dd	12.9	23.1		
alloxanthin†‡	allox	13.8	24.2		
diatoxanthin‡	dt	14.4	24.6		
lutein‡	lut	14.8	25.0*	255	448
zeaxanthin‡	zeax	15.1	24.9*	234	454
chlorophyll b†‡	chl_b	18.2	20.6	51.36	646
violaxanthin	viol	n/a	20.9		
crocoxanthin	croc	n/a	27.4		
echinenone	ech	n/a	28.1		
chlorophyll a†	chl_a	19.3	29.2	87.67	664
α,α - carotene‡	alpha	21.8	31.3	280	444
β,ε - carotene‡	beta	21.9	31.4	259.2	453

Pigments quantified and abbreviations as used in this text, average retention time (RT) for each method (Wright et al., 1991 used from 1995 to1999, Zapata et al., 2000 used from 2000 to 2007), and for those pigments mixed from powdered standards, extinction coefficients (α) applied and application wavelengths used. Additional comments: * Note elution order change between lutein and zeaxanthin with Zapata et al., 2000 method. † Denotes pigments used in CHEMTAX input ratios for composition determination. ‡ Denotes pigments used in assemblages analysis.

Table 4. Initial Pigment Ratio Matrices

Rodriguez et al., 2002:

Class/Pigment	chl_c3	chl_c2	chl_c1*	fuc	but	hex	allox	vio†	chl_b	NPchl_c2§	chl_a
Pyramimonas								0.055	0.945		1.000
Cryptophytes		0.174					0.228				1.000
Chemotaxonomic group	0.067	0.126		0.290	0.122	0.248					1.000
Diatoms		0.110	0.073	0.745							1.000
Haptophyte	0.141	0.144		0.011	0.080	0.916				0.054	1.000

Modification as used in this study:

Class/Pigment	chl_c3	chl_c2	chl_c1	fuc	but	hex	allox	vio	chl_b	NPchl_c2	chl_a
Prasinophytes									1.000		1.000
Cryptophytes		0.174					0.228				1.000
Mixed Flagellates		0.126		0.290	0.122	0.315					1.000
Diatoms		0.183		0.745							1.000
Type 4 Haptophytes		0.144		0.011	0.080	1.111					1.000

Pigments not quantified by HPLC in this study include: * chlorophyll c1, †violaxanthin and §non-polar chlorophyll c2-MGDG.

Table 5. Descriptive Grid Summary (%)

	Diatoms		Cryptophytes		Mixed Flagellates		Haptophytes		Prasinophytes	
	50%	1%	50%	1%	50%	1%	50%	1%	50%	1%
Climatology %Max/%Min Location of Max	55/11 coast & slope	60/31 ubiqui-tous	63/3 north coast	17/1 north shelf	29/4 shelf	33/17 ubiqui-tous	23/4 slope	19/7 slope	4/0 north	11/3 north coast
1995	High		High	High	Low	Low	Ave	Low	Low	Low
1996	High	High	Ave	Ave	High	High	Ave	Ave	High	Ave
1997	Ave	Ave	Ave	Ave	Low	High	High	Ave	Ave	High
1998	Low	High	Ave	Ave	High	High	High	High	Low	Ave
1999	Low	High	High	Ave	Ave	Ave	High	Ave	Ave	Low
2000	High	High	High	Ave	Ave	Low	Low	Low	Ave	Ave
2001	Low	Low	Low	Low	High	High	Low	Low	High	Low
2003	Ave	Low	Ave	High	Ave	Low	High	Ave	High	Low
2004	Low	Ave	High	Ave	Low	Low	High	High	High	High
2005	Low	Low	High	Ave	Low	High	Low	Ave	Low	High
2006	High	High	Low	Low	Ave	Low	Low	Ave	Ave	High
2007	High	High	Ave	Ave	Low	Ave	High	high	High	Ave

Average (climatological) percent of chl_a biomass of maximum and minimum contribution to the phytoplankton community and the overall grid description compared to the climatology for each year of the study, for each of the five main groups, at both the 50 and 1% light depths.

Table 6. Descriptive Grid Summary (µg L^{-1} chl_a)

	Diatoms		Cryptophytes		Mixed Flagellates		Haptophytes		Prasinophytes	
	50%	1%	50%	1%	50%	1%	50%	1%	50%	1%
Climatology Max/Min Loc. of Max	.97\.05 coast	.53/.06 south coast	.76/0 north shelf	.13/.00 north shelf	.19/.02 coast & shelf	.18/.03 coast & shelf	.07/.03 ubiqui-tous	.05/.01 ubiqui-tous	.04/.00 north coast	.03/.01 ubiqui-tous
1995	High		High	High	Low	High	Ave	High	High	Ave
1996	High	Ave	High	High	High	High	High	High	High	Ave
1997	Ave	Ave	Ave	Ave	Low	Ave	High	Ave	Ave	Ave
1998	Ave	Ave	Low	Low	Ave	Ave	Ave	Ave	Low	Low
1999	Ave	Ave	High	Ave	Ave	High	High	High	Ave	Ave
2000	High	Ave	High	Low	Ave	High	Low	Ave	Ave	Ave
2001	Low	Low	Low	Low	High	Low	Low	Low	High	High
2003	Low	Low	Low	High	Ave	Low	High	Ave	High	Low
2004	Low	Low	Low	Low	Low	Low	Low	Ave	Ave	Ave
2005	Ave	Low	High	Low	Ave	Low	Ave	Ave	Ave	Ave
2006	High	High	Low	Ave	High	High	High	High	Low	High
2007	Ave	Ave	Ave	Ave	Low	Ave	high	high	Low	Ave

Average (climatological) value (ug L^{-1} chl_a) of maximum and minimum contribution to the phytoplankton community and the overall grid description compared to the climatology for each year of the study, for each of the five main phytoplankton groups, at both the 50 and 1% light depths.

Table 7. Regression Results: Microscopy vs CHEMTAX

	1996 (n = 66)			1997 (n = 70)			1999 (n = 53)		
	m	b	R^2	m	b	R^2	m	b	R^2
Diatoms	0.90	-0.02	0.64*	0.80	-0.12	0.61*	0.97	0.13	0.56*
Crytophytes	0.92	0.01	0.71*	0.57	0.06	0.74*	0.77	-0.02	0.90*
Mixed Flagellates	0.88	0.20	0.42*	0.57	0.46	0.04	0.21	0.34	0.06
Haptophytes		n/a		-0.04	0.01	0.06		n/a	
Prasinophytes	0.12	0.01	0.03	-0.08	0.01	0.04	0.40	0.00	0.50*

Slope (m), intercept (b) and correlation coefficient (R^2) for biomass estimates of the five main phytoplankton groups using microscopy and CHEMTAX methods. Significant correlations ($p < 0.001$ $r_{0.05(2)n}$) are marked with an asterisk (*).

Table 8. Summary of assemblage findings.

Year	Clusters Observed (n)	Diatoms >50%	Cryptophytes >50%	Haptophytes >50%	Mixed Flagellates >50%	Prasinophytes >50%	Diatoms >90%	No Single Group Dominant	Timing of Sea Ice Retreat
1995	5	south shelf	north shelf		south slope		all coast, Marguerite Bay	north coast, central slope	late
1996	5	all slope	north coast north shelf		central shelf		all coast, Marguerite Bay	all shelf	average
1997	4	all slope, south coast	all shelf, Palmer				Marguerite Bay	north coast, south and central shelf	average
1998	4	south coast	north coast, Palmer		north slope, north shelf			south	average
1999	6	Marguerite Bay	all coast	north and south slope	all shelf		Marguerite Bay	all shelf, central slope	very early
2000	5	all slope, central and south shelf	north coast		north shelf		Marguerite Bay	inside north	early
2001	3				all			central slope, 300 line slope and shelf	early
2003	4	all slope, Marguerite Bay	inside north, south coast	central coast				all coast and shelf	late
2004	5	north shelf	all coast, south shelf	central slope			Marguerite Bay	all slope, north shelf	average

Table 8 (continued).

Year	Clusters Observed (n)	Diatoms >50%	Cryptophytes >50%	Haptophytes >50%	Mixed Flagellates >50%	Prasinophytes >50%	Diatoms >90%	No Single Group Dominant	Timing of Sea Ice Retreat
2005	4	south coast	all shelf, north and central coast				Marguerite Bay	all slope	very late
2006	6	north and south all, central coast and shelf	Palmer		500 line shelf and slope	central coast	central coast, inside south, Marguerite Bay	central slope	late
2007	6	all north, central shelf, south slope	all coast	central slope		south coast	far south	all shelf	early

APPENDIX D

MICROSCOPY DATA

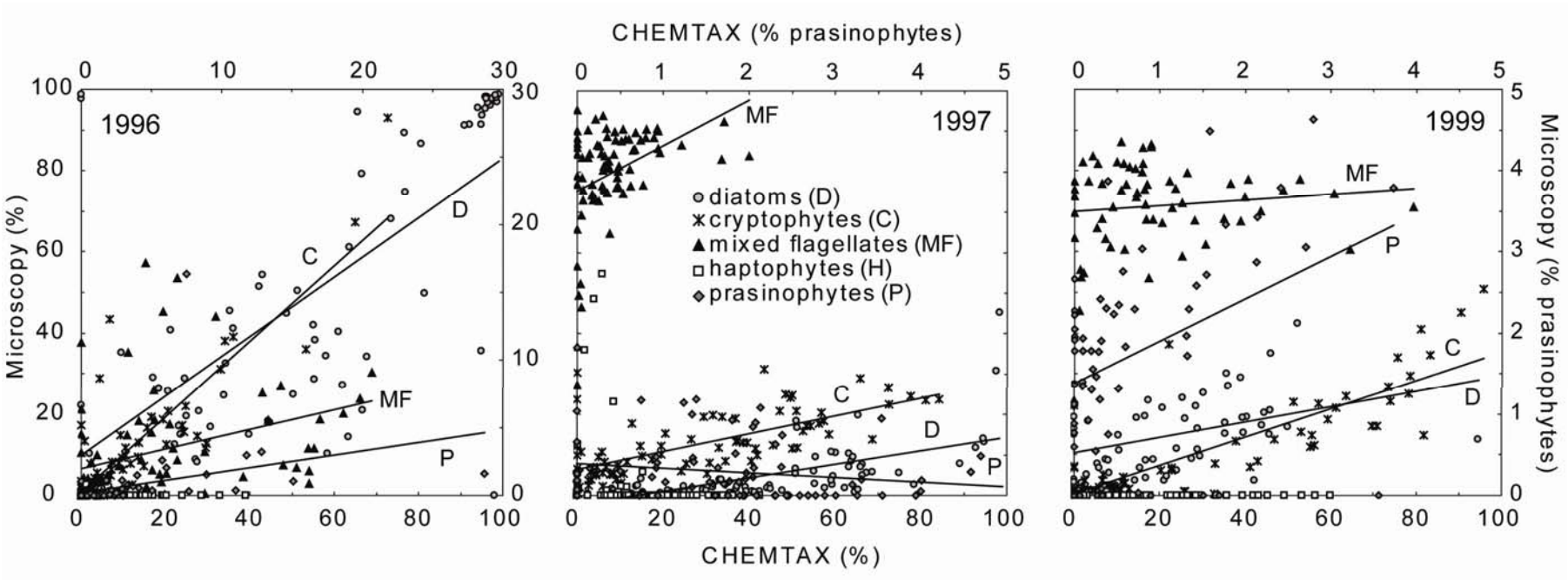
CHEMTAX (% prasinophytes)
1996
1997
1999
Microscopy (%)
Microscopy (% prasinophytes)
CHEMTAX (%)
diatoms (D)
cryptophytes (C)
mixed flagellates (MF)
haptophytes (H)
prasinophytes (P)
C
D
MF
P

ABSTRACT OF THE THESIS

Pigment Derived Phytoplankton Composition along the Western Antarctic Peninsula

by
Wendy Anne Kozlowski
Master of Science in Biology
San Diego State University, 2007

Current bio-optical models for remote sensing of chlorophyll a (chl_a) biomass and production are sensitive to changes in specific absorption. Variability in phytoplankton composition is tied to changes in spectral absorption; our ability to follow these changes would be enhanced by a better understanding of community composition. Examined in this study was a thirteen year span (1995-2007) of high-performance liquid chromatography (HPLC) pigments collected as part of the Palmer Long Term Ecological Research (PAL LTER) project along the western Antarctic Peninsula (wAP) between roughly -64 and -68° South. Phytoplankton composition was estimated using CHEMTAX analysis software, and presented here is the temporal and spatial distribution of those assemblages in both surface (50% $E_{0,PAR}$) and deep euphotic zone (1% $E_{0,PAR}$) waters. Diatoms and cryptophytes were found to be the two dominant groups at the surface. In the deep water sample, contribution to total chl_a was more evenly distributed between groups, with only diatoms ever consisting of more than 50% of the population. Spatially, diatoms were most abundant (in terms of μg L^{-1} chl_a) inshore along the entirety of the sampling grid, whereas cryptophyte and prasinophyte abundance was typically highest inshore only in the north. Mixed flagellate concentration was highest inshore in the south-eastern region but in shelf waters further north, and type 4 Haptophytes were most abundant along the length of the shelf region. Temporal distribution of groups is discussed in terms of anomalies calculated as yearly differences from the climatological means. Variability in space and time was examined using principle component analysis, and possible relationships between seasonal sea ice retreat and phytoplankton composition, as well as phytoplankton composition and primary production are discussed.